

Influence of Wax-Based Binder Formulations on Rheological  
Properties of Feedstocks Used in Low-Pressure  
Metal Injection

by

Ghalya ALI

THESIS PRESENTED TO ÉCOLE DE TECHNOLOGIE SUPÉRIEURE  
IN PARTIAL FULFILLMENT FOR A MASTER'S DEGREE  
WITH THESIS IN MECHANICAL ENGINEERING  
M. A. Sc.

MONTREAL, SEPTEMBER 19TH, 2018

ÉCOLE DE TECHNOLOGIE SUPÉRIEURE  
UNIVERSITÉ DU QUÉBEC



Ghalya ALI, 2018



This Creative Commons license allows readers to download this work and share it with others as long as the author is credited. The content of this work can't be modified in any way or used commercially.

**BOARD OF EXAMINERS**  
THIS THESIS HAS BEEN EVALUATED  
BY THE FOLLOWING BOARD OF EXAMINERS

Mr. Vincent Demers, Thesis Supervisor  
Department of Mechanical Engineering at École de technologie supérieure

Ms. Nicole Demarquette, Thesis Co-supervisor  
Department of Mechanical Engineering at École de technologie supérieure

Mr. Patrice Seers, President of the Board of Examiners  
Department of Mechanical Engineering at École de technologie supérieure

Mr. Éric David, Member of the jury  
Department of Mechanical Engineering at École de technologie supérieure

THIS THESIS WAS PRESENTED AND DEFENDED  
IN THE PRESENCE OF A BOARD OF EXAMINERS AND PUBLIC  
AUGUST 30TH, 2018  
AT ÉCOLE DE TECHNOLOGIE SUPÉRIEURE



## **ACKNOWLEDGMENT**

I would like to express all my gratitude to Mr. Vincent Demers, my thesis supervisor, for his great availability and great interest in this work. I would also like to thank Mrs. Nicole Demarquette, my thesis co-director of memory, who has supported me in my research. Many thanks also to all members of the jury for agreeing to judge this work.

Finally, I own my deepest gratitude to my husband, my children and my sisters for their unconditional support and love.



# **INFLUENCE DE LA FORMULATION DU LIANT À BASE DE CIRE SUR LES PROPRIÉTÉS RHÉOLOGIQUES DES MÉLANGES UTILISÉS DANS LE MOULAGE PAR INJECTION À BASSE PRESSION DES POUDRES MÉTALLIQUES**

Ghalya ALI

## **RÉSUMÉ**

Le moulage par injection à basse pression des poudres métalliques (LPIM) est une technologie de fabrication utilisée pour produire, d'une manière rentable, de petites pièces métalliques de forme complexes finale à partir d'une grande variété de métaux. Les avantages du procédé LPIM incluent des volumes de production élevés, une mise au mille élevée, une grande variété de matériaux (poudres céramiques et poudres métalliques), d'excellentes propriétés mécaniques, de bons finis de surfaces et de bonnes tolérances géométriques et dimensionnelles. Cependant, les efforts pour optimiser les propriétés mécaniques des matériaux métalliques LPIM impliquent typiquement le déliançage et le frittage en utilisant des charges dont la moulabilité optimale n'a pas encore été démontrée. Par conséquent, l'atteinte du plein potentiel du processus LPIM est encore limitée par la mauvaise compréhension des mécanismes fondamentaux qui régissent la moulabilité des mélanges LPIM. Jusqu'à présent, il n'y a pas de base de données que les ingénieurs peuvent utiliser pour concevoir une matière première appropriée et le lien entre la formulation du mélange et son impact sur la moulabilité n'est pas encore clair. Pour cette raison, l'objectif principal de ce travail est d'étudier l'influence des constituants à base de cire sur les propriétés rhéologiques des mélanges pour mieux comprendre et prédire les propriétés de moulabilité des mélanges poudre-liant utilisés dans le moulage par injection de poudre. Pour atteindre cet objectif, une campagne de caractérisation rhéologique a été réalisée en utilisant sept groupes de différentes formulations de mélanges composées de plus de 195 mélanges différents. Chaque famille de matières premières a été conçue pour discrétiser l'influence des formulations à un seul liant et à plusieurs liants sur la viscosité.

Dans cette étude, trois lots différents de poudre d'acier inoxydable 17-4PH ont été utilisés pour préparer différentes formulations utilisant une fraction volumique de 60 vol. % de poudre, cinq cires différentes (une cire de paraffine (PW), une cire d'abeille (BW), une cire de carnauba (CW) et deux cires microcristallines (MW1 et MW2)), deux agents tensioactifs (acide stéarique (SA) et acide oléique (OA)) et deux agents épaisseurs (éthylène-acétate de vinyle (EVA) et polyéthylène basse densité (LDPE)). Deux tailles de poudre différentes (12 et 3 µm) produites par pulvérisation à l'eau et une poudre produite par atomisation au gaz (12 µm). Les analyses de calorimétrie différentielle à balayage ont été réalisées pour évaluer le point de fusion de toutes les charges, tandis que les tests rhéologiques ont été effectués à 90 °C pour toutes les matières premières (c.-à-d. > que le point de fusion des liants) pour étudier l'influence des constituants du liant sur la viscosité des mélanges.

Il a été démontré que l'acide stéarique (SA) et l'acide oléique (OA) produisent le même effet tensioactif, et comme il est plus difficile de travailler avec l'acide oléique, il a été conclu qu'il

n'y a pas de réel avantage à utiliser cet agent tensioactif. Il a également été prouvé qu'une quantité aussi petite que 0.2 vol. % d'acide stéarique était suffisant pour produire l'effet tensioactif. De même, l'éthylène-acétate de vinyle (EVA) a été confirmé comme un bon constituant pour augmenter la viscosité et éventuellement adapter la viscosité des charges afin de diminuer la ségrégation. En comparaison, d'autres agents épaississants classiques tels que le polyéthylène basse densité (LDPE) peuvent également être utilisés comme agent épaississant mais au prix d'une augmentation trop importante de la viscosité des mélanges. Étant donné qu'aucune interaction significative entre SA et EVA n'a été observée, il a été proposé qu'une proportion aussi faible que 0.5 vol. % de SA pourrait être ajoutée dans des mélanges de cires EVA pour produire un effet tensioactif dans ce type de charges. Enfin, il a été démontré qu'une combinaison de deux agents tensioactifs (acide stéarique et acide oléique) dans des charges à base de cires EVA ne produit aucun effet significatif sur la viscosité par rapport à des charges similaires utilisant un seul agent tensioactif. Cette cartographie systématique des liants effectuée dans cette étude peut maintenant être utilisée comme première base de données complète pour mieux comprendre l'impact de chaque ingrédient et les interactions entre les liants sur la viscosité des mélanges afin d'adapter les propriétés des matières premières LPIM à l'avenir.

**Mots-clés:** LPIM; poudre métallique; formulation de liant; rhéologie; viscosité; mélange.

# **INFLUENCE OF WAX-BASED BINDER FORMULATIONS ON RHEOLOGICAL PROPERTIES OF FEEDSTOCKS USED IN LOW-PRESSURE METAL INJECTION**

Ghalya ALI

## **ABSTRACT**

Low-pressure metal injection molding (LPIM) is a powerful technology used to produce small complex net shape metallic parts from a large variety of metals in a cost-effective way. The advantages of LPIM process include high production volumes, high buy-to-fly ratio, wide variety of materials (both for ceramic powders and for metallic powders), excellent mechanical properties, good surface finishes, and good geometric and dimensional tolerances of the produced part. However, efforts to optimize the mechanical properties of LPIM metallic materials typically involve debinding and sintering using feedstocks whose optimal moldability has not yet been demonstrated. Therefore, achieving the full potential of the LPIM process is still limited by the poor understanding of the fundamental mechanisms underlying the moldability of LPIM feedstocks. So far, there is no database that engineers can use to design an appropriate feedstock and the link between the feedstock formulation and its impact on moldability is not yet clear. For this reason, the main objective of this work was to study the influence of wax-based binder systems on the rheological properties of feedstocks to better understand and predict the moldability properties of powder-binder mixtures used in low-pressure powder injection molding process. To achieve this objective, a rheological characterization campaign was carried out using seven groups of different feedstock formulations consisting in more than 195 different mixtures. Each feedstock family was tailored to discretize the influence of single-binder and multiple-binder formulations on viscosity.

In this study, three different 17-4PH stainless steel powder lots were used to prepare different feedstock formulations containing 60 vol. % of powder, five different waxes (one paraffin wax (PW), one beeswax (BW), one carnauba wax (CW), and two microcrystalline waxes (MW1 and MW2), two surfactants agents (stearic acid (SA) and oleic acid (OA)) and two thickening agents (ethylene vinyl acetate (EVA) and low-density polyethylene (LDPE)). Two different powder sizes (12 and 3  $\mu\text{m}$ ) produced by water-atomization and one powder produced by gas-atomization (12  $\mu\text{m}$ ) were selected to quantify the influence of powder size and powder shape on rheological behavior. Differential scanning calorimetry analysis were performed to assess the melting point of all feedstocks, while rheological tests were performed at 90°C for all feedstocks (i.e., above melting point of feedstocks) to study the influence of binder constituents on the feedstocks viscosity.

It was demonstrated that stearic acid (SA) and oleic acid (OA) produce the same surfactant effect, and since it is more difficult to work with oleic acid, it was concluded that there is no real advantage to use this surfactant agent in the future. It was also proved that a quantity as small as 0.2 vol. % of stearic acid was enough to produce the surfactant effect. Likewise, ethylene-vinyl acetate (EVA) was confirmed as a good binder constituent to increase the viscosity and possibly tailor the viscosity of feedstocks in order to decrease the segregation. In

comparison other conventional thickening agent such as low-density polyethylene (LDPE) can also be used as surfactant agent but at the price of a too significant increase in feedstocks viscosity. Since no significant interaction between SA and EVA was seen, it was proposed that a proportion as low as 0.5 vol.% of SA could be added into EVA-waxes mixtures to produce surfactant effect into that kind of feedstocks. Finally, it was demonstrated that a combination of two surfactant agents (stearic acid and oleic acid) into EVA-waxes based feedstocks produces no significant effect on viscosity compared to similar feedstocks using a single surfactant agent. This systematic binder mapping performed in this study can be now used as the first complete database to better understand the impact of each ingredient and interactions between binders on feedstocks viscosity in order to tailor the LPIM feedstocks properties in future.

**Keywords:** LPIM; metallic powder; binder formulation; rheology; viscosity; feedstock.

## TABLE OF CONTENTS

	Page
INTRODUCTION .....	1
CHAPITRE 1 LITERATURE REVIEW .....	3
1.1 Powder injection molding process .....	3
1.1.1 Comparison between LPIM & HPIM process .....	4
1.1.2 Mixing and powder-binder formulations .....	6
1.1.3 Injection molding .....	7
1.1.4 Debinding .....	8
1.1.5 Sintering .....	11
1.2 Feedstock constituents used in LPIM .....	12
1.2.1 Metallic powders .....	12
1.2.2 Binders .....	17
1.3 Rheological behavior of LPIM feedstocks .....	18
1.3.1 Influence of binder constituents on viscosity .....	19
1.3.2 Influence of particle size on viscosity .....	22
1.3.3 Influence of particle shape on viscosity .....	26
1.3.4 Influence of shear deformation rate on viscosity .....	27
1.3.5 Influence of temperature on viscosity .....	29
1.3.6 Influence of solid loading on viscosity .....	31
1.4 Injection performance of feedstocks .....	33
1.4.1 Moldability index model .....	33
1.4.2 Measurement of the feedstock's moldability .....	36
CHAPITRE 2 PROBLEM DEFINITION AND RESEARCH OBJECTIVE .....	39
2.1 Problem definition .....	39
2.2 Research objectives .....	39
CHAPITRE 3 EXPERIMENTAL METHODOLOGY .....	41
3.1 Feedstock formulations .....	41
3.1.1 Powder lots .....	41
3.1.2 Binder constituents .....	42
3.1.3 Feedstock preparation steps .....	46
3.2 Feedstock characterization .....	46
3.2.1 Thermal properties .....	46
3.2.2 Viscosity measurements and data processing .....	49
CHAPITRE 4 RESULTS AND DISCUSSION .....	55
4.1 Differential scanning calorimeter analysis .....	55
4.2 Study of thermal stability during rheological characterization .....	56
4.3 Quantification of the repeatability of the rheological tests .....	59
4.4 Influence of single waxes binder on viscosity .....	60
4.5 Influence of surfactant agents on viscosity of wax-based feedstocks .....	61
4.5.1 Use of stearic acid into single wax-based feedstocks .....	62

4.5.2	Use of oleic acid into single wax-based feedstocks.....	66
4.5.3	Comparison between surfactant agents.....	70
4.6	Influence of thickening agent on viscosity of wax-based feedstocks .....	71
4.6.1	Use of ethylene vinyl acetate into single wax-based feedstocks .....	72
4.6.2	Combination of stearic acid with ethylene vinyl acetate into single wax-based feedstocks.....	74
4.6.3	Comparison between thickening agents.....	82
4.6.4	Combination of stearic acid with ethylene vinyl acetate into multiple waxes-based feedstocks .....	83
4.6.5	Combination of stearic acid with, ethylene vinyl acetate and oleic acid into single wax-based feedstocks.....	85
4.6.6	Combination of stearic acid with, ethylene vinyl acetate and oleic acid into multiple waxes-based feedstocks.....	89
4.7	Influence of powder characteristics on viscosity of wax-based feedstocks.....	90
4.7.1	Impact of powder size on viscosity.....	90
4.7.2	Impact of powder shape on viscosity .....	95
4.8	Influence of binder on viscosity and slopes of the viscosity profiles .....	98
	CONCLUSION.....	101
	RECOMMENDATIONS .....	103
	APPEDIX I .....	105
	APPENDIX II .....	111
	REFERENCES .....	113

## **LIST OF TABLES**

	Page
Table 1.1	Comparison between LPIM & HPIM process (G Lamarre 2016).....
Table 1.2	Typical feedstocks used in HPIM and LPIM.....
Table 3.1	The list of binders used in our experimental study.....
Table 3.2	Binder constituents categories used in this study. ....
Table 4.1	Quantification of the repeatability of the viscosity profiles .....



## LIST OF FIGURES

	Page	
Figure 1.1	Typical MIM process (González-Gutiérrez, Stringari et al. 2012). ....	4
Figure 1.2	The main variants of the PIM process.....	5
Figure 1.3	Schematic view of LPIM injection press system with parts (Lamarre, Demers et al. 2017). .....	8
Figure 1.4	Different debinding cycles using (a) solvent extraction.....	9
Figure 1.5	Residual backbone polymer after solvent debinding.....	10
Figure 1.6	Debinding using an inert powder bed.....	11
Figure 1.7	Densification process, microstructure evolution in PIM sintering involves the.....	12
Figure 1.8	Morphology of metal powders (a) gas atomized powder.....	13
Figure 1.9	SEM of 17-4PH powders (a) the coarsest – about 20 $\mu\text{m}$ mean diameter,.....	14
Figure 1.10	Scanning electron micrographs of (a) agglomerated tungsten powder, (b) non- .....	15
Figure 1.11	Influence of solid loading on: (a) density and (b) viscosity .....	16
Figure 1.12	Influence of particle shape on: (a) density and.....	16
Figure 1.13	Diagram of viscosity concept.....	19
Figure 1.14	Viscosity of gas-atomized Inconel 718 superalloy powder with paraffin wax-based: (a) only paraffin wax, (b) with stearic acid) (Demers, Turenne et al. 2015).....	21
Figure 1.15	Viscosity profiles for feedstocks formulated from Inconel 718 .....	21
Figure 1.16	Viscosity profiles of (stainless steel 316L- .....	22
Figure 1.17	Viscosity as a function of shear rate for 50 vol. % of .....	23
Figure 1.18	Relative viscosity vs Small particle content for .....	24
Figure 1.19	Viscosity measurements for different particle size of 316L.....	25

Figure 1.20	Effect of particle shape on viscosity, adapted .....	26
Figure 1.21	Maximum solids loading for different shapes of.....	27
Figure 1.22	Dependence of feedstock viscosity on shear rate (Fareh and Demers 2016).....	29
Figure 1.23	Viscosity of feedstocks as a function of temperature .....	30
Figure 1.24	Correlation of viscosity and temperature for feedstocks .....	31
Figure 1.25	The shear viscosity dependence with shear rate for different .....	32
Figure 1.26	Relative viscosity versus volume fraction of solids .....	33
Figure 1.27	General moldability index vs. solid loading vol.% .....	35
Figure 1.28	Mold design and injected specimen: (a) rectangular dog bone shape,.....	36
Figure 1.29	Feedstock injected length: (a) Spiral flow lengths, adapted from ref.....	37
Figure 1.30	Comparison of the injected length and moldability index of feedstocks .....	38
Figure 3.1	SEM micrograph of 17-4 PH stainless steel powders (a) 12 $\mu\text{m}$ water.....	42
Figure 3.2	Appearance of the binders used in our study at room temperature. ....	43
Figure 3.3	Chemical formula of stearic acid (SA) and oleic acid (OA). ....	44
Figure 3.4	Differential scanning calorimeter (DSC).....	47
Figure 3.5	DSC results for binder constituents .....	48
Figure 3.6	DSC results for binder constituents (heating). .....	49
Figure 3.7	Anton Paar rotational rheometer and the method used. ....	50
Figure 3.8	Main test steps to perform tests using the rotational rheometer.....	51
Figure 3.9	Diagram for calculation viscosity and flow behavior index.....	53
Figure 4.1	DSC results for binder constituents .....	56
Figure 4.2	Viscosity profiles of feedstocks at different waiting time conditions. ....	58
Figure 4.3	Viscosity profiles of feedstocks in different test samples. ....	60

Figure 4.4	Viscosity profiles obtained with different single waxes-based feedstocks .....	61
Figure 4.5	Viscosity profiles obtained with different wax-stearic acid .....	64
Figure 4.6	Viscosity profiles obtained with different wax-based .....	68
Figure 4.7	Viscosity profiles obtained with paraffin wax-based feedstocks: (a) paraffin wax + stearic acid (PW-SA), and (b) paraffin wax + oleic acid (PW-OA). ....	71
Figure 4.8	Viscosity profiles obtained with different wax-based feedstocks: .....	73
Figure 4.9	Viscosity profiles obtained with different wax-based feedstocks: .....	76
Figure 4.10	Viscosity profiles obtained with different wax-based feedstocks: .....	80
Figure 4.11	Viscosity profiles obtained with paraffin wax-based feedstocks: (a) paraffin wax + stearic acid + Ethylene vinyl acetate (PW-SA-EVA) and (b) paraffin wax + stearic acid + low-density polyethylene (PW-SA-LDPE). ....	83
Figure 4.12	Viscosity profiles obtained with different multi waxes-based feedstocks: .....	85
Figure 4.13	Viscosity profiles obtained with different wax-based feedstocks: .....	87
Figure 4.14	Influence of two surfactant agents on the viscosity.....	90
Figure 4.15	Viscosity profiles of water atomized feedstocks for powder .....	93
Figure 4.16	Viscosity profiles of representative water atomized and gas atomized powder feedstocks (for same powder size of 12 $\mu\text{m}$ ).....	96
Figure 4.17	Flow behavior index according to feedstock formulations. ....	99
Figure 4.18	Evolution of the viscosity according feedstock formulations. ....	100



## **LIST OF ABREVIATIONS**

BW	Beeswax
CW	Carnauba wax
CIM	Ceramic injection molding
DSC	Differential Scanning Calorimetry
EVA	Ethylene–vinyl acetate
LDPE	Low-density polyethylene
LPIM	Low-pressure injection molding
MIM	Metal injection molding
MW1	Microcrystalline wax #1
MW2	Microcrystalline wax #2
OA	Oleic acid
PIM	Powder injection molding
PW	Paraffin wax
SA	Stearic acid
SEM	Scanning electron microscope
vol. %	Volume fraction



## LIST OF SYMBOLS

$n$	Power law index (-)
$K$	Constant (-)
$\eta$	Viscosity (Pa·s)
$R$	Gas constant (J·kg <sup>-1</sup> ·K <sup>-1</sup> )
$E$	Activation energy (J/mol)
$T$	Temperature
$\eta_o$	Viscosity at reference temperature (Pa·s)
$\dot{\gamma}$	Shear rate (s <sup>-1</sup> )
$\phi_m$	Maximum solid loading (%)
$\phi$	Solid loading (%)
$\eta_b$	Binder viscosity (Pa·s)
$\alpha_{STV}$	Moldability



## INTRODUCTION

In order to obtain a small complex shape part, the only manufacturing manner is probably casting. However, this technique may results in parts with low mechanical properties. Low-pressure metal injection molding (LPIM) is a relatively new technique, which gives the opportunity to produce the high shape complexity with high mechanical properties. LPIM technology takes advantage of feedstocks at low-viscosity to achieve high moldability at low-pressure, subsequently, more complex shape parts are manufactured. The low pressure required during injection is an opportunity to reduce the capacity of the injection press as well as the size of the tooling, therefore generating significant cost reductions compared to conventional high-pressure injection molding. This rapid fabricating process consists in mixing metallic powder with molten polymeric binder to obtain a feedstock, which is injected into a mold cavity to generate a complex shape. During debinding and sintering treatments, the binder is completely removed to obtain a near-net shape dense metallic component. Rheological behavior of powder-binder mixture has a direct impact on the successful mold filling for parts obtained from powder injection molding. Feedstock should be generally designed to minimize segregation, maximize flowability, maximize the strength of the molded component, maximize the solid loading potential and ease of debinding in order to minimize defects at all phases of manufacturing.

Assessing the full potential of the LPIM technique is still limited by a poor understanding of rheological behavior of feedstock. So far, there is no tool to predict the moldability of LPIM metallic feedstocks. This tool does not exist because of the lack of understanding on the feedstock formulation and its impact on the moldability of feedstock. Therefore, the aim of this work is to study the impact of wax-based binder systems on the rheological properties of feedstocks to better understand and predict the moldability properties of powder-binder mixtures used in LPIM process, and to have a big database that an engineer can use it to develop of LPIM feedstocks in the future.

This study is divided into five chapters; the first chapter is a literature review, which gives an overview of what exactly is the LPIM process with basic terminology. In that chapter, each

stage of LPIM process is explained clearly. In addition, the methods that are commonly used to prepare and characterize feedstocks are described in details. The experimental techniques that can be used to characterize LPIM feedstocks are also reviewed in this first chapter. The second chapter present the problem definition and research objective. The methodology used for the present work is described chapter 3. Chapter 4 reports the analysis of results and discussions.

## CHAPITRE 1

### LITERATURE REVIEW

#### 1.1 Powder injection molding process

Powder injection molding (PIM) is a cost-effective technology for producing small and complex shape parts. This manufacturing process consists in mixing metallic or ceramic powder with molten polymeric binder to obtain a feedstock (Figure 1.1a). The latter is then injected into a mold cavity to produce parts (Figure 1.1b) that are debound (Figure 1.1c) and sintered (Figure 1.1d) to completely remove the binder and obtain near-net shape dense components (Hausnerová 2010, Hidalgo, Abajo et al. 2013). The advantages of the PIM process include high production volumes, high buy-to-fly ratio, the possibility of using a wide variety of materials (both for ceramic powders and for metallic powders) excellent mechanical properties, good surface finishes, and good geometric and dimensional tolerances of the produced part (German 1996, Huang, Liang et al. 2003). High complexity of molded parts is achieved using low-viscosity feedstocks while high mechanical property originate from the granular microstructure (i.e., grains and grain boundaries structure) derived from the solid-state sintering. PIM may also eliminate some machining operations such as threads, serrations, waffle patterns, identification numbering and insignias that can be introduced into the mold during injection.

The first injection molding machine was built in the 1930's and used for ceramic-based feedstocks (Zlatkov, Griesmayer et al. 2008). The attention for ceramic powders increased significantly in the 1970s and 1980s to meet growing demands for material strength, particularly from the aerospace industry and from the medical technologies (Mangels 1994, Quevedo Nogueira, Bezerra et al. 2001). However, new forming processes such as slip casting and hot isostatic pressing were developed at the price of additional requirement for secondary finishing operations, resulting in additional costs (Medvedovski and Peletsman 2012). During this period, the plastic injection molding process developed rapidly the technology for molding plastic at high pressure into the cavity of a mold to form complex-shaped plastic parts close to

their final dimensions. This specific technique was then adapted to accommodate mixtures containing ceramic powders and polymeric binder (i.e., ceramic-based feedstocks), or metallic powder and polymeric binder (i.e., metallic-based feedstocks) where in both cases, the polymeric binder is only used as a media for powder transportation during the injection (i.e., the binder is removed by a debinding operation latter in the process).

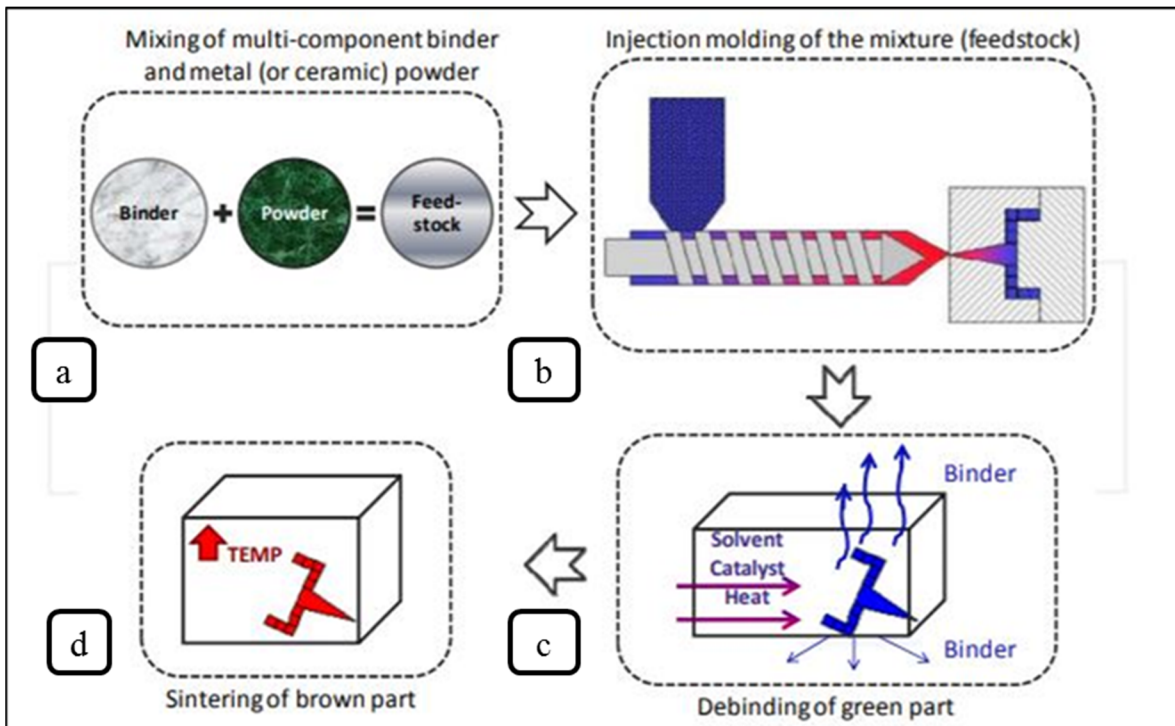


Figure 1.1 Typical MIM process (González-Gutiérrez, Stringari et al. 2012).

### 1.1.1 Comparison between LPIM & HPIM process

The PIM process presents two variations 1) high-pressure powder injection molding (HPIM) and 2) low-pressure powder injection molding (LPIM) as illustrated in Figure 1.2.

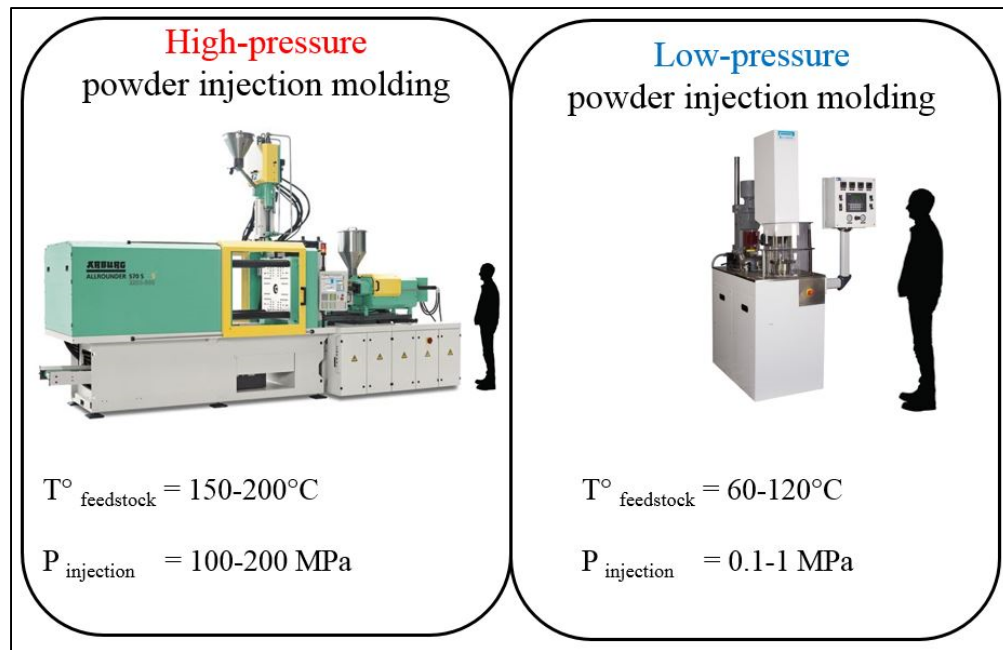


Figure 1.2 The main variants of the PIM process.

As described by their names, the main difference between these two processes originates from the pressure required during the injection operation. In the first case the high molecular weight binder used in HPIM (e.g., polyethylene, polypropylene, etc.) results in high-viscosity of the feedstock requiring an injection pressure up to 200 MPa and mold clamping forces of about 100 Tons (Fareh, Demers et al. 2016, Lamarre, Demers et al. 2017). In the second case, the low molecular weight binder used in LPIM (e.g., paraffin wax, beeswax, carnauba wax, etc.) produces a low-viscosity feedstock requiring an injection pressure generally lower than 1 MPa directly reducing the mold clamping forces (<1 Ton) and increasing the molding capabilities (Fareh, Demers et al. 2016, Lamarre, Demers et al. 2017). Therefore, LPIM demonstrates considerable processing benefits compared to the conventional HPIM technology including decrease of injection equipment size (illustrated in Figure 1.2 ) as well as decrease in tooling size directly resulting in a cost-effective technology for producing small and complex shape parts, either in high or in low production volumes (i.e., mass customization). Table 1.1 summarizes the main parameters of the two processes.

Table 1.1 Comparison between LPIM &amp; HPIM process (G Lamarre 2016).

	<b>HPIM</b>	<b>LPIM</b>
Maximum injection pressure (MPa)	200	< 0.8
Cost of tooling	High	Low
Volume of production	High only	Low and high
Viscosity of mixtures (Pa · s)	< 1000	< 10
Segregation	No	Yes

This project will focus in low-pressure powder injection molding process using low-viscosity mixtures for injection at low pressures. The emphasis will be given on the feedstock preparation and the injection stages of the LPIM process, as they are the two main points of the present work. A short description, with fewer details of the debinding and sintering stages will be also provided in this literature review.

### 1.1.2 Mixing and powder-binder formulations

During the mixing step, a fine metallic powder (with particles with a size of less than 20 µm in diameter) is mixed with a binder (usually a mixture of different polymers) to form a homogeneous mixture called feedstock (Mohamad Nor, Ismail et al. 2014). The main objective of the mixing process relies in coating the whole surface of each powder particle with binder. The powder used in HPIM and LPIM are commonly the same. The differences between these two processes are directly related to the binder used (see detail in section 1.2 below). Table 1.2, presents a list of typical binders used for each process. It can be seen from Table 1.2 that the ingredients forming the binders are almost the same. However the polymers used in HPIM technique (e.g., polypropylene (PP), high-density polyethylene (PE), polymethyl metacrylate (PMMA) and polyacetal (PA)) are not used in LPIM to reduce significantly the viscosity of the feedstock.

Table 1.2 Typical binder constituents used in HPIM and LPIM.

<b>HPIM</b>	<b>LPIM</b>
50PW-45PP-4SA	87.5PW-12.5SA
92PE-8PW	97.5PW-2.5EVA
58PMMA-24EVA-18SA	75PW-12.5SA-12.5EVA
69PW-20PP-10CW-1SA	50BW-50CW

PW: Paraffin wax; SA: Stearic acid; EVA: Ethylene–vinyl acetate; PW: Paraffin wax; CW: Carnauba wax; BW: Beeswax; PP: polypropylene; PE: high-density polyethylene; PMMA: polymethyl methacrylate.

In general, the rheological properties of feedstock depend on its powder characteristics (shape, average size, agglomeration, particle size distribution, surface texture, volume fraction, etc.) and its binder characteristics (molecular weight, solubility with other polymer, etc.) (Liu, Loh et al. 2002, Huang, Liang et al. 2003, Amin, Muhamad et al. 2014, Machaka, Ndlangamandla et al. 2018).

As mentioned above, one important parameter for feedstock is the volume fraction of powder and binder in the feedstock. If the volume percentage of the powder is high, the injection process will be difficult. On the other hand, excessive volume fraction of binders will result in high shrinkage of the final product leading in defects (Aslam, Ahmad et al. 2016). Note that the influence of these parameters will be specifically covered in the section 1.3 of this document because the main objective of this project is to characterize the rheological properties of LPIM feedstocks to better understand the role of each binder constituents on the viscosity and behavior of feedstocks during the injection stage.

### 1.1.3 Injection molding

The second stage is the molding process, where the molten feedstock is injected into the mold cavity to produce the green part (Machaka, Ndlangamandla et al. 2018). The process starts by increasing the feedstock temperature to exceed the melting point of the binder, then an injection

press forces the feedstock into the molding cavity using different injection principles represented in Figure 1.3. After the injection, the entrance point of the mold (also called the gate) is closed and the mold is opened to extract a green part. During and after injection, the characteristic of the feedstock such as temperature and pressure must be controlled to maintain suitable rheological behavior and guarantee proper mold filling.

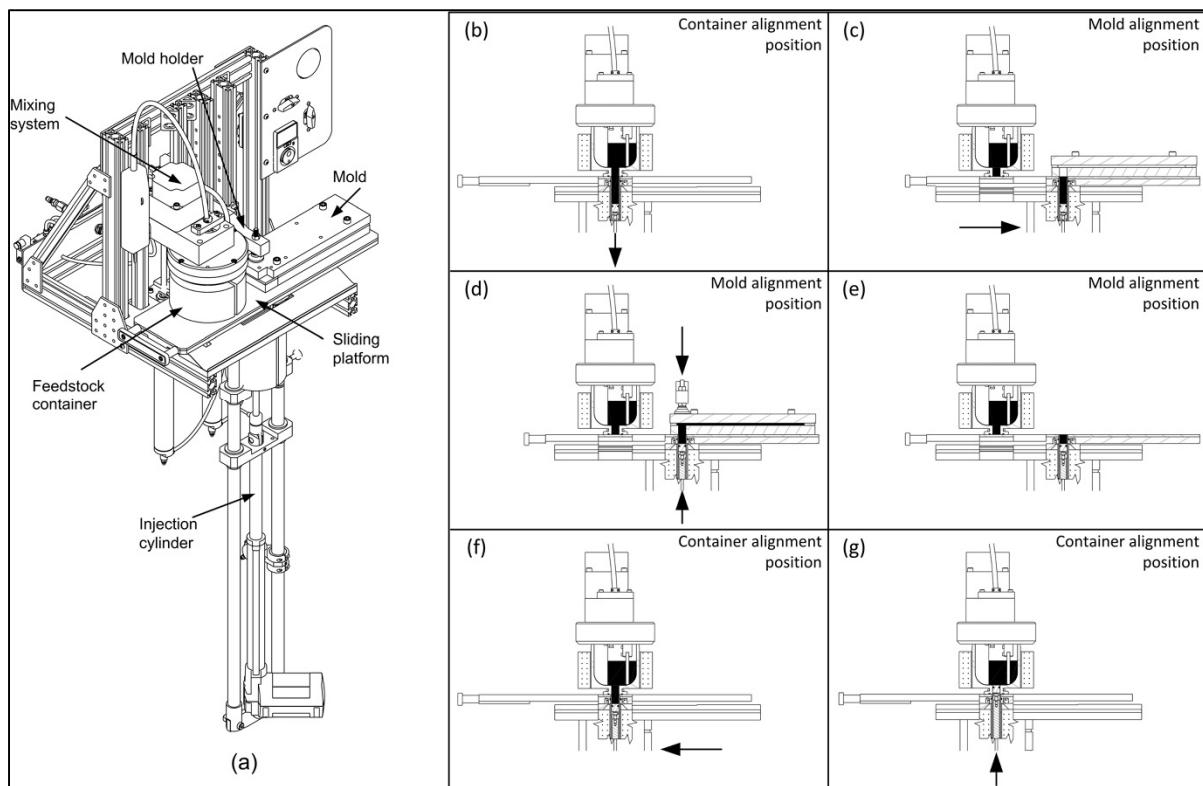


Figure 1.3 Schematic view of LPIM injection press system with parts (Lamarre, Demers et al. 2017).

#### 1.1.4 Debinding

The objective of this step is to remove partially or totally the binder from the green part. This binder removal process is usually performed by thermal decomposition or solvent extraction, which, in both cases, takes several hours as schematically represented in Figure 1.4. When the binder is removed, the component becomes fragile and should be handled with caution until sintering. Debinding rate is influenced by the particle size of the powder, packing arrangement

of the powder, viscosity of the binder, interaction between the binder components, vapor pressure of the binder, temperature, and gas pressure in the binder removal chamber. The goal in debinding is to remove the binder in the shortest time with the least defects on the component, such as pores, cracks, laminations, pinholes, etc.

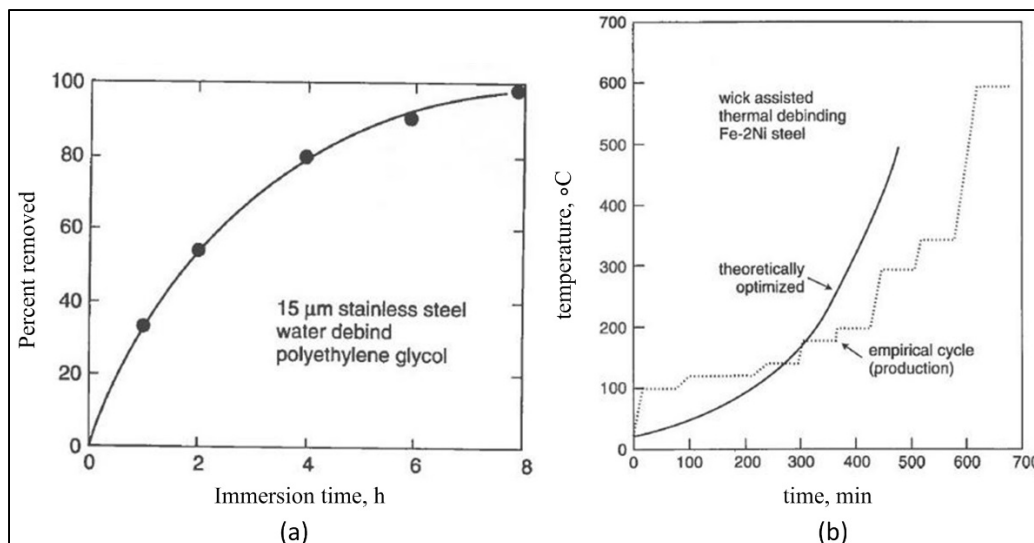


Figure 1.4 Different debinding cycles using (a) solvent extraction and (b) thermal extraction (German 1997).

For HPIM process, the binder is usually removed in two steps (Torralba, Ruiz-Román et al. 1997, Gonçalves 2001). First, low-molecular weight constituents (such as wax and other component that can be dissolved in water or chemical solvent) are removed from the bulk by either solvent extraction, direct sublimation, or evaporation. At that stage, the residual binder (consisting of high-molecular weight polymer such as PE, PP, etc.) acts as a backbone to maintain the shape of the debound component as shown in Figure 1.5. This residual binder (5-10% of the initial total binder) is then removed at the early stage of the sintering cycle (Kowalski 2005).

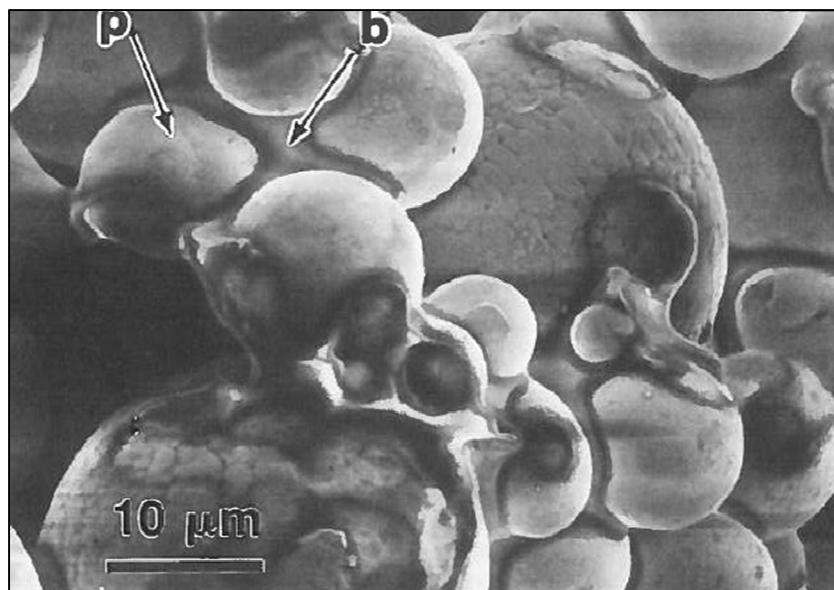


Figure 1.5 Residual backbone polymer after solvent debinding  
(HPIM process only) (German 1997).

For LPIM process, the binder is usually removed in one-step (Rei, Milke et al. 2002). Green component is embedded into inert powder (e.g., alumina powder), and all binder are removed by wicking during the thermal debinding at low temperature for long period (e.g., 250°C during 20 hours, as represented in Figure 1.6). Then pre-sintered at high temperature (e.g. 0.9 T<sub>m</sub>) is performed using the same debinding setup to maintain the shape and to provide some strength to the parts in order to facilitate handling up to the sintering stage.

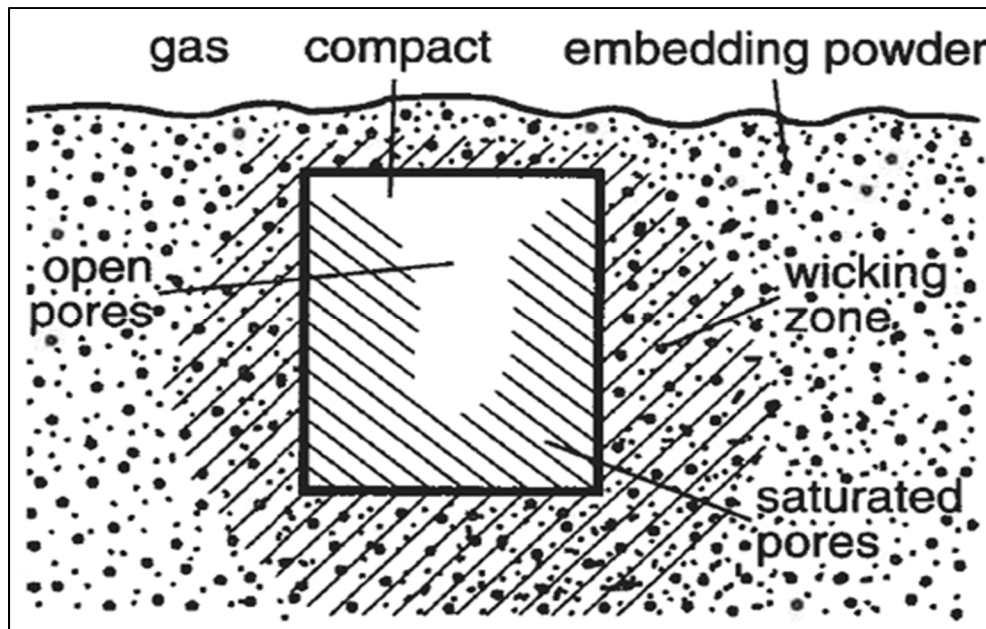


Figure 1.6 Debinding using an inert powder bed (Germanand Bose 1997).

### 1.1.5 Sintering

Sintering is the last step in the PIM process (HPIPM and LPIM use essentially the same process), where the debound part reaches the final density ( $> 95\%$  of the theoretical density). Sintering is a solid-state bonding process. During sintering the debound parts (metallic or ceramic) at a temperature close, but not exceeding, the melting point of the material, in order to promote the diffusion of the atoms between the powder particles. This step can last from few hours to several dozen hours (Gonçalves 2001, Kowalski 2005, AN 2012). As schematically represented in Figure 1.7, sintering eliminates the vacancies between loose-powders to form a dense component where the macroscopic shrinkage may reach several % varying typically between 10 and 25 compared to the initial dimensions of the green part. As the densification process occurs, the interstitial voids within debound part shrink in size and decrease in number. Generally speaking, complete densification does not occur following conventional sintering cycle, (i.e. density of 99% can be reached) while full densification can be achieved using a post-sintering cycle such as hot isostatic pressing (HIP) with the majority of the materials (Kowalski 2005).

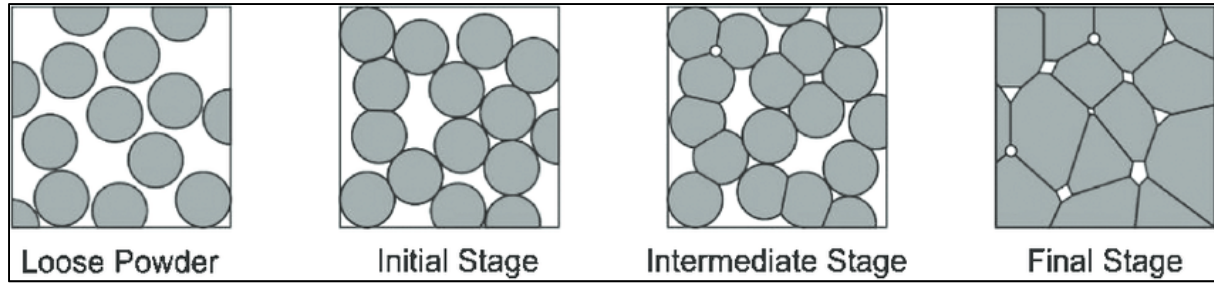


Figure 1.7 Densification process, microstructure evolution in PIM sintering involves the initial bonding of the particles, followed by pore rounding and grain growth by final stage (German and Bose 1997).

## 1.2 Feedstock constituents used in LPIM

This section reviews specific details about the two-feedstock constituents used in low-pressure metal injection molding (LPIM) process, which are metallic powders and binders. Properties of feedstocks are generally attributed to the powder and binders characteristics such as powder composition / properties and binder constituent to meet the higher solid loading with higher flowability.

### 1.2.1 Metallic powders

Stainless steel, iron, iron-nickel, nickel-based superalloys, cobalt-based superalloys, tool steel, titanium, titanium alloys, and copper are the powders that are most commonly used for the LPIM process (German and Bose 1997, Demers, Turenne et al. 2015, G Lamarre 2016, Lamarre, Demers et al. 2016, Demers V. 2017, Lamarre, Demers et al. 2017, Demers, Fareh et al. 2018, Machaka, Ndlangamandla et al. 2018). Attributes of a powder are the chemical composition, average particle size, particle size distribution, particle shape, interparticle friction and agglomeration (German 1990). The particle shape is directly related to the method of powder fabrication, including gas atomization, water atomization, plasma atomization, milling, and electrochemical treatment. As illustrated in Figure 1.8, gas atomization produces spherical particles while water atomization yields irregular particles, otherwise, electrochemical methods gives spongy particles of irregular contour (Park, Wu et al. 2009, AN

2012). The spherical particles improve the bulk density and reduce the viscosity of the mixtures, but produce parts, which are more brittle after debinding. Conversely, the irregular shape increases resistance after debinding, but exhibit higher viscosity leading to a decrease in the injection capability (Gonçalves 2001).

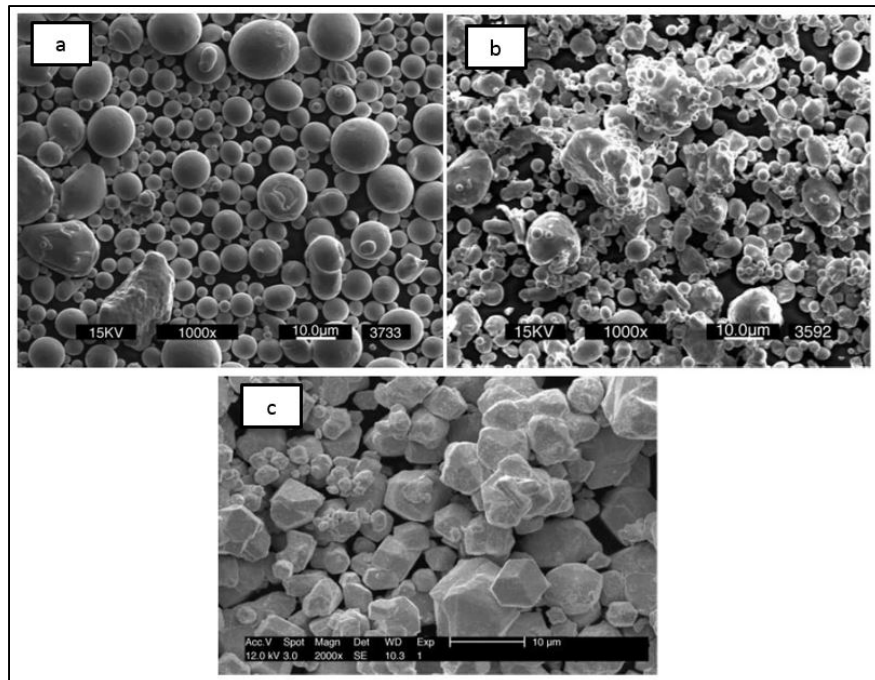


Figure 1.8 Morphology of metal powders (a) gas atomized powder stainless steel powder, (b) water atomized powder stainless steelpowder, and (c) a chemically reduced tungsten powder (AN 2012).

The average size of non-agglomerated particles as well as particles size distribution vary according to the chemical composition of the raw material and powder fabrication method, but finally are tailored by sieving operation to obtain an average particle size ( $d_{50}$ ) varying between 5 and 20  $\mu\text{m}$ , as illustrated in Figure 1.9. There are some antagonistic effects linked with the particles size: small particle sizes increase viscosity during molding due to their high surface area, but in counterpart increase the density during sintering due to its higher surface area; and vice versa for large particles. In addition, specific phenomenon such as formation of

agglomerations (represented in Figure 1.10) also increase with the decrease in particle size resulting in further increase in feedstock viscosity and leading to a decrease in moldability.

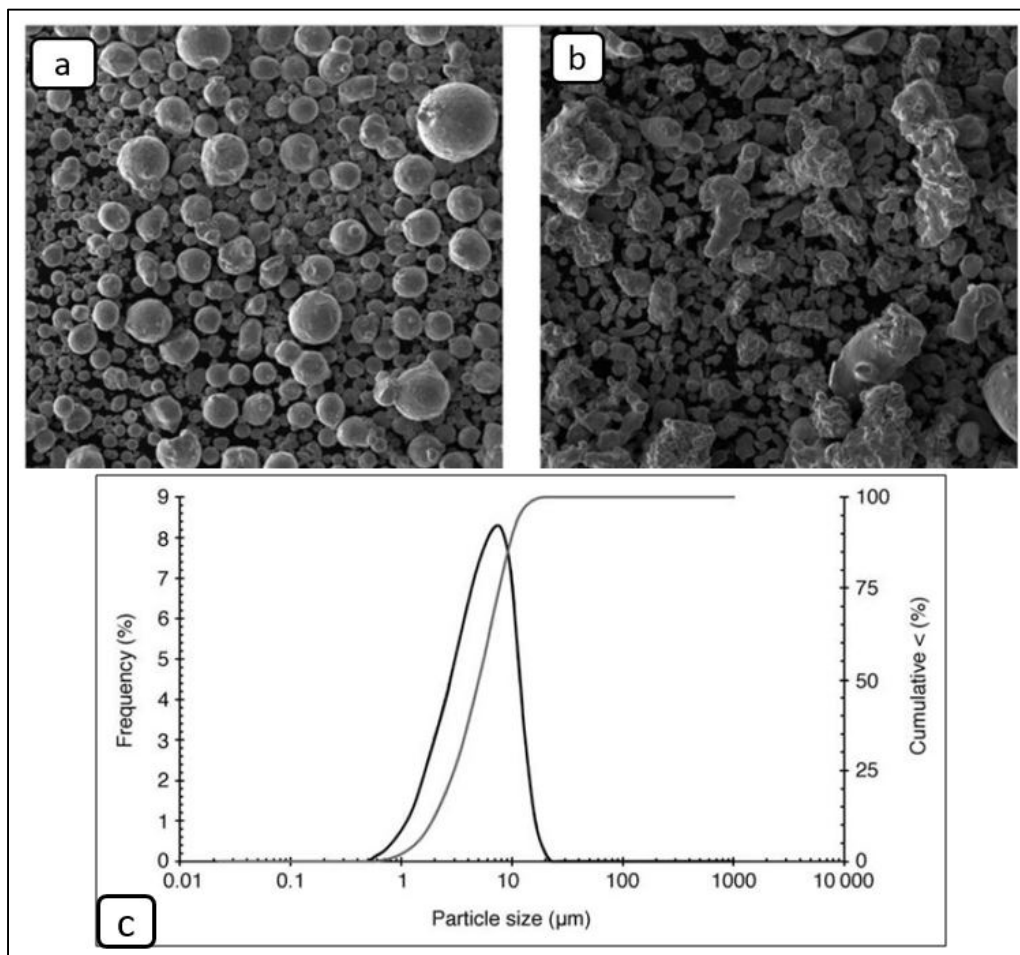


Figure 1.9 SEM of 17-4PH powders (a) the coarsest – about 20  $\mu\text{m}$  mean diameter,(b) The finest – about 3  $\mu\text{m}$  mean diameter and (c) A typical MIM powder particle size distribution (PSD) (AN 2012, Hausnerova, Mukund et al. 2017).

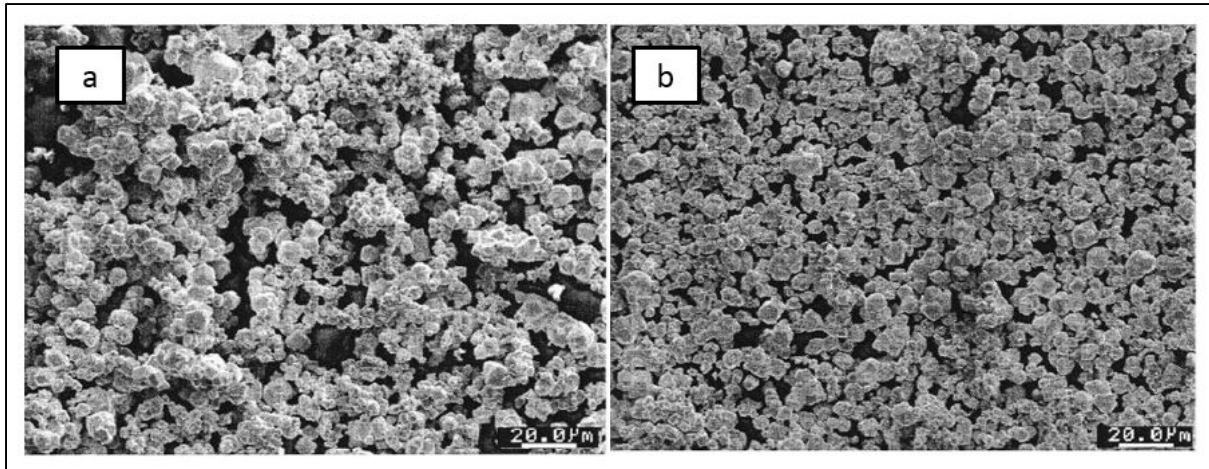


Figure 1.10 Scanning electron micrographs of (a) agglomerated tungsten powder, (b) non-agglomerated tungsten powder (Suri, Atre et al. 2003).

The volume fraction of powders (also called solid loading) is also an important attribute for LPIM feedstock representing the volumetric ratio between powder and binder. If the solid loading is too low, the viscosity of feedstock will be positively low (i.e., easy to inject), but the part will not retain its shape during the debinding operation due to the very low or absence of contact between particles. However, a too high solid loading may produce formation of voids in the mixture accompanied by a very high viscosity (i.e., sometime too high to be injected) due to high interparticle friction between powders. Therefore, an ideal solid loading is a value slightly below the critical solid loading (i.e., about 2 to 5% below the composition where the particles are packed together, as presented in Figure 1.11) to benefit both the moldability and sintering potential (Hidalgo, Jiménez-Morales et al. 2012). According to German and Bose (1997) (German and Bose 1997), the volume proportion of the powder is generally between 50 and 70 vol. % of powder. A proportion less than 50 vol. % is detrimental due to the low density of the part (weak contact between the powder particles), while a solid loading higher than 70% makes it difficult (or simply not possible) for the injection simply due to the too high viscosity.

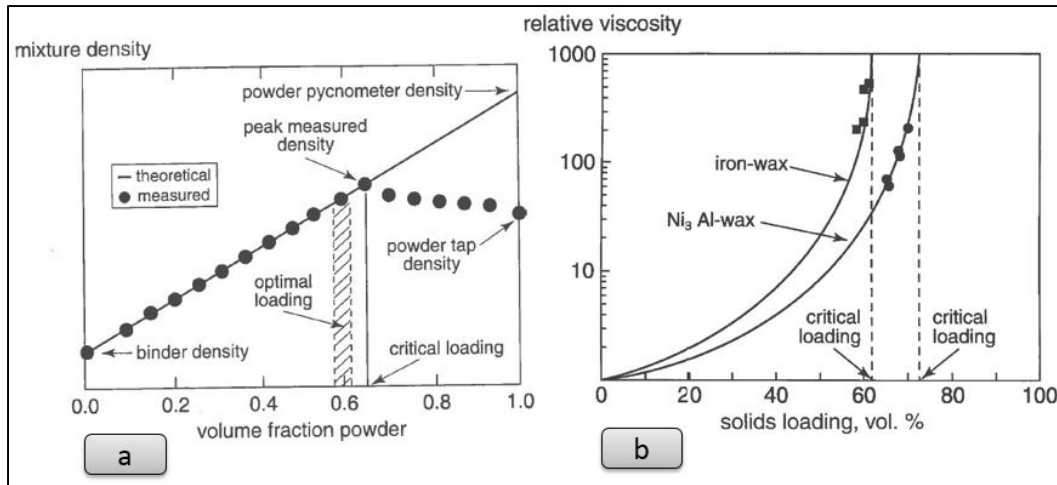


Figure 1.11 Influence of solid loading on: (a) density and (b) viscosity (German 1997).

Particle shape is normally studied using scanning electron microscope while sphericity can be used to quantify the roundness for a powder lot. In general, a spherical powder shape is suitable in PIM since higher packing and lower viscosity can be reached with spherical particles when compared to irregular shaped particles (see Figure 1.12). In addition, powders with wide size-distributions are favored due to their higher packing potential compared to mono-sized powders. Thus, the better powders are round and wide size-distributed.

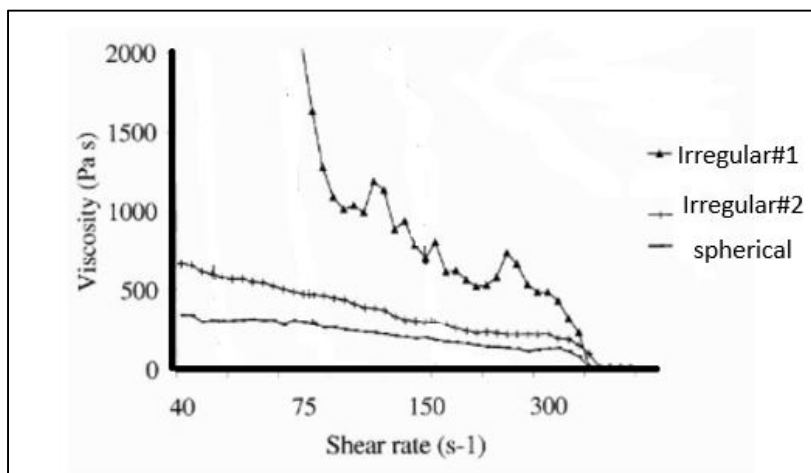


Figure 1.12 Influence of particle shape on: (a) density and (b) viscosity, adapted from ref. (Dihoru, Smith et al. 2000).

### 1.2.2 Binders

Binders play an important role in the success of LPIM process. During the injection process, the two functions of the binder are to first transport the powder into the mold cavity when the binder is in the liquid phase, and second to bond the powder particles to each other and maintain the shape after the injection when the binder is in the solid phase up to the debinding step (Vervoort, Vetter et al. 1996). Even though, the binder acts as a temporary vehicle to support metal powder especially during mixing and injection molding, it also plays an important role in the whole LPIM process by controlling the flowability of the feedstocks and the segregation of powder during and after injection, (segregation refers to the inhomogeneous distribution of powder particles in feedstocks) (German 1990, Schlechtriemen, Knitter et al. 2013, Kukla, Duretek et al. 2016).

As stated above, the main difference between binder system for HPIM and LPIM resides in the absence of backbone polymer for LPIM (e.g., HDPE, PP, PS, PVC, etc.), while the other type of binders constituents are present to meet the attributes link with flow characteristics, powder interaction, debinding, and other manufacturing consideration. The main constituent for LPIM feedstocks is wax-based binder, which are formed from one or more natural waxes or synthetic waxes (e.g., paraffin wax, beeswax, microcrystalline wax, carnauba wax, oxidized polyethylene waxes, montan wax, whale wax, wool wax, Candelilla wax, Japan wax, ouricury wax, sugar cane wax, ozokerite wax, ceresin wax and lignite wax) (Nishimura and Yoshino 1995, Adames 2007). Initially used in LPIM, wax-based binder systems have been used in ceramics to facilitate the debinding process; because of these kinds of binders are easy to eliminate. Zorzi et al. (Zorzi, Perottoni et al. 2003) demonstrated the potential of paraffin wax formulations to produce free of defect sintered alumina bodies with large cross-section and 98.5% of the theoretical density. The secondary binder constituent in LPIM feedstock is surfactant agent (e.g., oleic acid, peanut oil, fish oil, zinc stearate, etc.) which is added to the main binder formulations to increase the powder-binder interaction, promote the homogeneity of the feedstock, and decrease the viscosity of the feedstocks (German, Hens et al. 1991, Binet, Heaney et al. 2005, Hausnerová, Marcaníková et al. 2011, Demers, Turenne et al. 2015). The third binder constituent is a thickening agent (e.g., ethylene vinyl acetate (EVA) and low-

density polyethylene) used to increase the viscosity of feedstocks in order to prevent powder-binder separation.

In summary, LPIM binders typically include waxes, surfactant agent, and thickening agents used to improve homogeneity of powder-binder mixture, flowability of the feedstock, stability of the rheological properties over the time, mechanical properties of the green part, and minimize the debinding time as well as the interaction with the powder (Hens and German 1993, Suri, Atre et al. 2003, Liang 2004, Qu, Gao et al. 2004). Although several recipes exist for HPIM process and few recipes for LPIM, the influence of each binder constituent is not well understood in literature for LPIM feedstocks.

### 1.3 Rheological behavior of LPIM feedstocks

Rheological behavior of powder-binder mixture has a direct impact on the successful mold filling for parts obtained from powder injection molding. The feedstock viscosity is one of the most important rheological parameters influencing the success of the molding stage as identified by many researchers (Huang, Liang et al. 2003, Khakbiz, Simchi et al. 2005, Demers, Turenne et al. 2015, Fareh, Demers et al. 2016, Machaka, Ndlangamandla et al. 2018). The viscosity evaluates the resistance to flow of a certain fluid. Figure 1.13 presents the main factors that can help us to define viscosity. Suppose a fluid is contained between two plates and is sheared by the movement of the upper plate. The stress needed to shear this fluid is defined as F/A and the shear rate is defined as a velocity gradient at which one layer of fluid passes over an adjacent layer ( $\frac{dv_x}{dy}$ ).

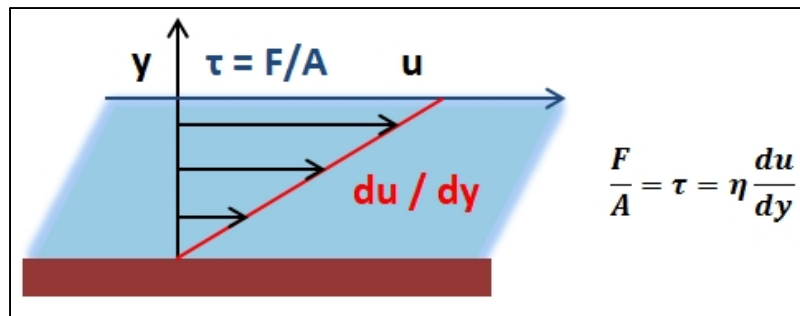


Figure 1.13 Diagram of viscosity concept.

According to Newton's law, the shear stress is linked to the shear rate in this simple case of the flow behavior by an equation:

$$\tau = \frac{F}{A} = \eta \frac{du_x}{dy} = -\eta \dot{\gamma} = -\eta \frac{u}{d} \quad (1.1)$$

Where ( $\tau$ ) is the shear stress, ( $\dot{\gamma}$ ) shear rate, ( $\eta$ ) viscosity of the fluid, ( $F$ ) force applied to the movable plate, ( $A$ ) area of the moving plate, ( $u_x$ ) velocity of the fluid at the specific position between the movable and fixed wall, ( $u$ ) velocity of the fluid in contact with the movable plate, and ( $d$ ) distance between the movable plate and the fixed wall.

The main variables influencing the viscosity of powder-binder mixtures are shear rate, temperature, solid loading, powder characteristics (shape and size), and binder composition (Liu, Loh et al. 2002, Rei, Milke et al. 2002, Sri Yulis, Khairur Rijal et al. 2009, Kukla, Duretek et al. 2016). This section summarizes the influence of each of these parameters specifically on melt viscosity of LPIM feedstocks.

### 1.3.1 Influence of binder constituents on viscosity

The viscosity of wax-based feedstocks generally decreases with shear rate, i.e. presents a shear thinning behavior (also called pseudoplastic effect) generally required for LPIM feedstocks between the mixing state (i.e., low shear rate) and the injection condition (i.e., high shear rate) as shown in Figure 1.14a (Demers, Turenne et al. 2015, Lamarre, Demers et al. 2017, Demers, Fareh et al. 2018).

As mentioned before, the low-viscosity binder constituents generally used in LPIM to tailor the properties of feedstocks are waxes, surfactant, and thickening agents. Surfactant agent has significant effects for improving the flow properties of LPIM feedstock by acting as a bridge between the metallic powder and the other binder constituents to enhance the homogeneity of the feedstock as well as the mixing properties. Thickening agent is generally used to increase the viscosity of the feedstock in order to prevent powder-binder separation and increase the strength of the green parts.

According to Li, et al. (Li, Liu et al. 2007), the content of stearic acid has an optimal value around 5 vol.% while the effect for improving the property of the feedstock is limited even when excessive surfactant is added. In this respect, Demers et al. (Demers, Turenne et al. 2015) established that an addition of only 1 vol.% of this surfactant agent into paraffin wax-based feedstock generates an important decrease in viscosity, and further increases of this constituent induce no effect on rheological behavior (see Figure 1.14b). Thus, the viscosity profile of paraffin wax-stearic acid group feedstock is characterized by a viscosity plateau at low shear rates, followed by a pseudoplastic behavior, and finally, a dilatant behavior, at high shear rates (seen on Figure 1.14b at shear rate  $> 400 \text{ s}^{-1}$ ) (Demers, Turenne et al. 2015, Demers, Fareh et al. 2018). More recently, Demers, et al. (2018) (Demers, Fareh et al. 2018) demonstrated that at least 5–10 vol.% of ethylene vinyl acetate should be added to paraffin wax to produce a thickening effect of the feedstock. However, these kinds of feedstocks exhibit, a near-Newtonian behavior with relatively high values of the viscosity on the entire shear rate range, as presented in Figure 1.15. In this respect, Figure 1.15 also shows that an addition of a small quantity of ethylene vinyl acetate (see the feedstock 39PW-1EVA) produces a significant decrease in viscosity values over the shear rate range, which is an unexpected result because the main objective of adding this constituent into paraffin wax is to increase the viscosity.

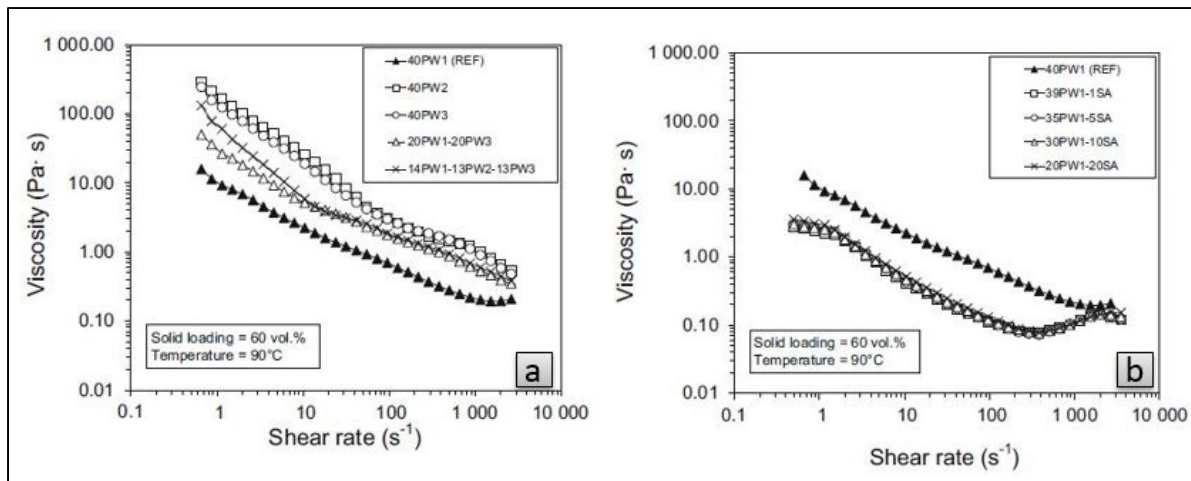


Figure 1.14 Viscosity of gas-atomized Inconel 718 superalloy powder with paraffin wax-based: (a) only paraffin wax, (b) with stearic acid) (Demers, Turenne et al. 2015).

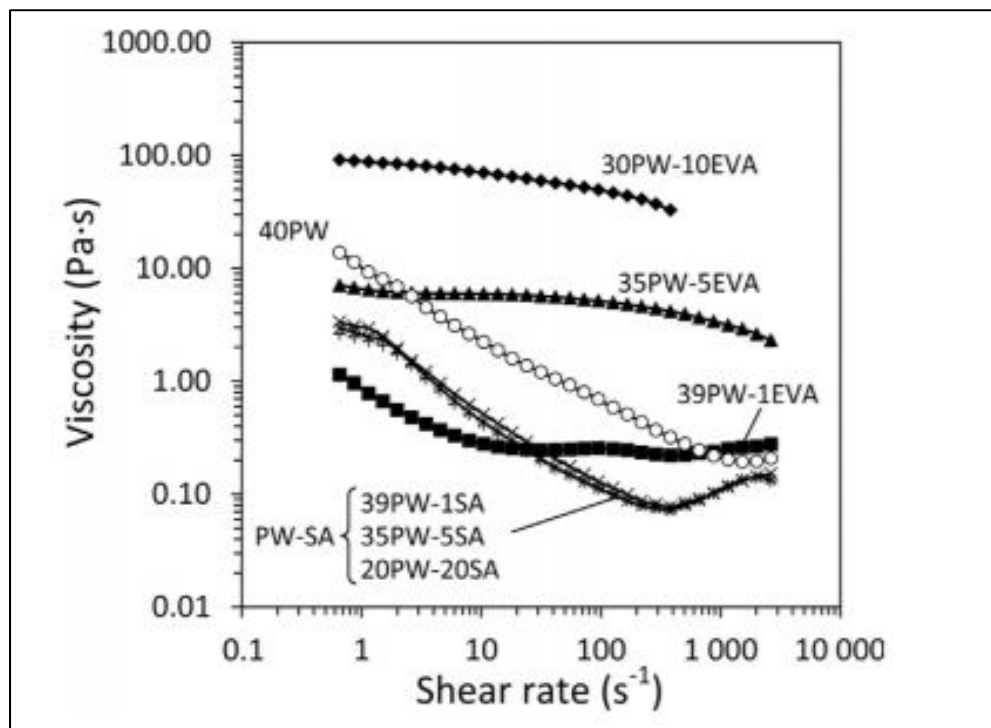


Figure 1.15 Viscosity profiles for feedstocks formulated from Inconel 718 superalloy powder with paraffin wax (PW) + surfactant agent (SA) + thickening agent (EVA) (Demers, Fareh et al. 2018).

In addition, Lamarre, et al (Lamarre, Demers et al. 2017) studied the impact of these three binder constituents on the rheological properties. The flow behavior of this kind of feedstock presented in Figure 1.16, (e.g., 30PW-5SA-5EVA) is characterized by a pseudoplastic behavior until a shear rate of  $100 \text{ s}^{-1}$  following with a near-Newtonian plateau, while presenting a comparatively high viscosity value over the rest of the high shear rate range.

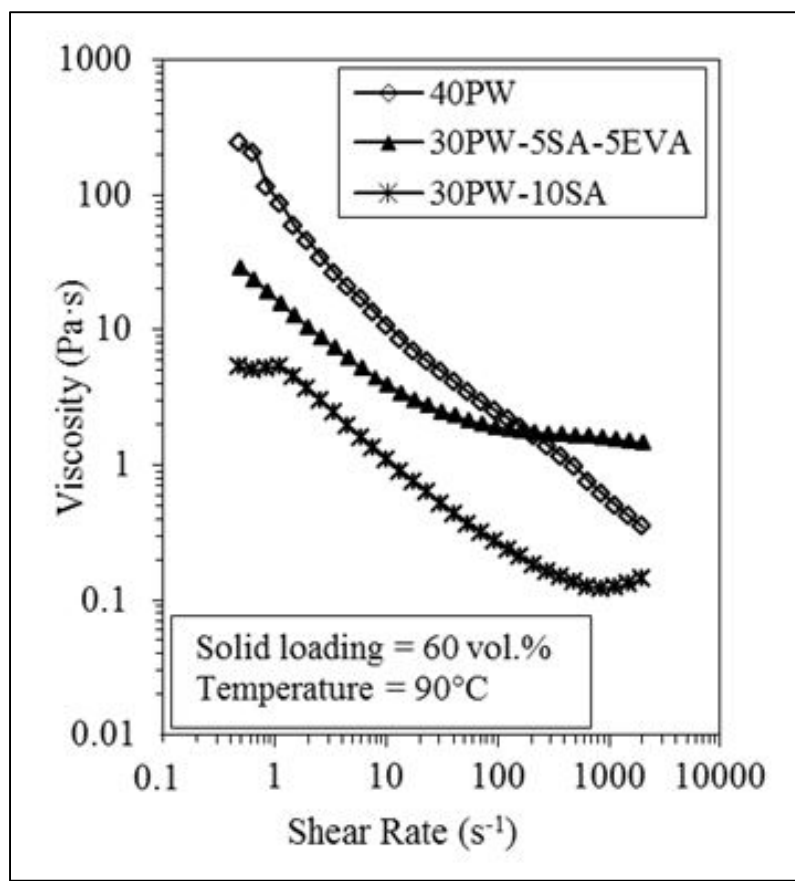


Figure 1.16 Viscosity profiles of (stainless steel 316L-wax-based binder) feedstocks (Lamarre, Demers et al. 2016).

### 1.3.2 Influence of particle size on viscosity

Typically, particle size distribution for LPIM technology varies between 0.1 and 20  $\mu\text{m}$ , with a  $d_{50}$  of about 10-12  $\mu\text{m}$  to produce a trade-off between injection and sintering properties (German and Bose 1997). For a given solid loading, small particle size results in a higher

feedstock viscosity since it has higher surface area and interparticle friction as shown in Figure 1.17. However, broad distributions where small particles fill the interparticle voids produce a suitable impact on viscosity. In this respect, German (AN 2012), highlighted that a mixture having a particle size ratio of small particles of 21  $\mu\text{m}$  (i.e. 21 vol.% of the total amount of powder) produces a 24-fold decrease in the viscosity value as shown in Figure 1.18. This approach finally shows that it is possible to increase solid loading and decrease the viscosity of feedstock at the same time by using a proper powder size distribution. In this respect, the conclusions drawn by Honek, et al. (Honek, Hausnerová et al. 2005), also shown that a higher value of the maximum powder loading can be obtained with a widest particle sizes distribution, whereas the lowest value is attained for powder with a high fraction of small particles.

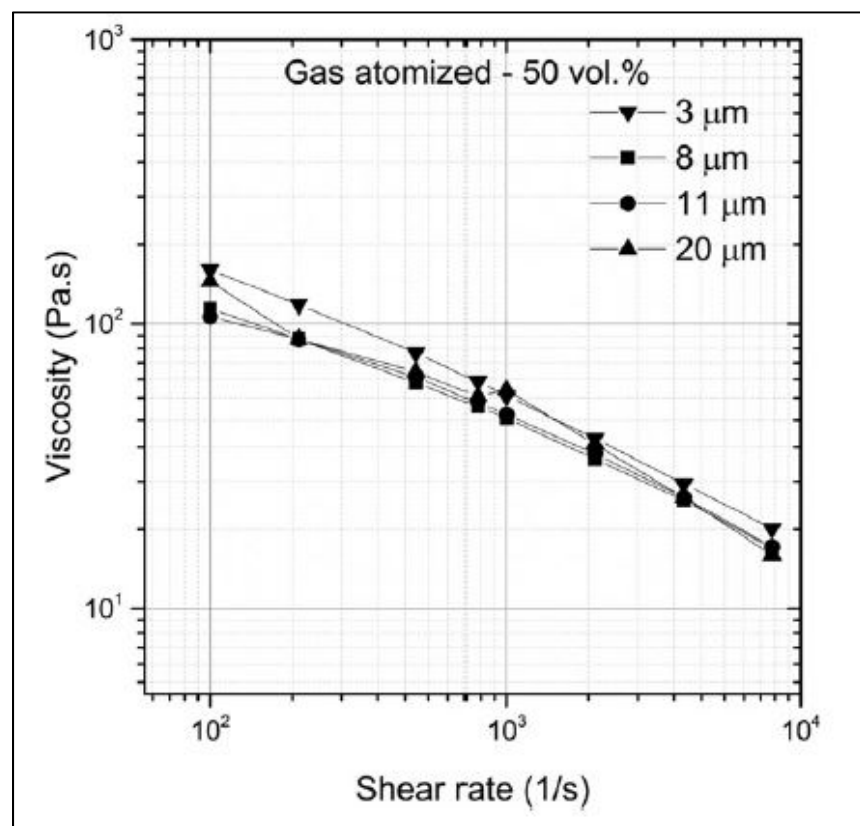


Figure 1.17 Viscosity as a function of shear rate for 50 vol. % of gas atomized feedstocks, the viscosity increases with a decrease in particle size (Hausnerova, Mukund et al. 2017).

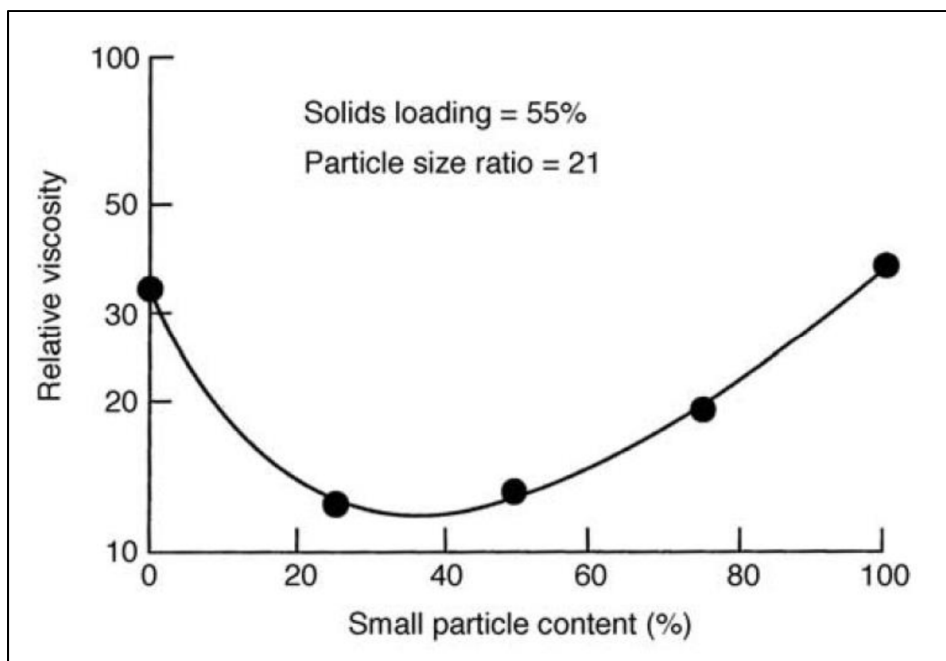


Figure 1.18 Relative viscosity vs Small particle content for a specific particle shape (AN 2012).

Likewise, Sotomayor, et al. (Sotomayor, Várez et al. 2010) have elucidated that viscosity of feedstocks decreases with an increase in shear rate where the flow behavior becomes more pseudoplastic for finer particle size (see Figure 1.19).

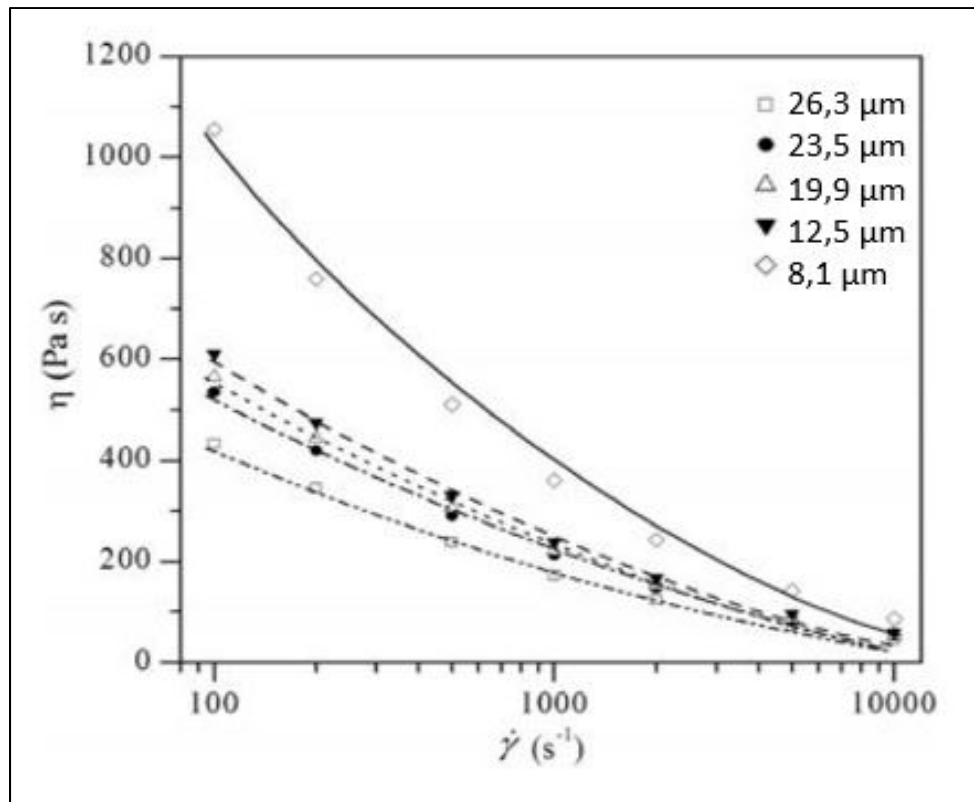


Figure 1.19 Viscosity measurements for different particle size of 316L stainless steels feedstocks at fixed loading, adapted from ref. (Sotomayor, Várez et al. 2010).

In summary, there is an antagonistic effect to define an ideal powder particle size where small particles reduce molding defects, decrease the speed of debinding, and promote a faster sintering, but in counterpart those small particles increase feedstock viscosity, sintering shrinkage and agglomeration(Honek, Hausnerová et al. 2005). Therefore, an ideal powder lot should combine large and small particles in a tailored particle size distribution, providing simultaneously high packing, and appropriate viscosity during molding (German and Bose 1997).

### 1.3.3 Influence of particle shape on viscosity

The particle shape also has an impact on the feedstock viscosity, as irregular shaped particle would exhibit higher interparticle friction and low packing density, resulting in feedstocks with higher viscosity, as illustrated in Figure 1.20. Although there was an opposite effect shown in this figure for the fine irregular particles (3 and 8  $\mu\text{m}$ ), but this impact was accepted for the effect of particle shape on flow behavior of powder-binder mixtures.

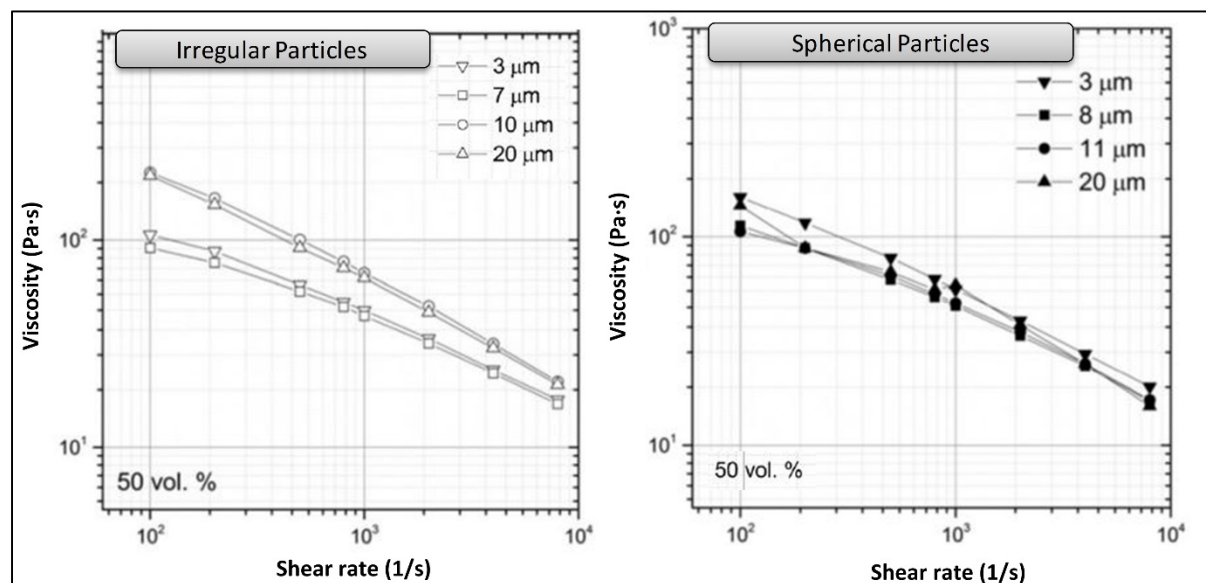


Figure 1.20 Effect of particle shape on viscosity, adapted from ref.  
(Hausnerova, Mukund et al. 2017).

Optimal particle flowability is achieved by using spherical particle powders for their better flowability and low interparticle friction. Therefore, the critical solid loading for spherical particle is higher than that achievable by any other shape. The influence of different particle shape on the relative viscosity of feedstock according to the solid loading is presented in Figure 1.21, where it is evident that the spherical shape powder produces the best flowability attributes.

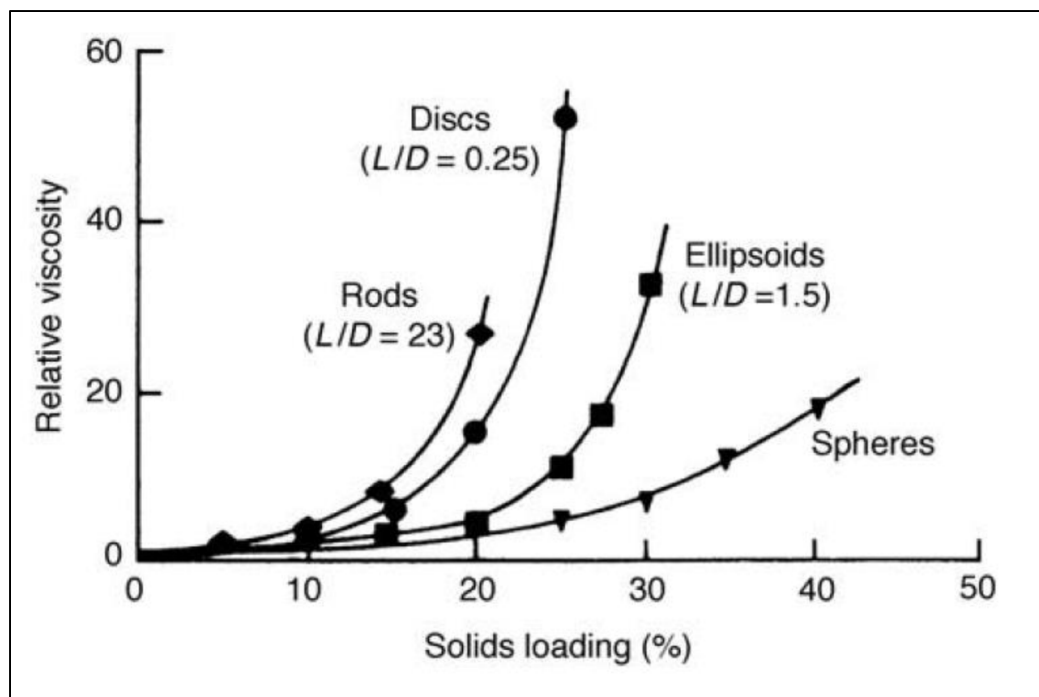


Figure 1.21 Maximum solids loading for different shapes of glass particles (AN 2012).

However, an ideal particle shape is still under debate due to the poor compact strength after debinding compare to the one obtained with irregular particle. Indeed, the low interparticle friction associated with spherical powder, which was suitable during injection stage, may produce too much brittle part or component slumping during debinding. Some authors have proposed solution to this issue by blending spherical and irregular shape particles together to obtain the advantages of both (R.M. German 1995).

### 1.3.4 Influence of shear deformation rate on viscosity

LPIM feedstocks normally exhibit a shear thinning (pseudoplastic) behavior on the majority of the shear deformation rate range, where the viscosity decreases with an increase in shear rate as presented in Figure 1.22. At a given temperature, this suitable behavior leads to fill the die cavity completely under low-pressure (during high shear rate) and prevent segregation after injection (during low shear rate). This pseudoplastic behavior is explained by particle or binder

molecule ordering with the flow. The following power law model (Eq. 1.2) widely reported in the literature (Park, Wu et al. 2009) can describe this behavior, and can be applied to study the effect of the binder on the rheological behavior of the molten feedstocks (Hidalgo, Abajo et al. 2013, Demers, Turenne et al. 2015).

$$\eta = k\dot{\gamma}^{n-1} \quad (1.2)$$

Where  $\eta$  is the feedstock viscosity,  $k$  a constant,  $\dot{\gamma}$  the shear rate and  $n$  is the shear sensitivity index. The pseudoplastic ( $n < 1$ ) and near-Newtonian ( $n \approx 1$ ) behavior of feedstocks are acceptable in powder injection molding. Through the mixing and the injection steps, a pseudoplastic behavior is more desirable to promote a decrease in viscosity of feedstocks with increasing shear deformation during mold filling. However, a near-Newtonian behavior could be quite acceptable during the injection phase if the viscosity values remain acceptable for molding over the whole shear rate range (Demers, Turenne et al. 2015, Demers, Fareh et al. 2018). Generally, the value of  $n$  should be as small as possible, to maximize the viscosity changes during and after the mold filling. Before and after injection, the feedstock viscosity should be as high as possible to prevent powder-binder separation in the injection channel of the injection press, as well as within the injected part. However, the viscosity during the injection operation must be as low as possible, to increase the moldability potential of the feedstock, or in other words, to increase the complexity of the part that can be molded. The value of flow behavior index ( $n$ ) is calculated from the  $(n - 1)$  slope of graph drawn between the log-log values of shear rate and viscosity as illustrated Figure 1.22.

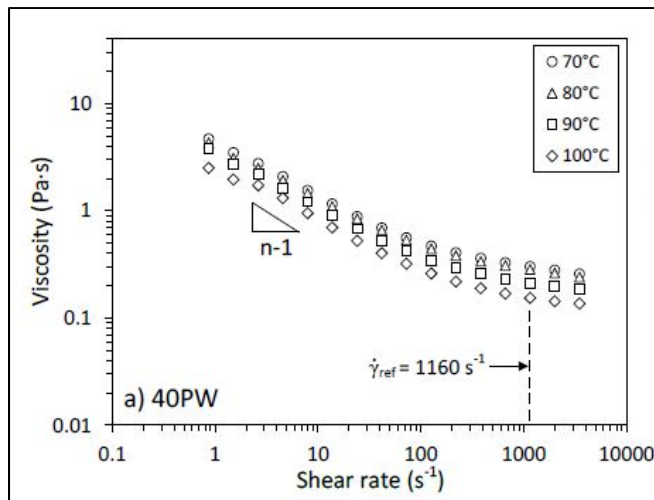


Figure 1.22 Dependence of feedstock viscosity on shear rate (Fareh and Demers 2016).

### 1.3.5 Influence of temperature on viscosity

The relation between the temperature and the viscosity was also widely studied (Mobilallegh, Morshedian et al. 2005, Fareh, Demers et al. 2017, Machaka, Ndlangamandla et al. 2018). This temperature-dependence of viscosity can be described by an Arrhenius equation (Equation (1.3)) indicating that the viscosity of a feedstock decreases with an increase in temperature visible in Figure 1.22.

$$\eta = \eta_{To} \exp\left(\frac{E}{RT}\right) \quad (1.3)$$

Where  $R$  is the gas constant,  $T$  is the temperature in Kelvin unit,  $E$  is the flow activation energy,  $\eta$  is the feedstock viscosity at a given temperature, and  $\eta_{To}$  is the viscosity at reference temperature. Large values of flow activation energy ( $E$ ) show a high sensitivity of viscosity to temperature, and this has an adversely effect on the flow manners during injection molding (Amin, Muhamad et al. 2012). If the viscosity is very sensitive to the temperature variation, any small fluctuation of temperature during molding will produce viscosity changes, generating stress concentration in the molded part, resulting in cracking and distortion. Moreover, sudden viscosity changes could cause a reduction in the flowability of feedstock

during injection. Therefore, the value of ( $E$ ) should be as small as possible to minimize significant changes of feedstock viscosity between the hot and cold zones in the injection press or in the mold (Demers, Turenne et al. 2015, Fareh, Demers et al. 2016). Furthermore, the value of  $E$  depends to the composition of binder formulations and can be estimated by plotting the Napierian logarithm of feedstock viscosity against the inverse of the temperature as illustrated in Figure 1.23. The  $E/R$  coefficient represents the slope of the resulting linearization curve as described by the Equation (1.4).

$$\ln \eta = \ln \eta_{To} + \frac{E}{RT} \quad (1.4)$$

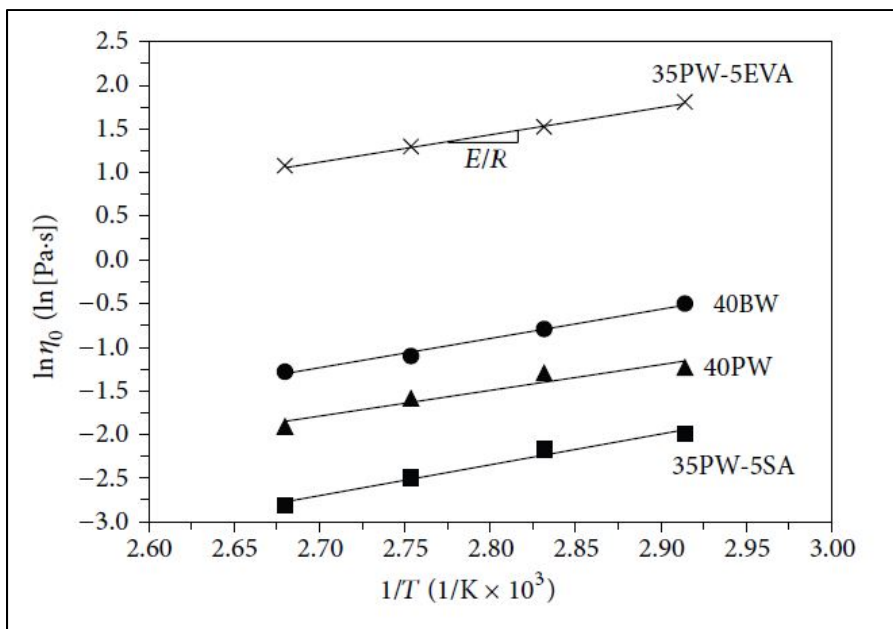


Figure 1.23 Viscosity of feedstocks as a function of temperature  
(at  $\dot{\gamma}_{ref} = 1160 \text{ s}^{-1}$ ) (Fareh, Demers et al. 2016).

It is reported in the literature that feedstocks containing finer particles size exhibit higher flow activation energy compared to the feedstocks formulated with coarser particle size. As explained by Tatt et al. (Tatt, Muhamad et al. 2012), finer particles have larger surface area enhancing the particle-particle interaction and heat dissipation through the green part. In addition, it is evident that the flow activation energy value correlated with the solid loading of the powder (see Figure 1.24), where a decrease in the value of  $E$  values is generally linked with

an increase in solid loading (Sotomayor, Levenfeld et al. 2011). Therefore, the feedstock with a higher powder loading could be more appropriate for the injection stage from a thermal stability point of view (Abdoos, Khorsand et al. 2014).

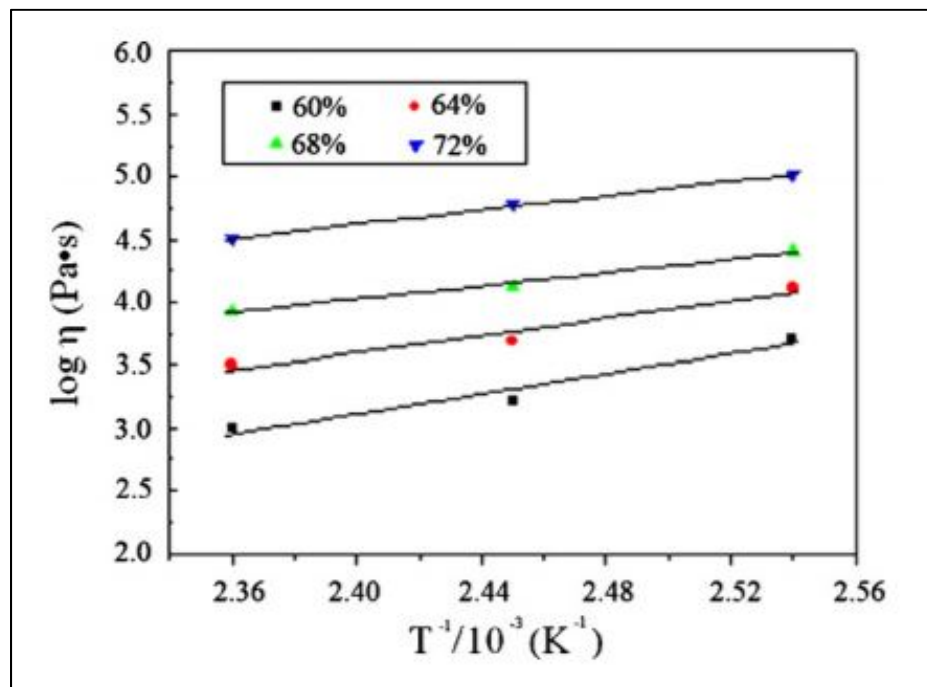


Figure 1.24 Viscosity as a function of  $1/T$  for feedstocks with different powder loadings (Li, Li et al. 2007).

### 1.3.6 Influence of solid loading on viscosity

It well known that the viscosity of a feedstock increases with an increase in the volume fraction of powder, as illustrated in Figure 1.25 (Sotomayor, Vález et al. 2010).

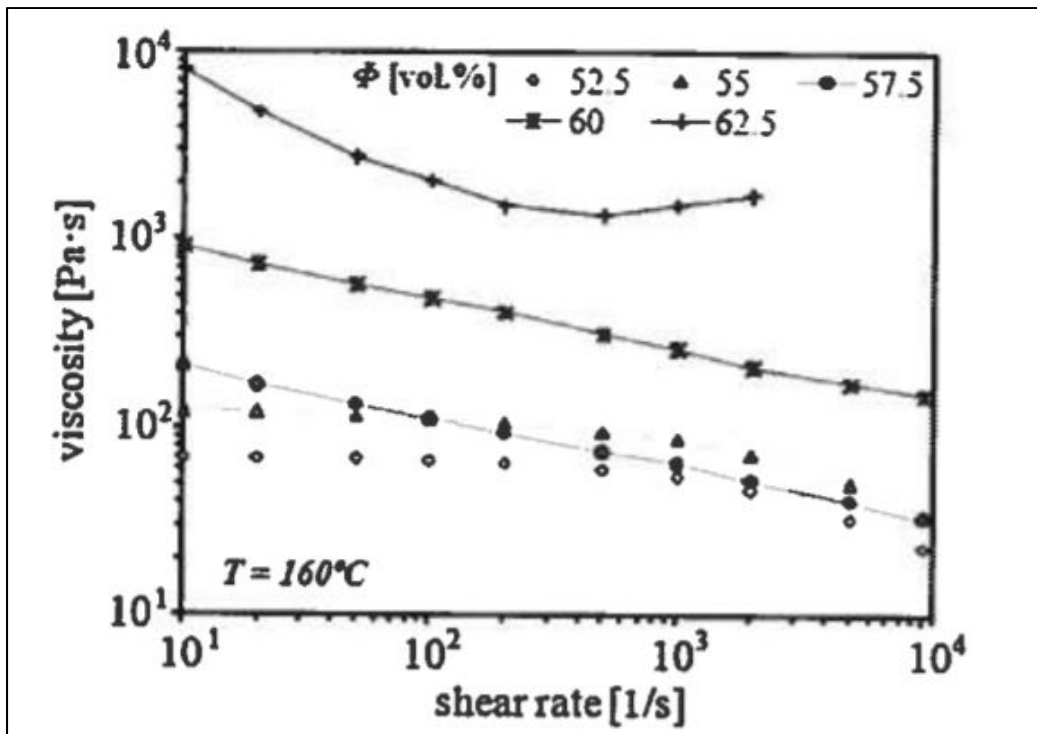


Figure 1.25 The shear viscosity dependence with shear rate for different percentages of solid loadings for 160°C (Hidalgo, Jiménez-Morales et al. 2012).

In the literature, several mathematical models can be found to describe the relationship between the viscosity and the solids loading where the most popular is that of Quemada (equation (1.5)):

$$\eta = \eta_b \left(1 - \frac{\phi}{\phi_m}\right)^{-2} \quad (1.5)$$

Where  $\eta_b$  is the binder viscosity,  $\phi$  is the solid loading, and  $\phi_m$  is the maximum solid loading. As presented in Figure 1.26, the value of viscosity become infinite as the solids loading approaches the maximum solid loading value, describing the fact that all particle are interlocked together resulting in a flow impediment.

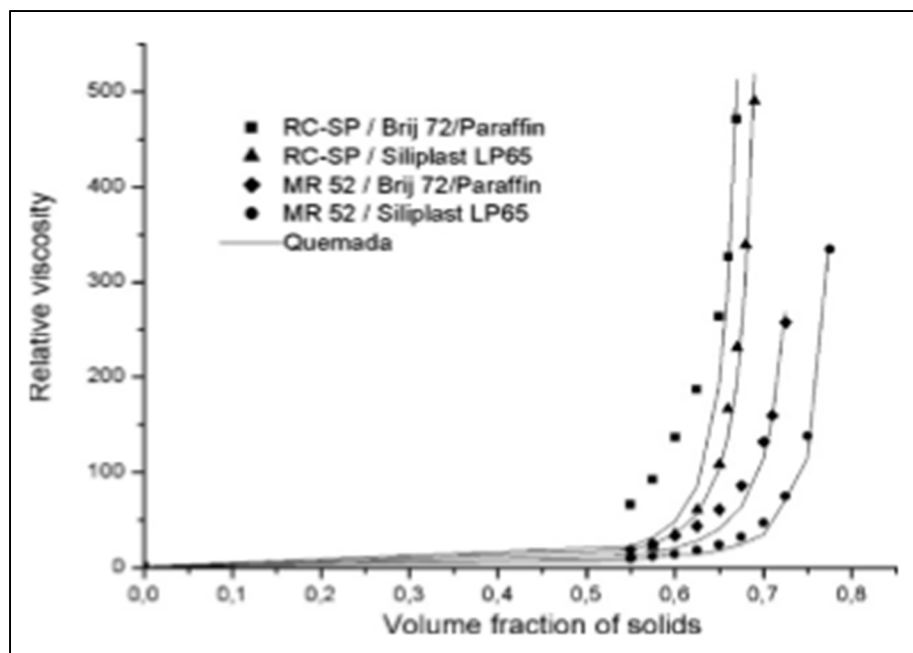


Figure 1.26 Relative viscosity versus volume fraction of solids with the use of the Quemada model (Loebbecke, Knitter et al. 2009).

## 1.4 Injection performance of feedstocks

In general, the injection properties of feedstocks could be assessed using the calculation of the moldability index (using Weir's model) or by measuring the feedstock moldability. These considerations are reported below.

### 1.4.1 Moldability index model

The general rheological properties of feedstock is evaluated by the moldability index (moldability is the ability of the mixture to be injected into the mold cavity), which has been first proposed by Weir for polymers, and then used for 15 years in PIM to include the effect of the three parameters introduced above (Weir, Doyle et al. 1963):

$$\alpha_{STV} = \frac{1}{\eta_o} \frac{\left| \frac{\partial \ln \eta}{\partial \ln \dot{\gamma}} \right|}{\frac{1}{\partial \frac{T}{T}}} \quad (1.6)$$

Where  $\eta$  is viscosity,  $\eta_o$  the reference viscosity,  $\dot{\gamma}$  shear rate,  $T$  temperature, and  $\alpha_{STV}$  moldability index for PIM feedstocks and simplifying the equation (1.6) into:

$$\alpha_{STV} = \frac{1}{\eta_o} \frac{|n - 1|}{E/R} \quad (1.7)$$

Where  $n$  is a flow behaviour exponent,  $E$  is the flow activation energy, and  $R$  is the gas constant. The subscripts  $S$ ,  $T$ ,  $V$  of  $\alpha_{STV}$  represent the effect of shear sensitivity, temperature sensitivity, and viscosity respectively. It was determined that a viscosity value lower than 10 Pa·s (commonly measured at a shear rate of 100 s<sup>-1</sup>) was appropriate to fill mold cavity completely using the LPIM feedstock (Lamarre, Demers et al. 2017). The higher the value of  $\alpha_{STV}$ , the better the general moldability properties, where from a molding perspective, the best feedstock candidate corresponds to the highest value of the moldability index (i.e., lowest value of  $\eta_o$ ,  $n$ , and  $E$ , concurrently) also represented in Figure 1.27 for a LPIM of ceramic feedstock (Hidalgo, Jiménez-Morales et al. 2012).

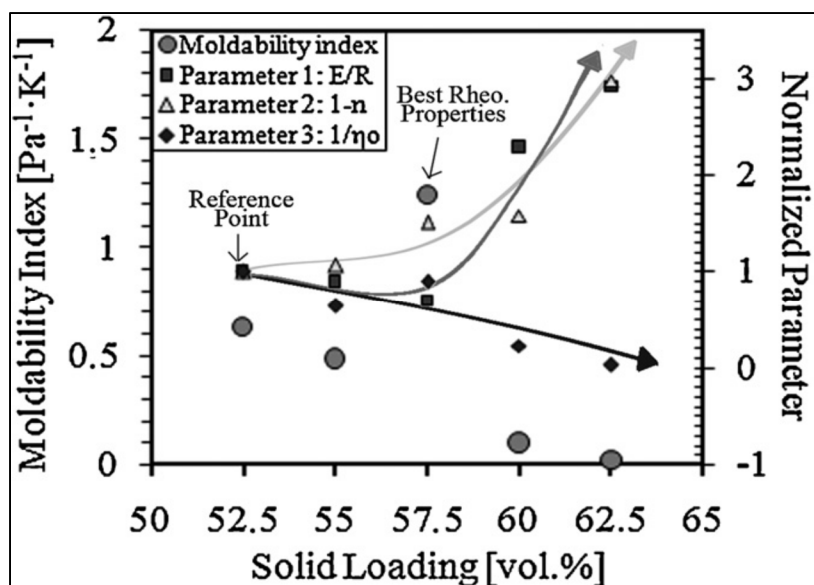


Figure 1.27 General moldability index vs. solid loading vol.% (Hidalgo, Jiménez-Morales et al. 2012).

This original model has been used successfully to optimize solid loading (Hidalgo, Jiménez-Morales et al. 2012, Abdoos, Khorsand et al. 2014, Abdoos, Khorsand et al. 2014, Ghanbari, Alizadeh et al. 2015) and feedstock formulations (Mohd Amin, Ibrahim et al. 2014). For example, Ghanbari et al. (Ghanbari, Alizadeh et al. 2015) demonstrated that the solid loading of LPIM feedstocks have a significant impact on moldability index which can be doubled with a five-percentage points change in solid loading (i.e. 54 to 59 vol. %). In addition, Hidalgo et al. (Hidalgo, Jiménez-Morales et al. 2012) have indicated that the optimal solid loading can create the highest value of moldability index for LPIM ceramic feedstock. Furthermore, Fareh et al. (Fareh, Demers et al. 2016) have demonstrated that the moldability properties of feedstocks are controlled by the proportion of the major binder. Finally, Lamarre et al. (Lamarre, Demers et al. 2017) have established that the best moldability properties were obtained with the feedstock containing paraffin wax and stearic acid.

### 1.4.2 Measurement of the feedstock's moldability

Real moldability of feedstock is usually obtained using real scale injection in order to determine the best candidate powder-binder attributes producing higher moldability while minimizing segregation of powder and binder constituents. Moldability of LPIM feedstocks is carried out using different types of mold cavities typically zigzag mold, rectangular shape, wedge shape, spiral shape, or any cavity representing the injection process (Figure 1.28).

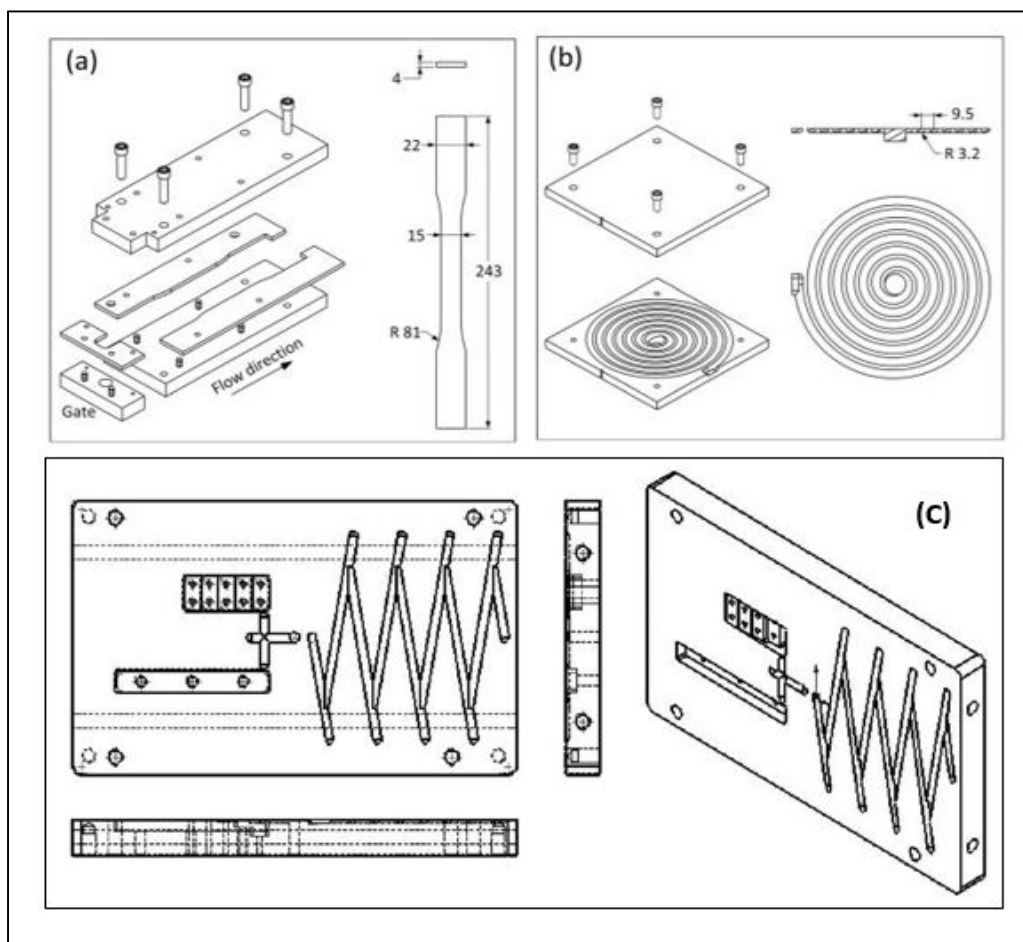


Figure 1.28 Mold design and injected specimen: (a) rectangular dog bone shape, (b) spiral shape and (c) zigzag mold (dimensions in millimeters) (Karataş, Sözen et al. 2008, Cheng, Hwang et al. 2009, Lamarre, Demers et al. 2017).

Typically, an injection press is used to inject the feedstocks into one of the mold presented above in Figure 1.28 to quantify experimentally the achievable injected length as illustrated in Figure 1.29. These injected length values can then be used to validate the moldability index obtained with the Weir's model (presented in section 1.4.1) and quantify the capacity of the model to predict the injection performance of powder-binder mixtures. Note that the experimental validation of this simple model has received very little attention in the literature but it is of primary importance for future development and optimization of low-pressure powder injection molding feedstock, which is, so far, done by trial and error method.

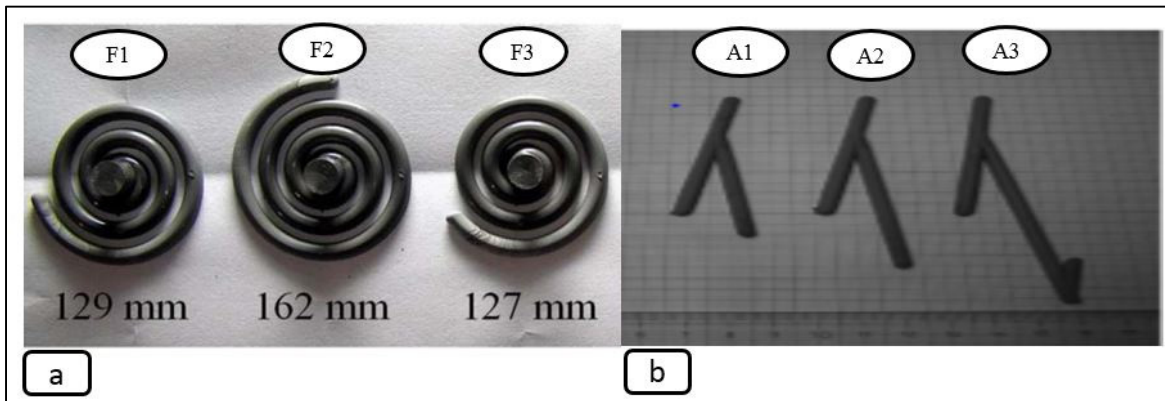


Figure 1.29 Feedstock injected length: (a) Spiral flow lengths, adapted from ref. (Cheng, Hwang et al. 2009) and (b) Zigzag flow test adapted from ref. (Karataş, Sözen et al. 2008).

Mangels, et al. (1983) (Mangels and Williams 1983) suggested the connection between the spiral flow distance (*SFD*) and the viscosity of feedstock (see Equation (1.8), and found that the greater the spiral flow distance, the better the injection moldability of feedstock.

$$SFD = C/\eta \quad (1.8)$$

Where: ( $\eta$ ) feedstock viscosity and ( $C$ ) constant. Our research team (Demers V. 2017) has recently confirmed for LPIM feedstock that an increase in moldability index values was correlated with an increase in injected length for simple feedstock formulations (Figure 1.30). However, large rheological database is not available in literature to assess the moldability properties of different feedstock constituents.

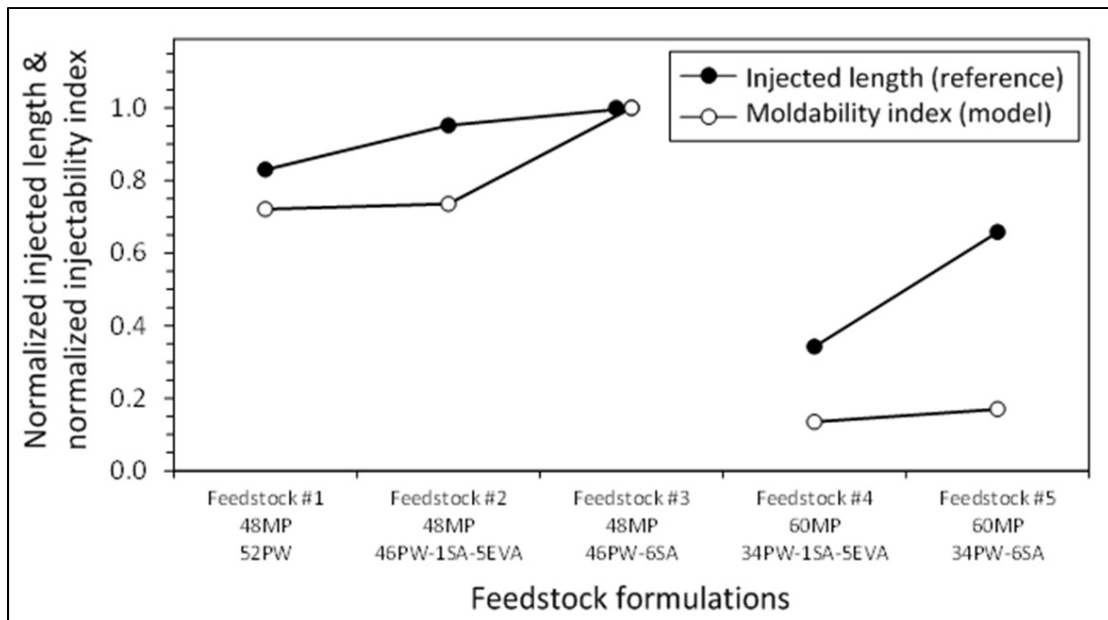


Figure 1.30 Comparison of the injected length and moldability index of feedstocks at 70°C for viscosity values obtained at  $100\text{ s}^{-1}$  (Demers V. 2017).

## **CHAPITRE 2**

### **PROBLEM DEFINITION AND RESEARCH OBJECTIVE**

#### **2.1 Problem definition**

Based on the literature review, it is well known that rheological behavior of powder-binder mixture has a direct impact on the successful mold filling for parts obtained from powder injection molding. This rheological behavior depends on shear rate, temperature, solid loading, powder shape, powder size, and binder composition. Although trends qualifying the influence of these parameters are well known (see particularly the section 1.3 of this document), it is clear that data available in literature are not sufficient to assess the moldability properties of feedstock and optimize feedstock formulations as well as final properties of the manufactured components. So far, the efforts to optimize the mechanical properties of LPIM metallic materials typically involve debinding and sintering using feedstocks whose optimal moldability has not yet been demonstrated. Therefore, assessing the full potential of the LPIM technique is still limited by a poor understanding of the fundamental mechanisms underlying the moldability of LPIM feedstocks linked with the rheological behavior of feedstock specifically on a poor understanding of the impact of binder constituents on rheological behavior.

#### **2.2 Research objectives**

The main objective of this work is to study the influence of wax-based binder systems on the rheological properties of feedstocks to better understand and predict the moldability properties of powder-binder mixtures used in low-pressure powder injection molding process.

The specific objectives of the current project are:

- ✓ Obtain the viscosity profiles at constant temperature and constant powder solid loading for single-binder and multiple-binder system formulated from wax-binder, surfactant agent, and thickening agent.

- ✓ Determine the threshold proportion producing the surfactant and thickening effect.
- ✓ Calculate the rheological parameters describing each feedstocks (i.e., flow behavior index, and reference viscosity)
- ✓ Propose a design tool describing the impact of each binder on viscosity

This project will finally produce the first complete database describing the influence of each binder constituents that is still missing today to develop optimal feedstock for LPIM process.

## **CHAPITRE 3**

### **EXPERIMENTAL METHODOLOGY**

This chapter presents the experimental procedures used to prepare the feedstock formulations, characterize their thermal properties, and obtain their rheological behaviors.

#### **3.1 Feedstock formulations**

##### **3.1.1 Powder lots**

In this study, three different powder lots were used. The first powder lot is a water-atomized stainless steel 17-4PH powder (Epson Atmix Corporation, Japan) with a typical near-spherical or ligament shape and an average particle size of 12 µm (Figure 3.1a). This latter powder lot was used as a reference material in this study. This high-strength material generally consists of 17% of Chromium and 4% of Nickel while water or gas atomization technique provides powder lot with interesting properties such as small particle size, high packing density, and low cost raw material suitable for metal injection molding. This precipitation-hardening stainless steel is widely used in the aerospace, chemical, petrochemical, and many other sectors for its high strength and good corrosion resistance.

Two other powder lots were also used to better understand fundamental mechanism highlighted with the first powder lot. On one hand, water-atomized stainless steel 17-4PH powder (Epson Atmix Corporation, Japan) with a typical near-spherical shape and an average particle size of 3 µm (Figure 3.1b) was used to quantify the influence of powder size on rheological behavior. On the other hand, gas-atomized stainless steel 17-4PH powder (Sandwick Osprey, UK) with a typical spherical shape and an average particle size of 12 µm (Figure 3.1c) was used to quantify the influence of powder shape on rheological behavior.

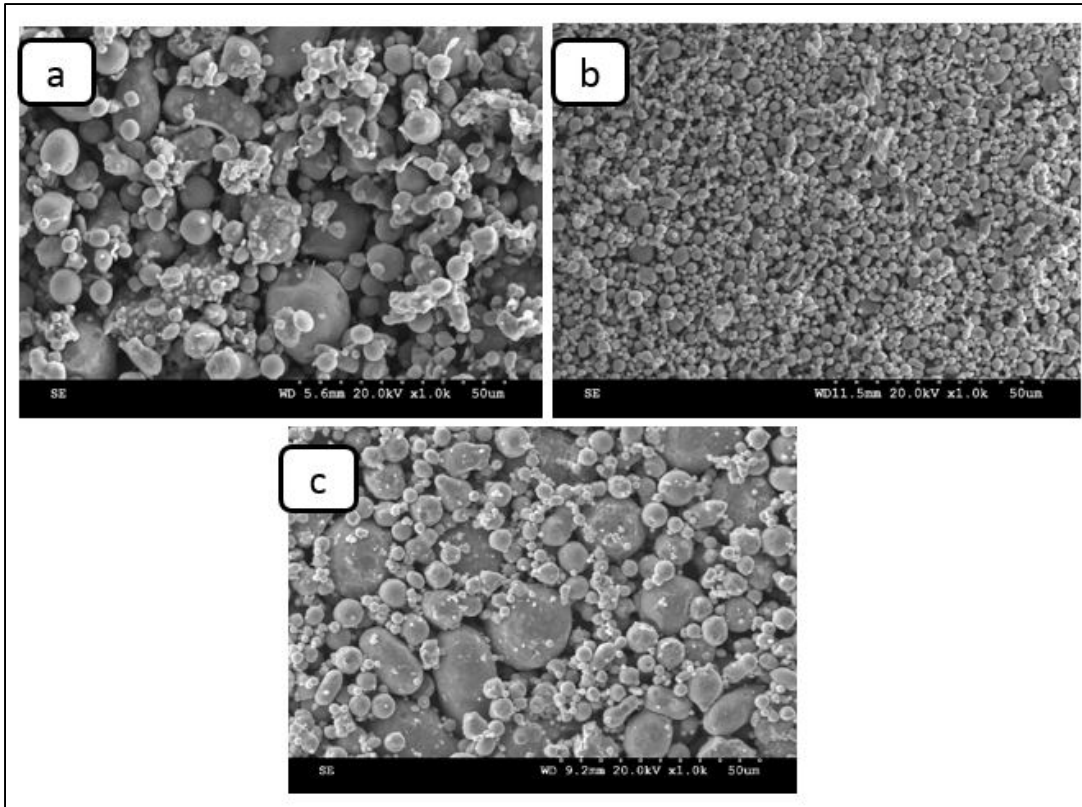


Figure 3.1 SEM micrograph of 17-4 PH stainless steel powders (a) 12  $\mu\text{m}$  water atomized by Atmix, (b) 3  $\mu\text{m}$  water atomized by Atmix, and (c) 12  $\mu\text{m}$  gas atomized by Osprey.

### 3.1.2 Binder constituents

In this study, the binders were formulated from three main constituents which are i) the filler material, ii) the surfactant agent, and iii) the thickening agent. The filler binders were taken amongst five different waxes (i.e., used as a single-binder or combined together): one paraffin wax (PW), one beeswax (BW), one carnauba wax (CW), and two microcrystalline waxes (MW1 and MW2). Paraffin and microcrystalline waxes originate from petroleum. Microcrystalline waxes have a higher melting point than paraffin and are generally more stable but more expensive than paraffin. In general, these kinds of waxes are inexpensive and can be removed easily in debinding stage. Natural wax (beeswax (BW) and carnauba wax (CW) are more rigid at room temperature, but they are very liquid at high temperature. Surfactant agents

such as stearic acid (SA) and oleic acid (OA) were used for enhancing the homogeneity of the feedstock and mixing properties. Finally, thickening agents such as ethylene vinyl acetate (EVA) and low-density polyethylene (LDPE) were employed to manage the viscosity properties of LPIM feedstock. These latter constituents were used to tailor the viscosity of feedstock in order to prevent powder-binder segregation. All of these specific filler binder constituent, surfactant and thickening agents were selected due to their intensive use in LPIM (Choi, Lyu et al. 2014, Demers, Turenne et al. 2015, Fareh and Demers 2016, Fareh, Demers et al. 2016, Fareh, Demers et al. 2016, Lamarre, Demers et al. 2016, Demers V. 2017, Fareh, Demers et al. 2017, Lamarre, Demers et al. 2017, Demers, Fareh et al. 2018). Appearance of these binders at room temperature is presented in Figure 3.2. In general, waxes (natural or synthetic) are supplied in the form of blocs, flakes or granules; EVA or LDPE in the form of granules; SA in the form of flakes; and oleic acid in the liquid state. Figure 3.3 shows the chemical formula of stearic acid (SA) and oleic acid (OA).



Figure 3.2 Appearance of the binders used in our study at room temperature.

The physical properties of the components used in this work are reported Table 3.1.

Table 3.1 The list of binders used in our experimental study.

Constituent	Melting point (°C)	Density (g.cm <sup>-3</sup> )
Paraffin wax (PW)	55	0.90
Microcrystalline wax #1 (MW1)	55	0.90
Microcrystalline wax #2 (MW2)	70	0.90
Beeswax (BW)	65	0.96
Carnauba wax (CW)	84	1.00
Stearic acid (SA)	62	1.00
Oleic acid (OA)	13	0.895
Ethylene–vinyl acetate (EVA)	86	0.94
Low-density polyethylene (LDPE)	85-140	0.91–0.94

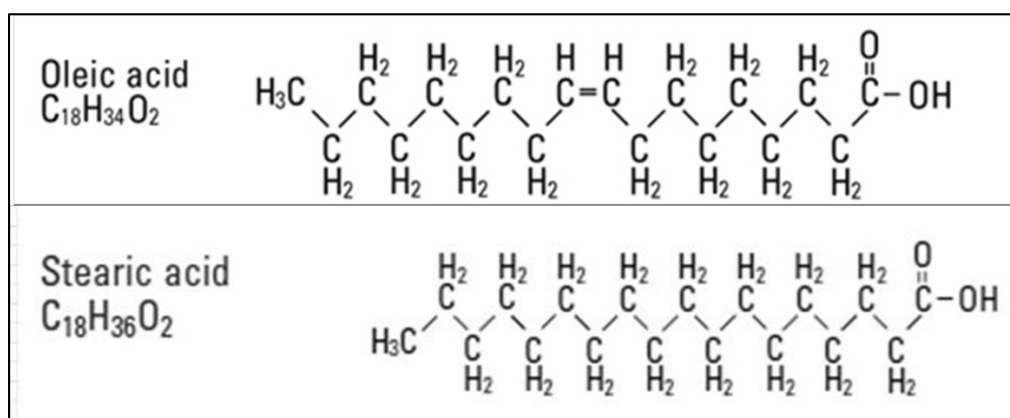


Figure 3.3 Chemical formula of stearic acid (SA) and oleic acid (OA).

In the framework of this study, these polymer constituents were mixed with metallic powder to formulate more than 195 different feedstocks according to seven feedstock families reported in Table 3.2. These seven categories of feedstock families were tailored to discretize the

influence of single-binder and multiple-binder formulations on viscosity. For example, the feedstock family #1 was built to measure the influence of each single-binder on viscosity, while the feedstock families #2 to #7 were developed to better understand the chemical interaction between binders, determine threshold proportion producing measurable effect (e.g, surfactant or thickening effects), and their general influence of multi-binder formulation on rheological behavior.

Table 3.2 Binder constituents categories used in this study.

<b>Feedstock family</b>	<b>Binder constituents</b>
1	Influence of waxes "only" on viscosity.
2	Influence of stearic acid (SA) on viscosity of wax-based feedstocks
3	Influence of oleic acid (OA) on viscosity of wax-based feedstocks
4	Influence of Ethylene vinyl acetate (EVA) on viscosity of wax-based feedstocks
5	Influence of SA+EVA on viscosity of single wax-based feedstocks
6	Influence of SA+EVA on viscosity of multi wax-based feedstocks
7	Influence of stearic acid SA+OA+EVA on viscosity of wax-based feedstocks

The solid loading of all feedstocks was kept constant at 60 vol. % of powder and they are referenced by their polymer volume fractions (vol. %), which were determined at room temperature. For example, the feedstock 13PW-12BW-12CW-0.5SA-0.5EVA-2OA is a mixture containing 60 vol. % of powder with 13 vol. % of PW, 12 vol. % of BW, 12 vol. % of CW, 0.5 vol. % of SA, 0.5 vol. % of EVA and 2 vol. % of OA. Because it is more convenient to work with weight fraction (wt. %), this value was then converted in terms of volume fraction of powder using Equation (3.1).

$$vol\%_{powder} = \left[ 1 + \left( \frac{\rho_{powder}}{\rho_{binder}} \right) \left( \frac{1}{wt\%_{powder}} - 1 \right) \right]^{-1} \quad (3.1)$$

Where  $vol\%_{powder}$  is the volume fraction of powder,  $wt\%_{powder}$  is the weight fraction of powder, and  $\rho_{powder}$  is the density of the powder, and  $\rho_{binder}$  is the density of the binder (see Table 3.1 for the density values).

### **3.1.3 Feedstock preparation steps**

After the exact quantity measurement of the powder and binders, the mixing process started with successive steps. First, the metallic powder heated for 15 minutes at the heater temperature of 300°C. Next, the temperature of the heater dropped to 130 C with stirring of the powder. Then, the main wax added. After that, the surfactant and thickening agents added in the same time. Finally, the temperature of the heater increased from 150 to 200 °C depended on the binder type with continuous flipping.

Once the liquid feedstock obtained which is not yet homogeneous. In other words, this mixture presents small bubbles stuck in the liquid, which are going to prevent the good homogeneity of the mixture. Therefore, the feedstock cooled. In this step, the cooling wax shrinks and forces the bubbles to get out. Then the mixture heated again. The idea is to repeat the operation until all the bubbles disappear and get a homogeneous mixture.

## **3.2 Feedstock characterization**

As demonstrated in the literature review section, the viscosity of feedstock is a useful rheological characteristic and a key parameter that can be used to study the moldability of feedstocks in different conditions. This section thus describes the methodology used to obtain thermal properties, viscosity profiles from all feedstocks and the method used to analyze the data.

### **3.2.1 Thermal properties**

Melting point of each single binder constituent and feedstock (i.e. blended binder) were obtained using a differential scanning calorimetry (DSC) technique. DSC tests were performed

with a PerkinElmer Pyris 1 (Figure 3.4) for temperatures ranging from 20 to 120°C, a heating rate of 10°C/min under a nitrogen gas flow rate of 20 ml/min. Specimens with a mass ranging from 20 to 40 mg were encapsulated in standard aluminum hermetic pans.

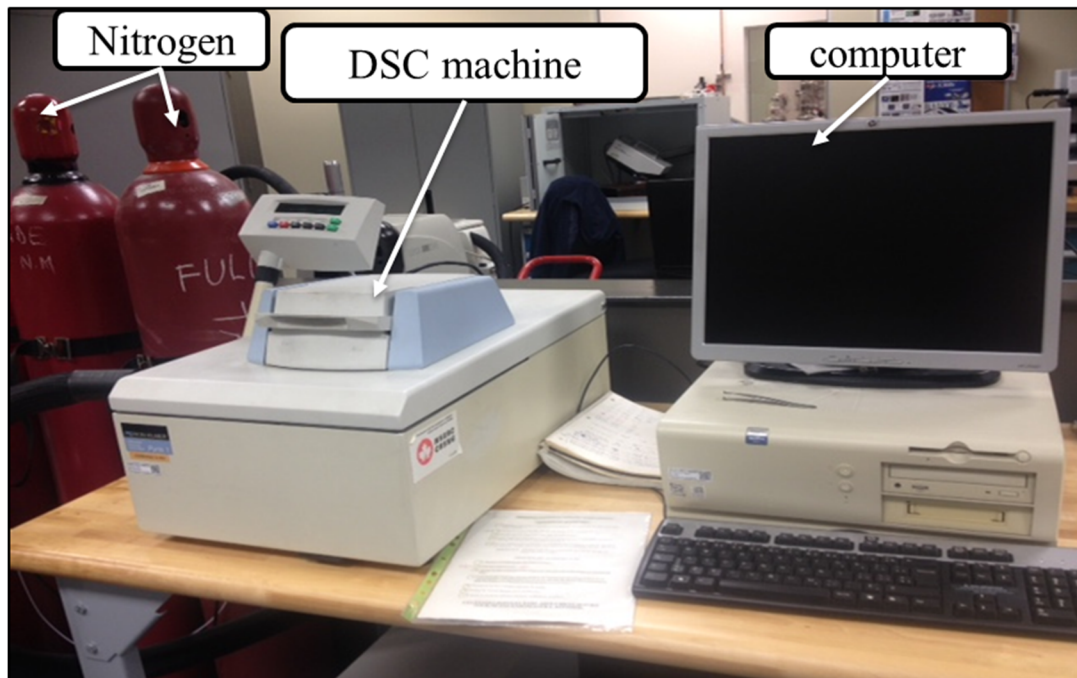


Figure 3.4 Differential scanning calorimeter (DSC).

As specified by ASTM D3418, the DSC graphs were recorded from the second heating cycle to erase previous thermal history and to maximize thermal contact between the pan and specimen. When the feedstock exhibited several melting points (i.e. more than one DSC peak due to a multi-binder formulation), the feedstock melting point was determined from the last peak obtained during a heating cycle as indicated by a black arrow on the example presented in Figure 3.5. Likewise, it is shown in this figure, there is not possible to measure the melting point of the mixture contained only 40EVA, Because EVA is used as a secondary binder component to increase the viscosity of the mixture to prevent the powder-binder segregation.

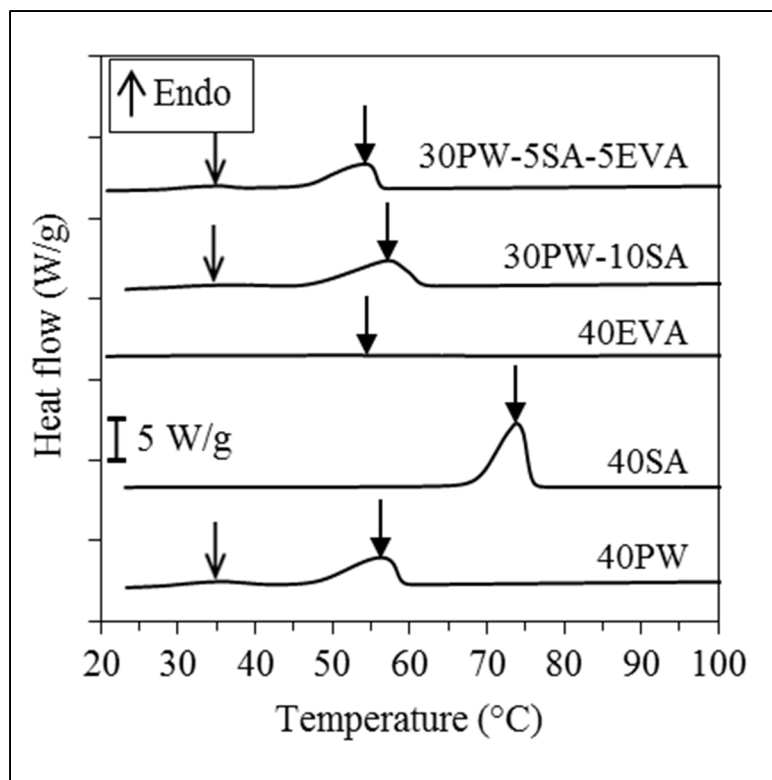


Figure 3.5 DSC results for binder constituents  
(Lamarre, Demers et al. 2016).

For a given feedstock, this maximum melting temperature provides the minimum temperature for powder-binder mixing and minimum injection temperature. The DSC graphs were also used to assess the solubility (interaction) between polymers when they are mixed together where polymer soluble in each other produce a final melting point different than the single constituent. For example, Figure 3.6 shows that carnauba wax, beeswax, ethylene vinyl acetate, oleic acid, and stearic acid exhibit a certain degree of solubility because the melting points of the single binder.

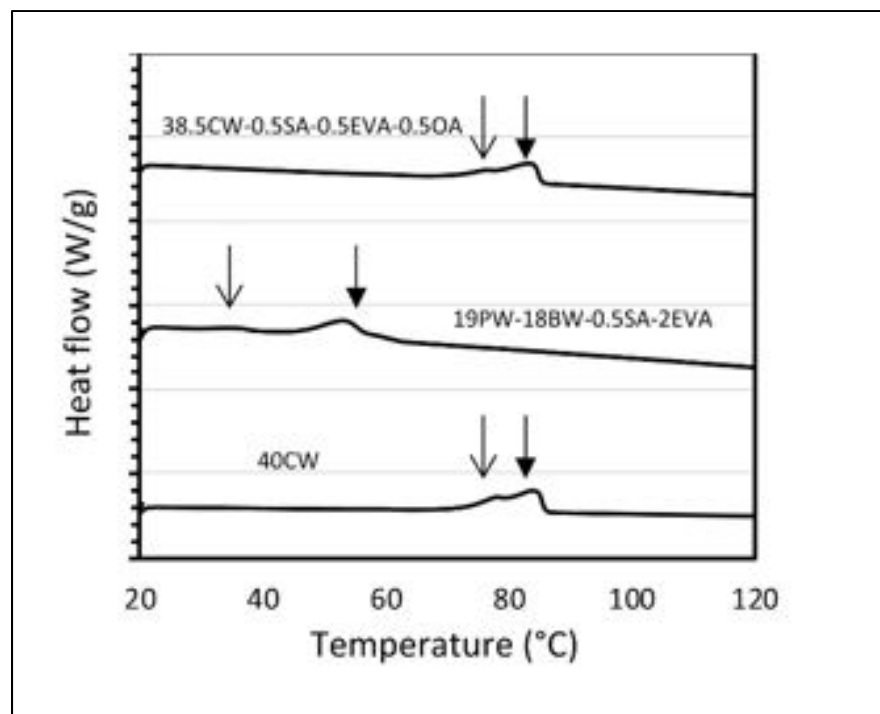


Figure 3.6 DSC results for binder constituents (heating).

### 3.2.2 Viscosity measurements and data processing

Feedstocks viscosity was measured using an Anton Paar MCR 302 rotational rheometer using the concentric-cylinder C-PTD 200 and a Peltier temperature-controlled measuring system presented in Figure 3.7.

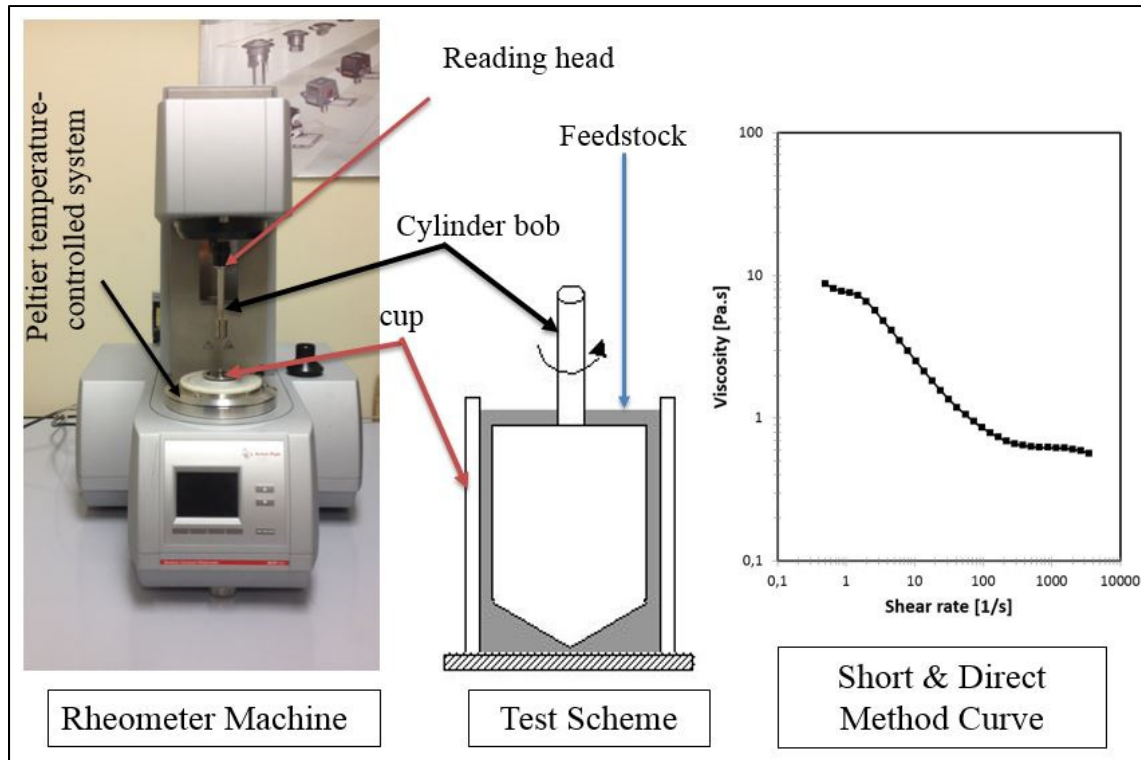


Figure 3.7 Anton Paar rotational rheometer and the method used.

The solid feedstock was placed into a metallic container (outside the rheometer) and warmed at 90°C (i.e., above the melting point of the binder) using a heating plate as illustrated in Figure 3.8b. In this study, this specific heating temperature was fixed at 90°C, which corresponds to a higher melting point than the one of the wax-based binders generally used in literature. At the same time, the empty cup cylinder was placed into the Peltier temperature-controlled system at 90°C while the bob cylinder was preheated at 90°C outside the rheometer using a hot water beaker as represented in Figure 3.8a. This procedure was implemented to eliminate the dwell time (generally around 5 minutes) required for temperature homogeneity (i.e., thermal equilibrium between the feedstock and the measurement cylinder) and thus, to avoid segregation of low-viscosity feedstocks that may occur during this dwell period. In this respect, our research team has developed rheological methodology specifically for testing low-viscosity feedstocks in (Fareh, Demers et al. 2017). This technique consists in measuring the viscosity profile of feedstocks in 2 minutes instead of 30 minutes as it is usually done. This procedure was used to minimize the segregation of the powder-binder mixtures but this

approach will be discussed and refined in the results section (see section 4.1) because it was demonstrated that the technique might produce thermal stability issues. For this reason, each lot of feedstocks were re-tested several times (i.e., same feedstock sample in the rheometer) to guarantee thermal equilibrium between the mixture and the equipment. The molten feedstock was then stirred by hand (i.e. in molten state). After that, it poured into the cup cylinder (previously placed in the rheometer). The preheated bob cylinder was take-off the water, dried using Tork® H1 Kraft Roll towels, installed into the reading head of the rheometer (Figure 3.8c), and introduced into the molten feedstocks. In order to minimize or avoid segregation of feedstock, the test was started (Figure 3.8d) as soon as the bob is introduced into the cup using a short cycle as described in (Fareh, Demers et al. 2017). The molten feedstock was tested at a constant temperature of 90°C using shear rates ranging from 0.5 to 3000 s<sup>-1</sup>.

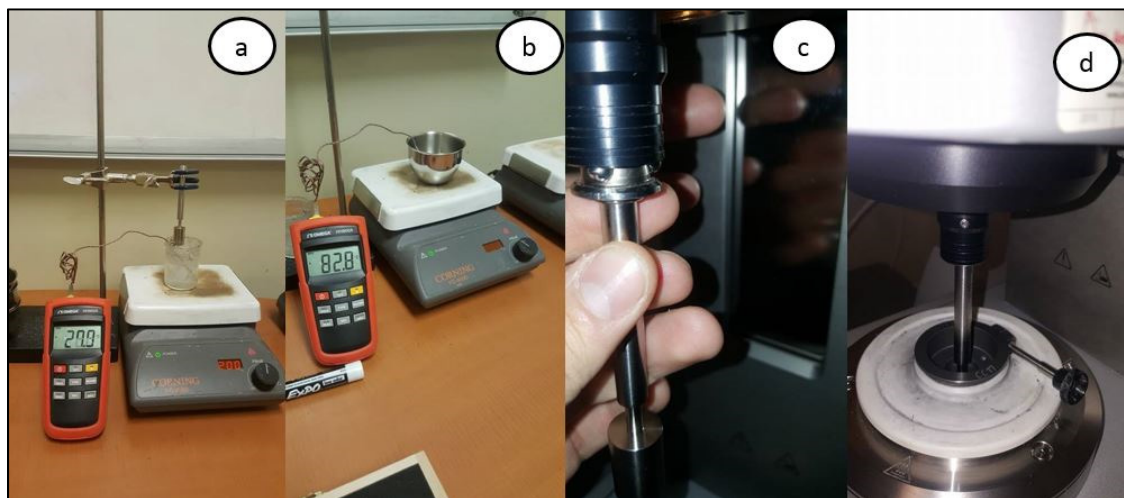


Figure 3.8 Main test steps to perform tests using the rotational rheometer.

Based on the data displayed by the rheometer, the viscosity according to the shear rate was plotted for the 200 feedstocks. As it was explained in the literature review section, low shear rate represents the mixing stage or the state of the feedstock after the mold filling where high viscosity is required to prevent segregation, while high shear rate represents the injection where low viscosity value is appropriate to enhance the complete filling of the mold cavity without defects. The minimum and maximum viscosity values can be correlated with the feedstock behavior during the injection and mixing steps of the process, while the flow behavior index

is a parameter characterizing the transition from the mixing to the injection step. From this perspective, our data analysis was divided in three parts according to the Figure 3.9:

- First, from the viscosity profiles, the curve were divided into two values in term of viscosity ( $\eta_1$  (Pa·s): maximum viscosity obtained at low shear rate ( $\dot{\gamma} = 1 \text{ s}^{-1}$ ) and  $\eta_2$  (Pa·s): minimum viscosity obtained at typical injection shear rate ( $\dot{\gamma} = 100 \text{ s}^{-1}$ )).
- Second, the curves were divided into two sections in term of the flow behavior index value. The first one ( $n_1$ ) is around the shear rate ( $1 \text{ s}^{-1}$  and  $100 \text{ s}^{-1}$ ), where the slope of the viscosity profile curve decrease and the second sector ( $n_2$ ) is around ( $100 \text{ s}^{-1}$  and  $3500 \text{ s}^{-1}$ ), where the slope becomes constant as shown in Figure 3.9. The slope was calculated to determine the flow behavior index  $n$  as stated in the power law Equation 1.2 presented above in this document.
- Third, the variation in viscosity was calculated using the equation 3.2:

$$\Delta\eta = \eta_1 - \eta_2 \quad (3.2)$$

Where:  $\eta_1$  is the maximum viscosity obtained at low shear rate ( $\dot{\gamma} = 1 \text{ s}^{-1}$ ) and  $\eta_2$  is the minimum viscosity obtained at typical injection shear rate ( $\dot{\gamma} = 100 \text{ s}^{-1}$ ).

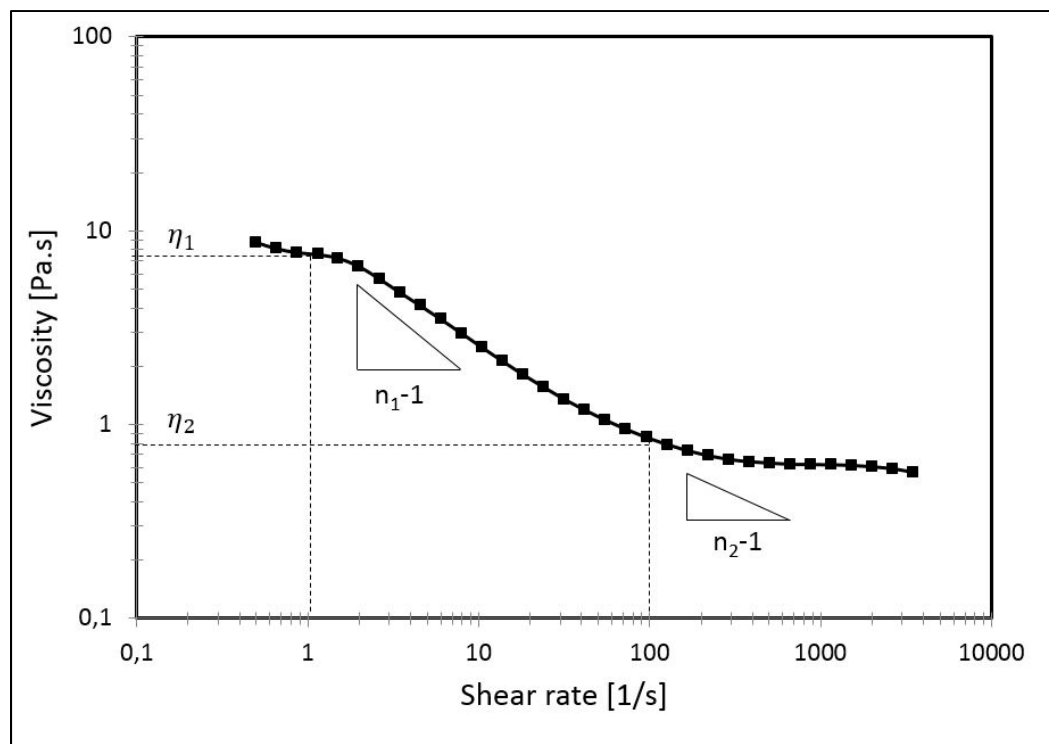


Figure 3.9 Diagram for calculation viscosity and flow behavior index.



## CHAPITRE 4

### RESULTS AND DISCUSSION

This chapter is divided into eight sections to evaluate the melting point of feedstocks, quantify the repeatability of rheological tests, study the influence of thermal stability, and asses the influence of binder constituents on viscosity. For more clarity, it was proposed to use two different scales for the y-axis of the viscosity profiles where low-viscosity and high-viscosity feedstocks were presented along a scale up to 30 and 200 Pa·s, respectively.

#### 4.1 Differential scanning calorimeter analysis

Figure 4.1 presents differential scanning calorimetry (DSC) results for typical feedstocks used in the framework of this study. Ten feedstocks were selected to assess the melting point for each constituent in different typical proportions. These tests were used to define the maximum melting point value in order to set the minimum temperature used for all rheological tests (i.e. higher than the melting point of all feedstocks for the current project). The feedstock melting point was determined from the last peak obtained during a heating cycle as indicated by a black arrow in Figure 4.1. The feedstock formulated entirely with Carnauba wax (40CW) exhibits the higher melting point (85°C), while an addition of surfactant and thickening agents into this wax does not affect significantly the melting point of this previous single-wax binder. It was also noted that a combination of surfactant and thickening agents into beeswax-based feedstocks generates almost the same melting point (around 66°C) regardless of the proportions of ingredients. Likewise, an addition of surfactant and thickening agents in paraffin wax-based feedstocks and microcrystalline wax feedstocks create roughly the same melting point (around 56°C) regardless of the proportions of ingredients. However, an addition of beeswax or the combination of beeswax and Carnauba wax in to PW-SA-EVA produces a slight decrease in melting point (around 53°C) regardless of the proportions of ingredients.

Overall, results demonstrate that the melting points of all selected feedstock were lower than 90°C, which was chosen for all rheological tests presented in the next sections.

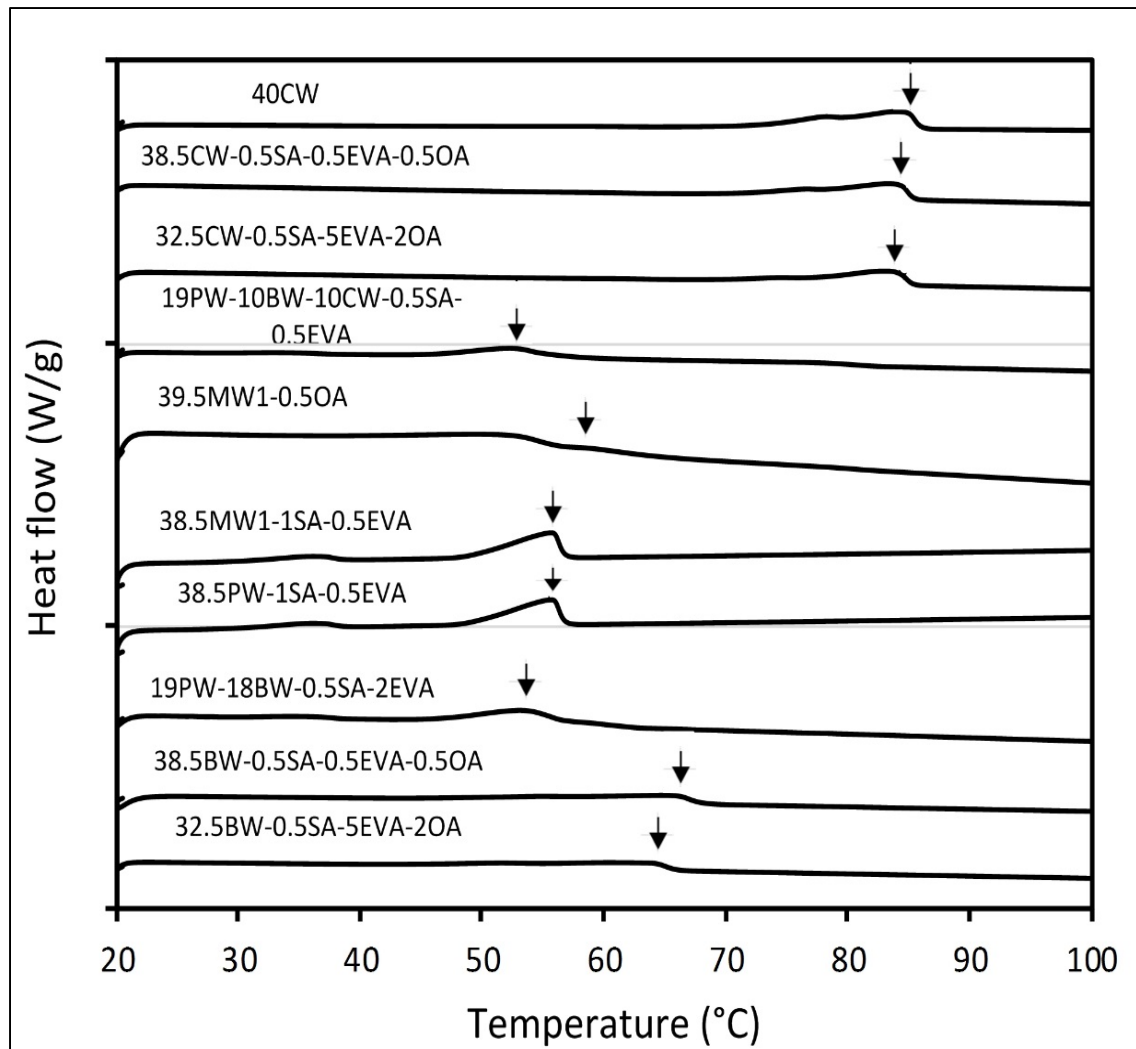


Figure 4.1 DSC results for binder constituents.

#### 4.2 Study of thermal stability during rheological characterization

The rheological tests presented in this section were performed for studying the impact of thermal stability on viscosity profiles and improve, if necessary, the testing protocol developed by a previous student in our research group. This student had demonstrated that the time between the introduction of the mixture into the rheometer and the start of the test must be minimized to avoid segregation of powder and binder (Fareh 2016). However, in the framework of the present project, it was realized that the test duration must be long enough to achieve the thermal stability between the rheometer and the feedstock (rheometer and

feedstock must be at 90°C), but must be short enough to prevent the segregation. On one hand, if the feedstock and the measurement equipment are not at the same temperature, this may produce a measurement error as long as the LPIM feedstocks are generally very sensitive to the temperature changes. On the other hand, if the time required to reach this thermal stability is too long (or if an exaggerated dead time is sustained before to start the test), low-viscosity feedstocks will segregate while producing, still again, a measurement error as long as the LPIM feedstocks are very sensitive to the solid loading changes. Therefore, the purpose of this section is to validate and improve the “short time testing” methodology developed by F. Fareh (Fareh 2016), previous student in our group, and highlight potential thermal stability that may occur when this kind of short time testing method.

Figure 4.2 presents the viscosity profiles of four different feedstocks obtained at different waiting conditions. The condition “No waiting” means that the molten feedstock was introduced into the rheometer and directly tested using the short time testing protocol developed by F. Fareh. This specific protocol consists in heating the feedstock at the given testing temperature outside the rheometer (as detailed in Figure 3.8 above), poured the molten feedstock into the rheometer, introduce hot testing mandrel into the molten feedstock (also detailed in Figure 3.8), and obtain the viscosity profile using a full testing cycle taking two minutes. The conditions “waiting 2 min” and “waiting 4 min” mean that the feedstock previously tested using the “No waiting” cycle was retested using the same molten sample directly after the first test (i.e., after 2 minutes poured into the barrel), and directly after the second test (i.e., after 4 minutes into the barrel).

For different feedstocks, it is clear that the curves obtained in “No waiting” (i.e., blue curves) are detached from the two other curves meaning that the testing conditions have been changed between the first and the two other tests. Since no parameter in the test methodology was changed, it is suggested that the feedstock was simply not thermally equilibrated during the first test, and this phenomenon appears irrespectively to the binder constituents. On one hand, it is interesting to note that this difference between the first and the second viscosity profile is sometime accentuated at the beginning of the test (i.e., left part of the curve obtained at low shear rate as indicated by a black arrow in Figure 4.2). On the other hand, this difference

between the first and the second viscosity profile tends to decrease reaching the values obtained with the second profile at the end of the first profile as indicated by a white arrow (i.e. the viscosity values obtained at high shear rate are very close because the test is performed from low to high shear rate). After the thermal equilibrium is reached, the second and third profiles are very repeatable for all feedstock formulations. It should also be noted that this phenomenon was sometimes not really visible especially when the thermal equilibrium was already reached due to rather long artificial dead time before starting the test (i.e. enough time spent before to perform the first profile which is not shown in Figure 4.2). In this respect, it was decided to enhance the testing protocol by introducing a thermal equilibrium stage consisting in two minutes of blending before to record the viscosity profile.

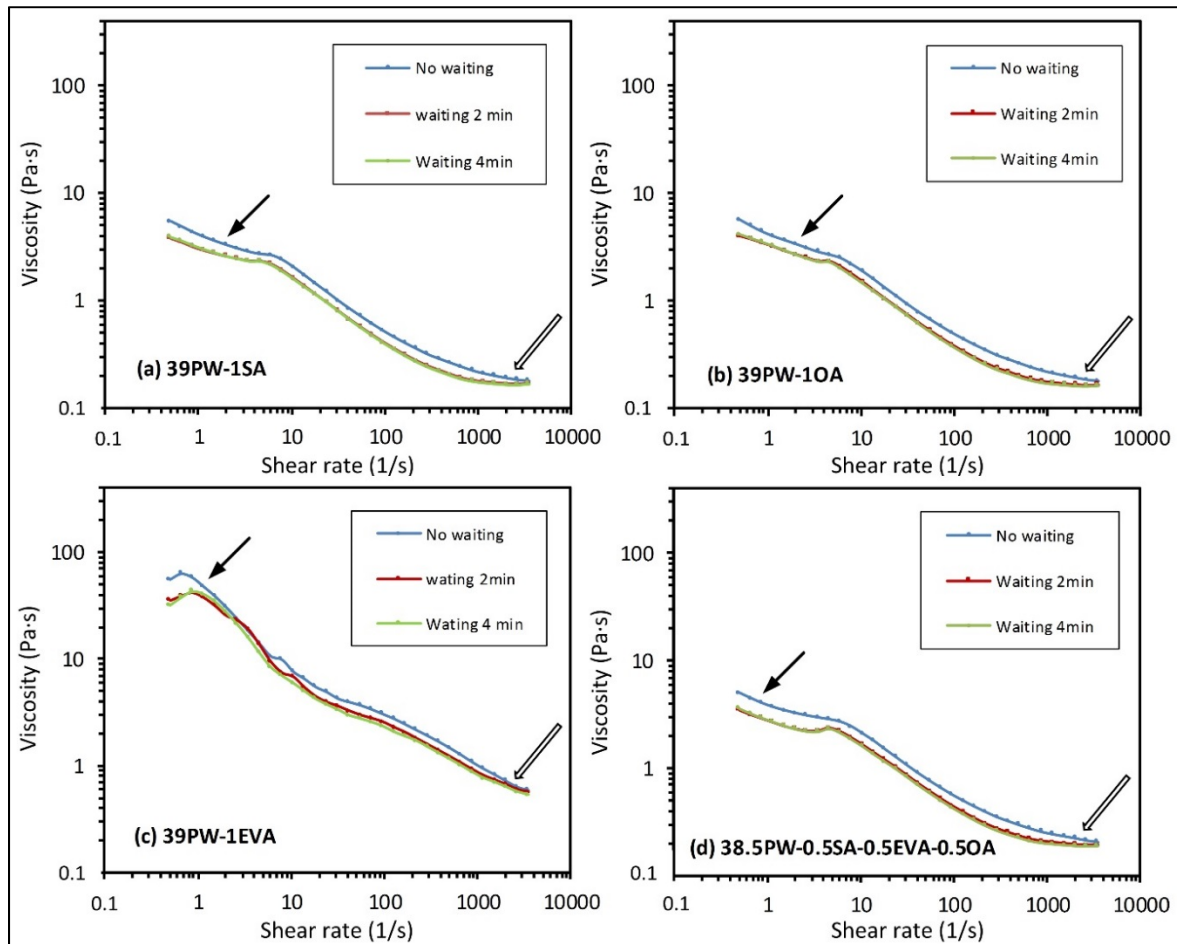


Figure 4.2 Viscosity profiles of feedstocks at different waiting time conditions.

### 4.3 Quantification of the repeatability of the rheological tests

Due to the very high quantity of tests planned during this Master project (i.e., more than 240 rheological profiles were obtained during this study), it was not possible to quantify the repeatability of each testing conditions. For this reason, this section proposes to quantify specifically the repeatability for two typical LPIM feedstocks (one low-viscosity and one high-viscosity feedstock) by calculating the variability of the viscosity profiles for the same feedstocks using different samples, and finally state the assumption that this variability can be reasonably apply to the rest of the project. Figure 4.3 illustrates the viscosity profiles obtained with different feedstocks recipes tested several time using the new test protocol developed above in section 4.1 and different samples (i.e., different molten mixture). In general, the viscosity profiles of feedstocks are very repeatable by their overlapping and sometime indistinguishable profiles. In order to assess the repeatability of these two feedstocks, it is proposed to calculate the average value of the viscosity obtained at a shear rate of  $100\text{ s}^{-1}$  and standard deviation of these average values as shown in Table 4.1.

Note that this reference shear rate value corresponds to the shear rate generally experienced by LPIM feedstocks during a typical injection. Values reported in Table 4.1 indicate that the standard deviation values calculated from these two typical feedstocks are relatively low (i.e. 0.07 Pa·s maximum) while this maximum values will be used to confirm the influence of binder constituents on viscosity values for the rest of this project.

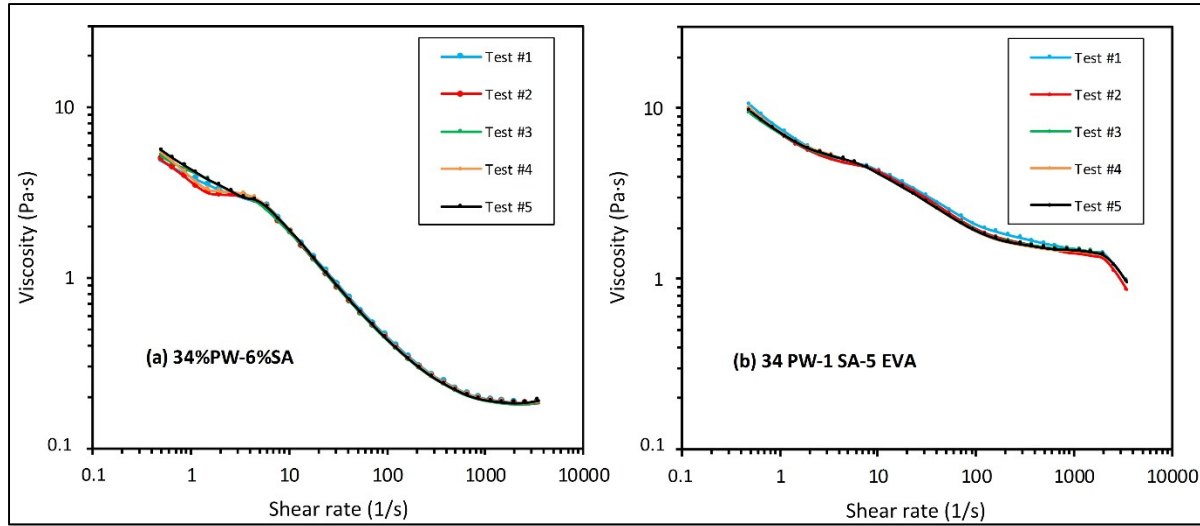


Figure 4.3 Viscosity profiles of feedstocks in different test samples.

Table 4.1 Quantification of the repeatability of the viscosity profiles

	Average viscosity at $100\text{ s}^{-1}$ (Pa·s)	Standard deviation (Pa·s)
34PW-5EVA-1SA	1.99	0.07
34PW-6SA	0.45	0.01

#### 4.4 Influence of single waxes binder on viscosity

In LPIM process, the wax is generally blended with other polymeric constituents to reach the proper rheological properties. Although that single wax binder is rarely used alone into the feedstock, this section studies the impact of each single binder on the viscosity of feedstocks to obtain simply a baseline that could be used in the framework of this study.

For feedstocks contained 40PW, 40MW1and 40MW2, it was impossible to measure the viscosity profiles of these feedstock because the contact of these waxes with the powder particle and the wettability were very poor at this solid loading, results the very thicker feedstock. For this reason, the solid loading of these feedstocks was changed to 57 vol. % of metallic powder and 43 vol. % of wax. These kinds of feedstocks were used only as references.

Figure 4.4 illustrates the viscosity profiles obtained with the 5 different single wax-based feedstocks. All single wax-based feedstocks exhibit a shear thinning effect follow by a near-Newtonian plateau visible at high shear rate. The feedstock producing the highest viscosity is constituted from the microcrystalline wax #1 (MW1) while the one producing the lowest viscosity is made from the paraffin wax (PW).

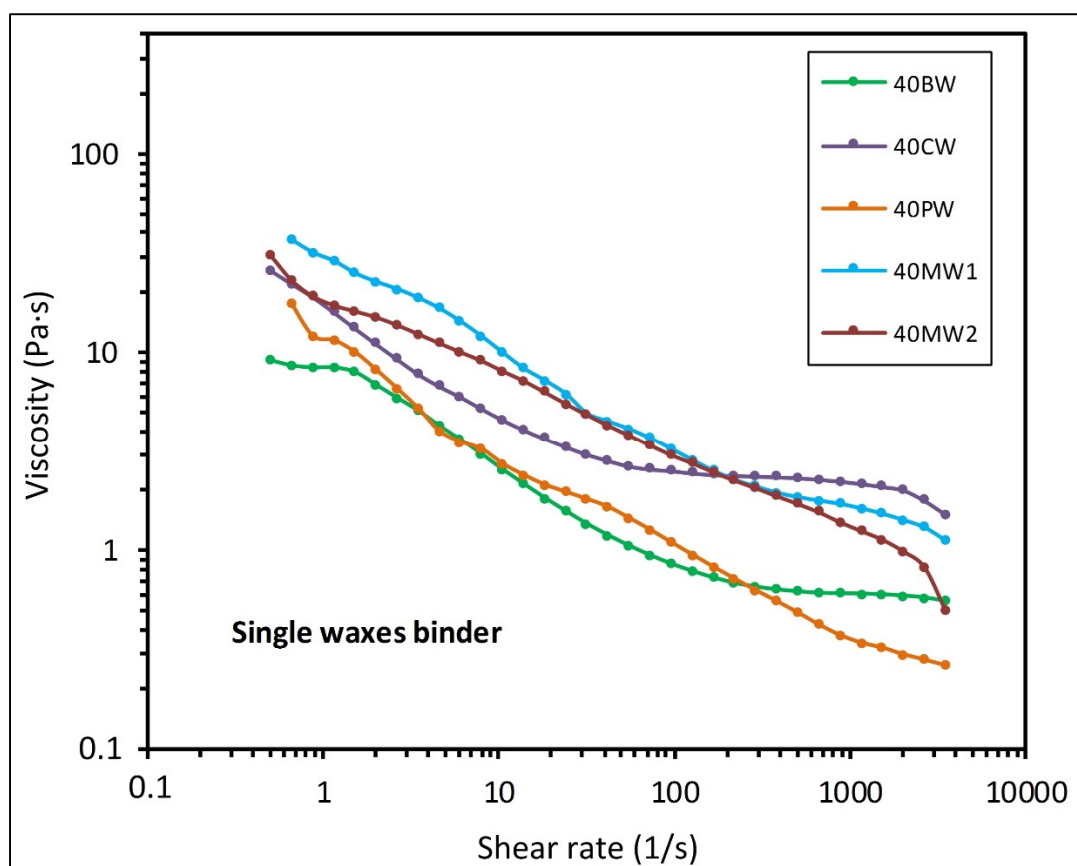


Figure 4.4 Viscosity profiles obtained with different single waxes-based feedstocks.

#### 4.5 Influence of surfactant agents on viscosity of wax-based feedstocks

The stainless steel 17-4PH powder typically has hydrophilic surface where organic binders such as waxes have generally low wettability on powder surface (i.e., difficulty to spread molten wax on solid particle). Consequently, a surfactant agent is often used during feedstock preparation in order to improve the wetting of powders and enhance the chemical bond between

powders and main binders. In this study, two different surfactant agents namely, stearic acid and oleic acid were used.

#### 4.5.1 Use of stearic acid into single wax-based feedstocks

As mentioned above, the proportion of stearic acid into the different waxes (PW, BW, CW, MW1, and MW2) has been changed to determine the threshold proportion (if exists) promoting the surfactant effect and better understanding the impact of this specific constituent on feedstock viscosity. Stearic acid is a saturated fatty acid generally used as a surfactant and softening agent in fabrication of soaps, cosmetics, detergents, lubricants, softening and release agents. At room temperature, it appears like a white granulated solid. Viscosity profiles obtained with five different wax-stearic acid based feedstocks are presented in Figure 4.5 where proportion of stearic acid (SA) was changed from 0.1 to 5 vol. %. In general, the viscosity value for all wax-SA-based feedstocks decreases with an increase of shear rate. This corresponds to the shear thinning behavior generally required for LPIM feedstock by generating a low viscosity value at high shear rate (i.e., during the injection stage of the process) and a high viscosity at low shear rate (i.e., during the mixing stage of the process or directly after the injection into the mold). Indeed, high viscosity is desirable during mixing to avoid segregation and maintain the homogeneity of the feedstock. In counterpart, the viscosity during injection phase is expected to be as low as possible to promote the mold filling and minimize the molding defects.

All viscosity profiles (except the one obtained with the CW-SA feedstock) present almost the same trend, where a near-Newtonian plateau is observed at low shear rate (e.g., between 0.5 and 2 s<sup>-1</sup> or up to 6 s<sup>-1</sup> for PW-SA feedstock). Then it followed by a clear shear thinning behavior, where the viscosity decreases as the shear rate increases (e.g., from 2 to 800 s<sup>-1</sup>), and where a second near-Newtonian plateau is finally seen at high shear rate (e.g., up to 3 500 s<sup>-1</sup>). The first plateau-like behavior is generally explained by the lack of binder molecule chains alignment due to the too low shear deformation applied at low speed. This plateau was observed for all feedstocks excepted for the one containing carnauba wax where the curves seem to start to stabilize at constant viscosity around 30 Pa·s. Although it was not possible to

test the feedstock at a shear rate value below  $0.5 \text{ s}^{-1}$ , this first plateau is anticipated and possibly visible at very low shear rate (left hand side of the curves in Figure 4.5c). At low shear rate, some PW-SA feedstocks (Figure 4.5a) demonstrate a hook in the viscosity profile characterized by a slight decrease in viscosity with increasing shear rate from  $0.5$  to  $0.9 \text{ s}^{-1}$  followed by an slight increase in viscosity with increasing shear rate from  $0.9$  to  $2 \text{ s}^{-1}$ . Hausnerova et al. (Hausnerova, Kasparcova et al. 2016) reported that this change from pseudoplastic to dilatant behavior at low shear rate can be explained by the difficulty to form particles layers leading in particles sliding over each other and producing an increase in viscosity. The second pseudoplastic behavior (i.e., the one observed from  $2$  to  $3000 \text{ s}^{-1}$  for all feedstocks) was explained by a restructuration of the mixture where polymer chains and particles alignment is promoted with increasing of shear rate. At high shear rates, the pseudoplastic regime is followed by a Newtonian-like plateau where entire binder molecules chains are aligned and where an increase in shear rate does not change the viscosity value.

For the PW-SA feedstocks (Figure 4.5a), the influence of the surfactant proportion is only visible at low shear rate (i.e.,  $< 10 \text{ s}^{-1}$ ). The minimal proportion of  $0.2$  vol. % of stearic acid into the paraffin wax seems to be required in order to decrease the viscosity below  $10 \text{ Pa}\cdot\text{s}$ , and where an increase from  $0.2$  to  $5$  vol. % produces a slight increase in viscosity, which is only visible on the first plateau. For all other feedstocks used in this study, similar rheological behavior was observed regardless of the proportion of surfactant. This is an important conclusion because several research teams use given stearic acid proportion as high as  $5$  vol. %, while the results presented in Figure 4.5 confirm that a quantity as small as  $0.2$  vol. % is enough to produce the surfactant effect.

Results presented in Figure 4.5b-c show that there is no impact of this surfactant agent on viscosity compared to the singles binder feedstocks. In this respect, it can also be concluded that stearic acid can be successfully used to significantly decrease the viscosity values specifically at high shear rate corresponding to the injection phase of the process.

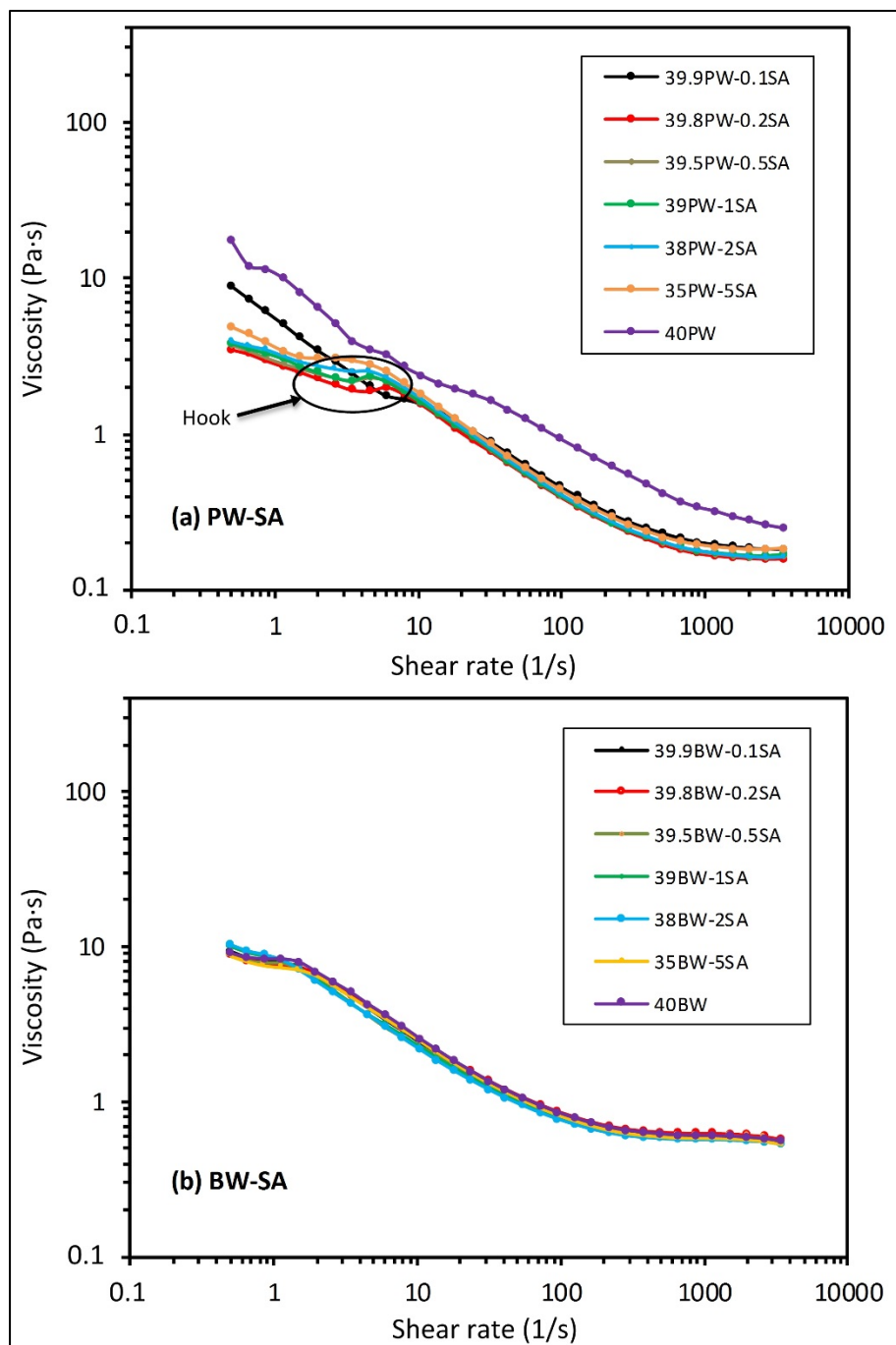


Figure 4.5 Viscosity profiles obtained with different wax-stearic acid based feedstocks: a) paraffin wax + stearic acid (PW-SA), b) beeswax + stearic acid (BW-SA), c) carnauba wax + stearic acid (CW-SA), d) microcrystalline wax #1 + stearic acid (MW1-SA), e) microcrystalline wax #2 + stearic acid (MW2-SA).

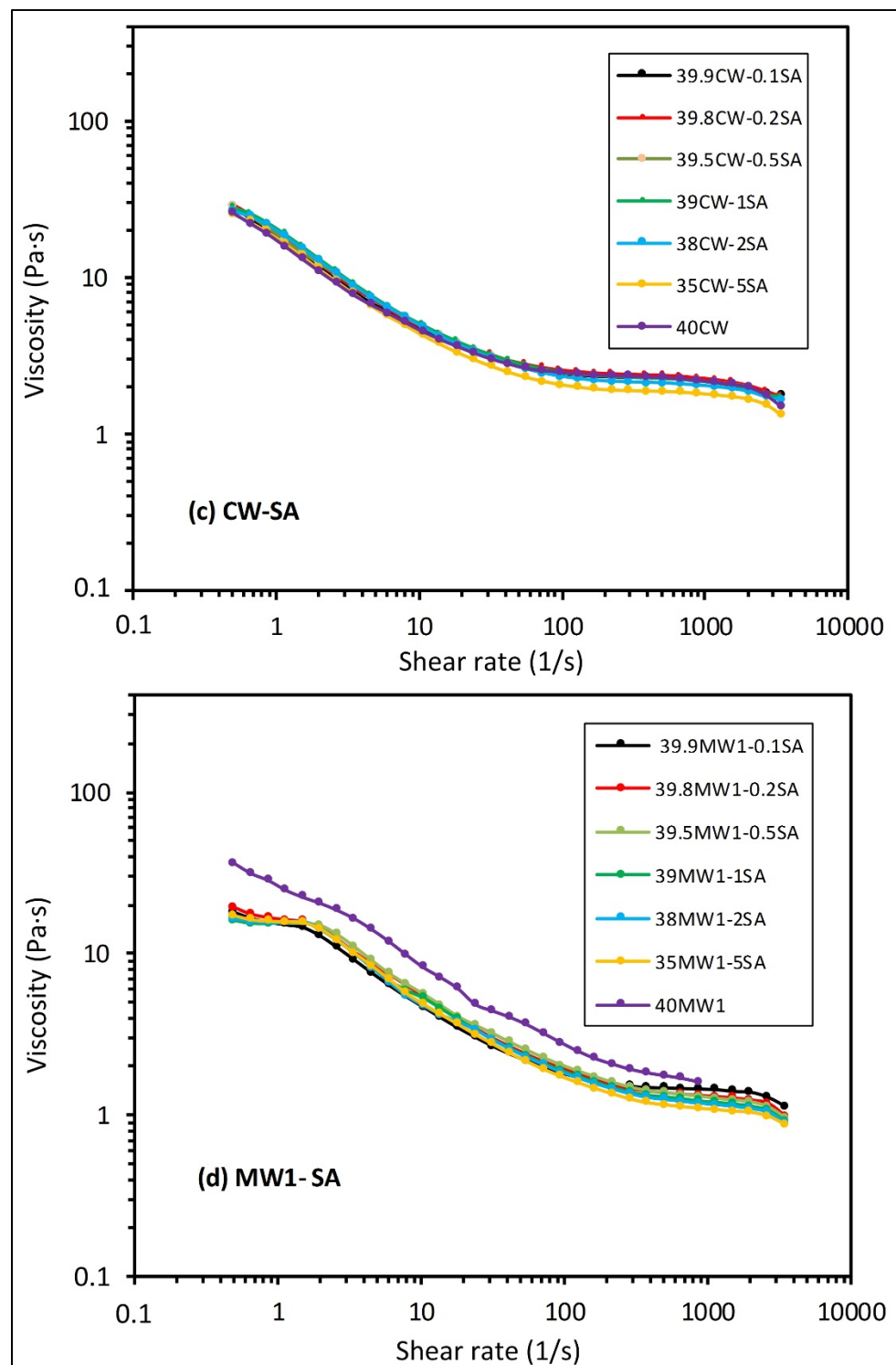


Figure 4.5 (continued)

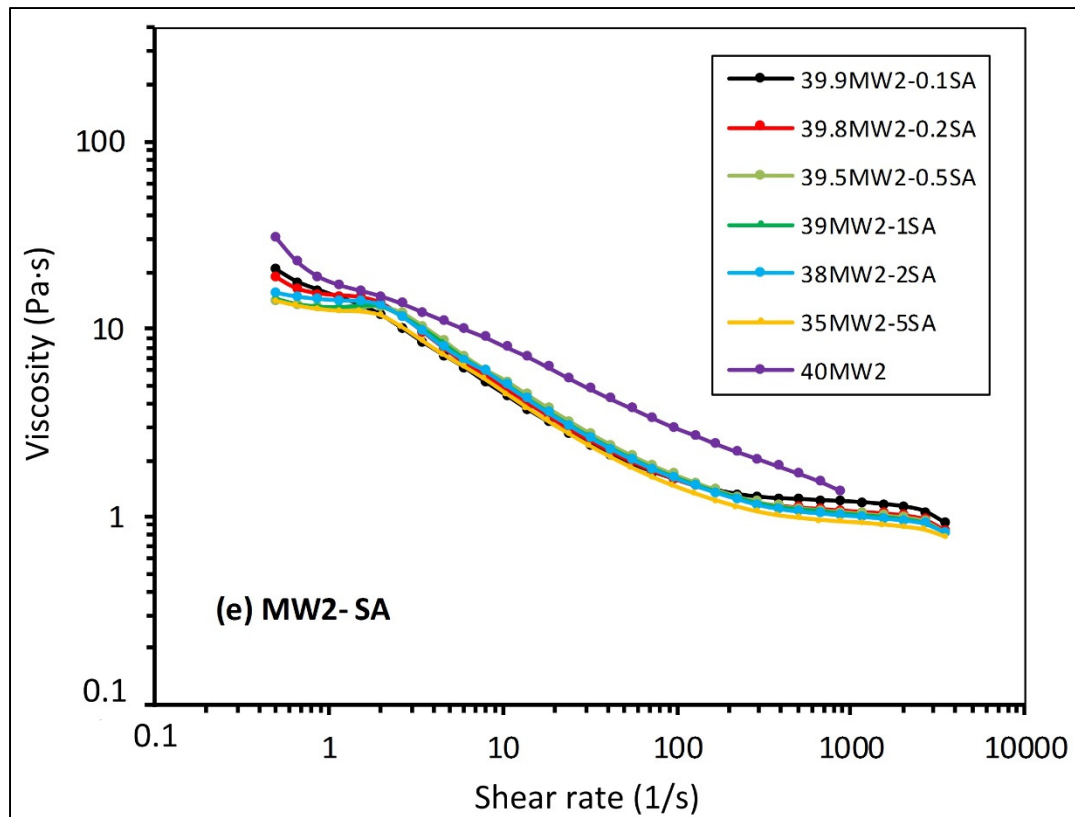


Figure 4.5 (continued)

#### 4.5.2 Use of oleic acid into single wax-based feedstocks

A second surfactant agent was tested in the framework of this study. Compared to stearic acid, which is solid at room temperature, the oleic acid has the particularity to be liquid at temperature above 13°C. This oil is a monounsaturated fatty acid present in many foods, and used as a component of soap and as an emulsifying agent. The proportion of oleic acid (OA) into different five waxes (PW, BW, CW, MW1, and MW2) has been changed from 0.5 to 5 vol. % (excepted for PW-based feedstock where 0.1 and 0.2 vol.% were added) to determine if a threshold proportion exist to promote the surfactant effect and to better understand the impact of this specific constituent on feedstock viscosity. Note that the small proportions ranging from 0.1 to 0.5 vol. % of oleic acid were difficult to measure due to its liquid state at room temperature (i.e., difficult to cut one drop in two parts). If this low-quantity

would be tested in future, it is thus proposed to increase the volume of the feedstock in order to minimize the possible error that may occur during the feedstock preparation.

The evolution of viscosity according to the shear rate for these five wax-OA based feedstocks is reported in Figure 4.6. The viscosity of all feedstocks decreases as the shear rate increases, which can be identified as the shear thinning behavior commonly desired for LPIM feedstocks. As described above, this kind of rheological behavior is explained by particle or binder molecule ordering with the flow. All wax-OA-based feedstocks generate roughly similar rheological behavior regardless of the proportion of surfactant. Indeed, the viscosity graphs are characterized by a near-Newtonian plateau for shear rates lower than  $2\text{ s}^{-1}$ , followed by a pseudoplastic behavior up to  $800\text{ s}^{-1}$ , and a second near-Newtonian behavior for shear rate values higher than  $800\text{ s}^{-1}$ . The first yield plateau behavior is generally explained by the lack of binder molecule chains alignment due to the too low shear deformation applied at low speed. This plateau was seen for all feedstocks excepted for the carnauba wax feedstock where the curves seem to stabilize at constant viscosity around  $30\text{ Pa}\cdot\text{s}$  for shear rate below  $0.6\text{ s}^{-1}$ .

For the PW-OA feedstocks (Figure 4.6a), a hook in the viscosity profile at low shear rate (i.e.,  $<8\text{ s}^{-1}$ ) is visible for specific oleic acid proportions varying from 0.1 to 1 vol. %. In this respect, it is interesting (and also surprising) to see that an increase in 2 to 5 vol. % of oleic acid into paraffin wax produce a double effect consisting in a significant increase in viscosity as well as the appearance of a shear thinning effect instead of a plateau at low shear rate. In other words, it can be stated that a quantity as small as 0.2 vol. % of oleic acid into PW-based feedstock seems to be sufficient to achieve the surfactant effect but an addition of high quantity of this surfactant agent annihilate the first plateau-like generally observed at low shear rate. Furthermore, results presented in Figure 4.6b-c show that there is no impact of this surfactant agent on viscosity compared to the singles binder feedstocks. As seen in previous section, blending of surfactant with different waxes produce different viscosity level as well as different values at which the second plateau occurs.

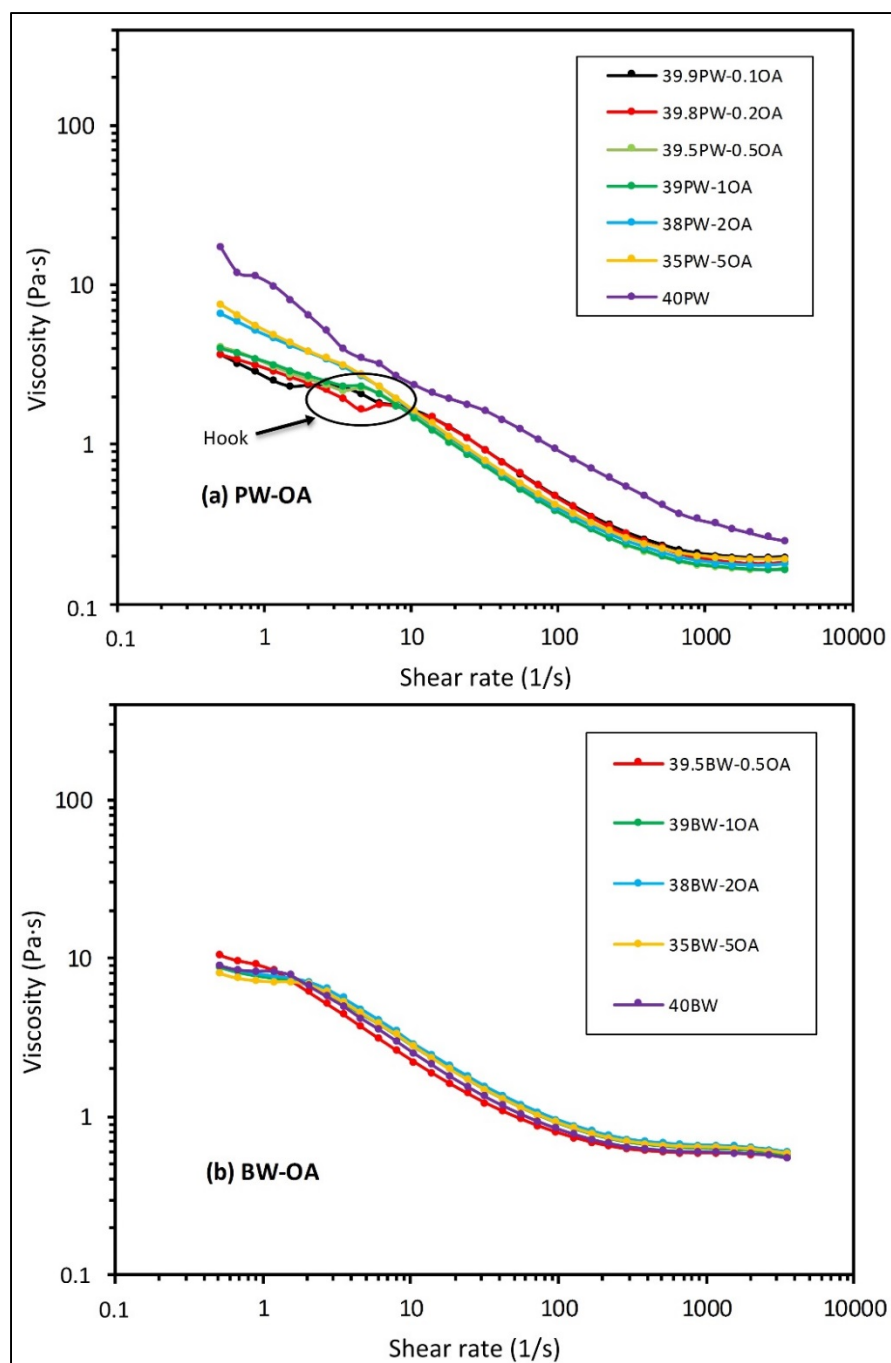


Figure 4.6 Viscosity profiles obtained with different wax-based feedstocks: a) paraffin wax + oleic acid (PW-OA), b) beeswax +oleic acid (BW-OA), c) carnauba wax + oleic acid (CW-OA), d) microcrystalline wax #1 + oleic acid (MW1-OA), e) microcrystalline wax #2 + oleic acid (MW2-OA).

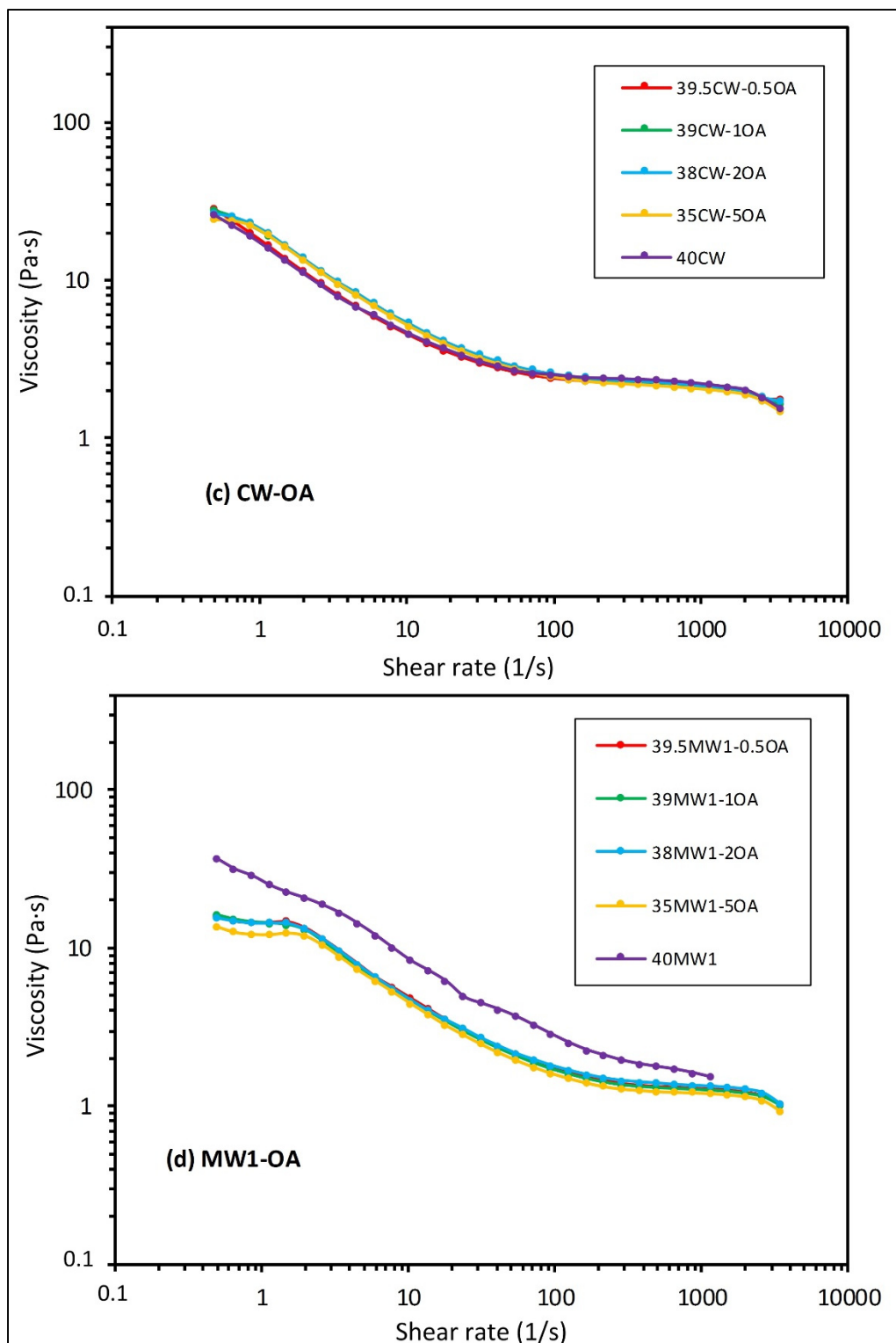


Figure 4.6 (Continued).

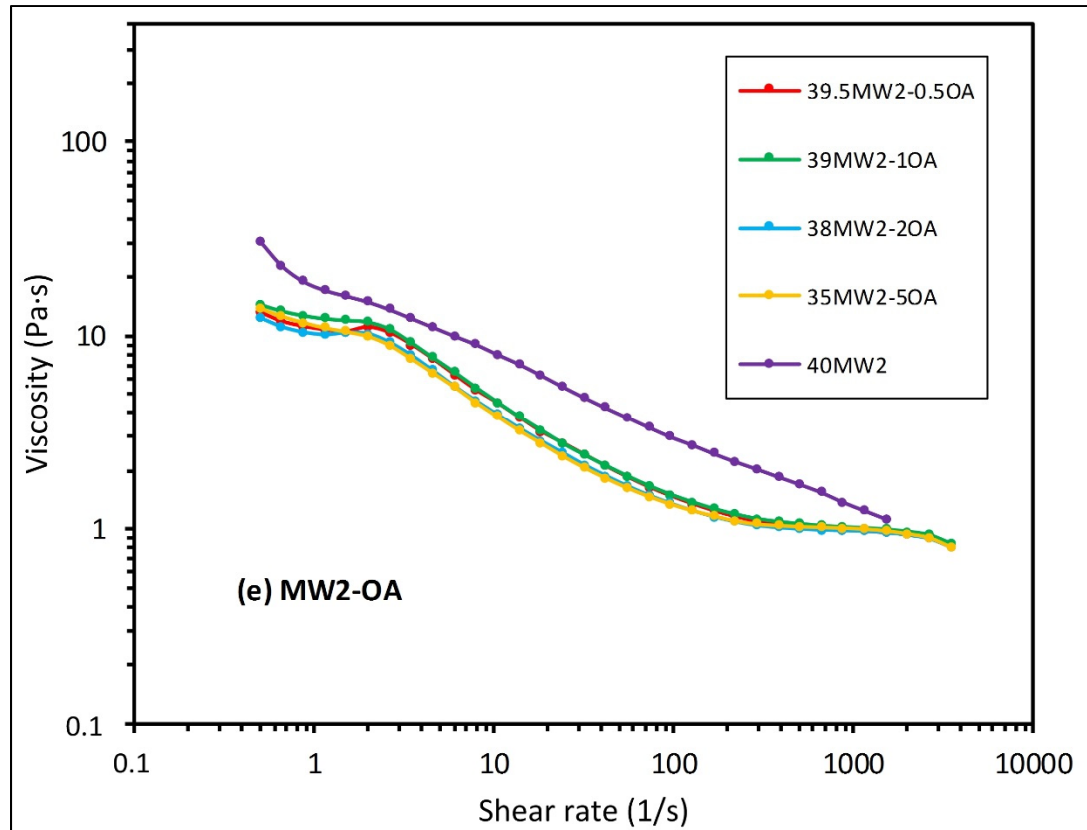


Figure 4.6 (Continued).

#### 4.5.3 Comparison between surfactant agents

In this work, two types of surfactant agents were used for enhancing the powder-binder interaction, promoting the homogeneity of the feedstock, and decreasing the viscosity of the feedstocks. Figure 4.7 summarizes the impact of surfactant agents on the viscosity of paraffin wax-based feedstocks (i.e., data extracted from Figure 4.5a and Figure 4.6a). It is interesting to note that these surfactant agents produce almost the same effect on viscosity profiles. Indeed, the viscosity values obtained at low and high shear rates are similar, and the shear thinning effect is visible in the similar shear rate range. However, it is interesting to highlight that high viscosity values (around 8-10 Pa·s) are not obtained in the same proportion range. For PW-SA feedstocks, high viscosity is obtained when proportion of SA is very small while viscosity profile turn to high viscosity value when the proportion of OA becomes large (2 and 5 vol. %) for PW-OA feedstocks, where large proportion of SA has no detrimental impact on viscosity.

From this study, it can be concluded that these two surfactants proposed different advantages and limitations. On one hand, it is suggested to use the stearic acid (SA) as a surfactant agent instead of using oleic acid (OA) when small quantity must be used due to the difficulty in measurement of very small amount of oleic acid (i.e., not suitable to use small quantity). However, oleic acid seems to presents a certain advantage in increasing viscosity at low shear rate (e.g., during the blending phase of the process) without producing any change in low viscosity visible at high shear rate (i.e., during the injection phase). It is propose to study this interesting trend in a future work involving real scale injection to confirm this potential beneficial influence of oleic acid on moldability of feedstocks.

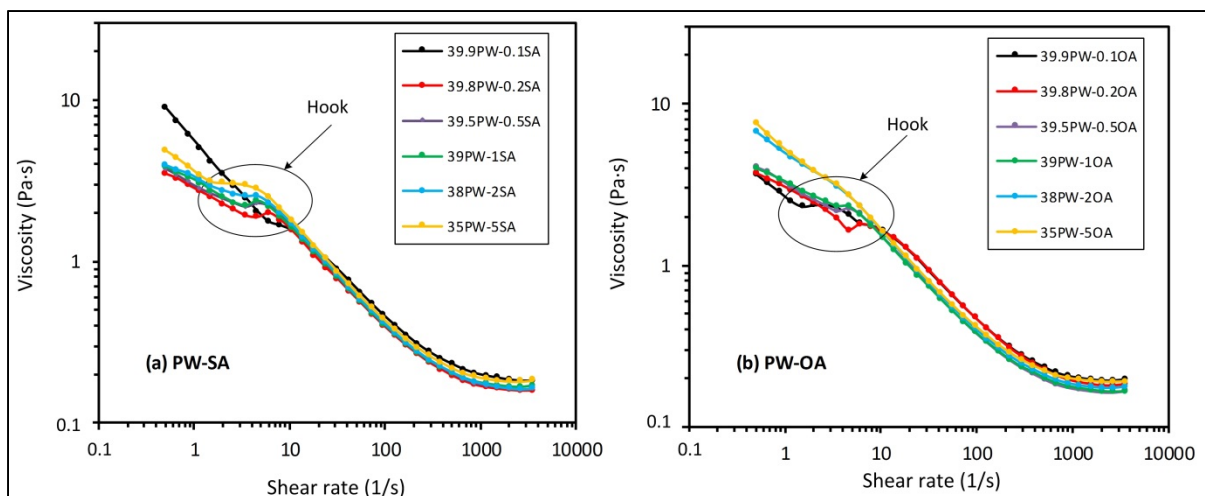


Figure 4.7 Viscosity profiles obtained with paraffin wax-based feedstocks: (a) paraffin wax + stearic acid (PW-SA), and (b) paraffin wax + oleic acid (PW-OA).

#### 4.6 Influence of thickening agent on viscosity of wax-based feedstocks

As stated above, thickening agent is generally used to increase the viscosity of feedstocks in order to prevent powder-binder separation and increase the strength of the green parts after the injection. This section presents the rheological results obtained with different feedstocks formulation containing ethylene vinyl acetate or low-density polyethylene into single wax-based or multiple-waxes-based feedstocks.

#### **4.6.1 Use of ethylene vinyl acetate into single wax-based feedstocks**

Three different waxes (PW, MW1, and MW2) were used to study the impact ethylene vinyl acetate (EVA) on the viscosity of feedstocks. It was decided to vary the EVA proportion of 0.5, 1, and 2 vol. % to determine its threshold proportion promoting thickening effect. Our previous group study has demonstrated that a very small quantity of EVA blended with paraffin wax could produce an intricate surfactant effect (Demers, Turenne et al. 2015). Surprisingly, the results presented Figure 4.8 shows that a small proportion of EVA produces almost no changes in viscosity profiles which is in opposite with our previous group results. In this study, viscosity of all wax-EVA-based feedstocks decreases with an increase of shear rate (shear thinning behavior). The viscosity values at low and high shear rates are probably too high to create homogeneous feedstocks during the mixing stage at low shear rate and to be properly injected at high shear rate. However, an erratic rheological behavior was clearly visible in all curves that was explained by a certain inhomogeneity of the feedstocks generated by the absence of surfactant agent generally required to promote the contact of powder with the rest of binders.

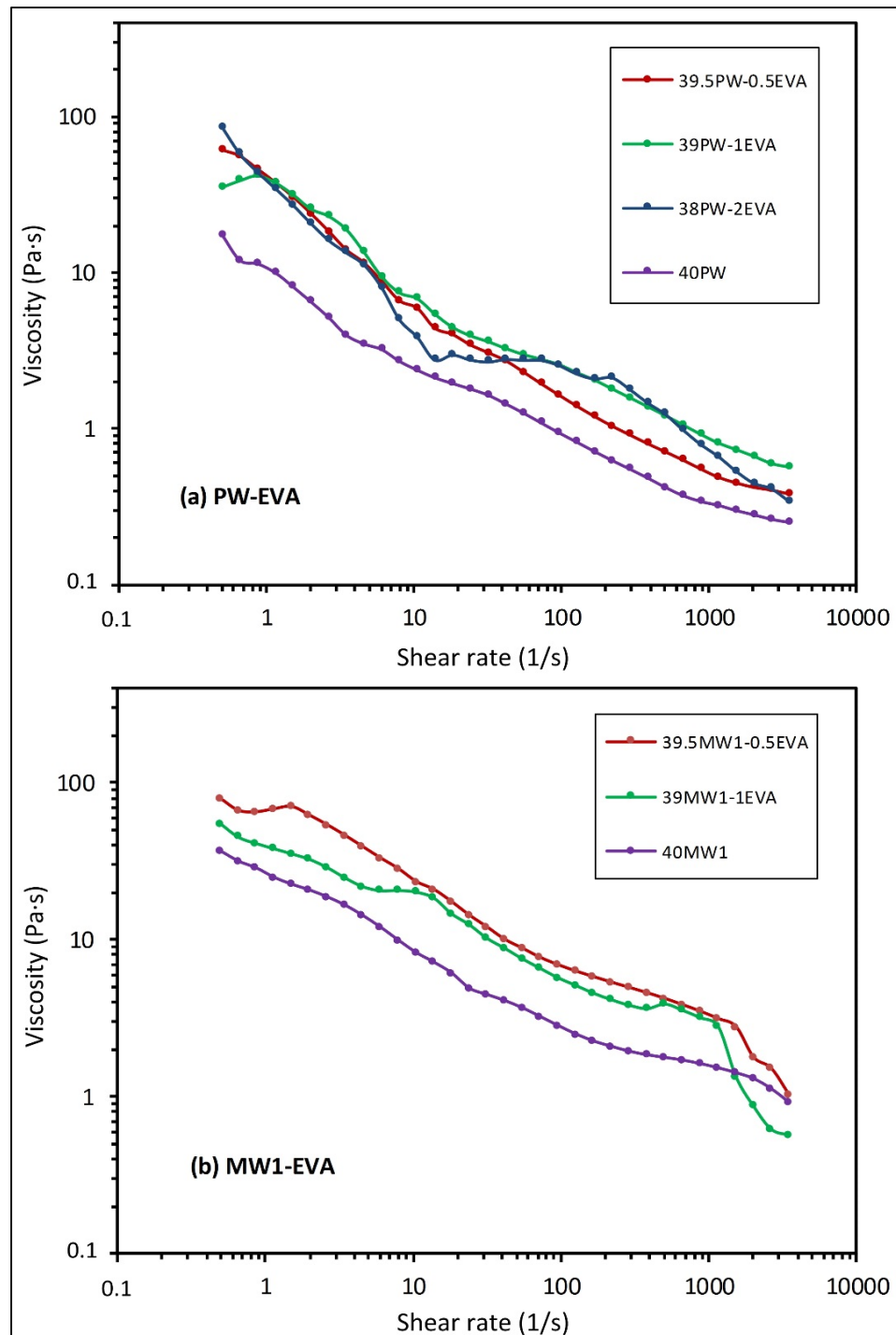


Figure 4.8 Viscosity profiles obtained with different wax-based feedstocks:a) paraffin wax + Ethylene vinyl acetate (PW-SA), b) microcrystalline wax #1 + Ethylene vinyl acetate (MW1-EVA), and c) microcrystalline wax #2+ Ethylene vinyl acetate (MW2-EVA).

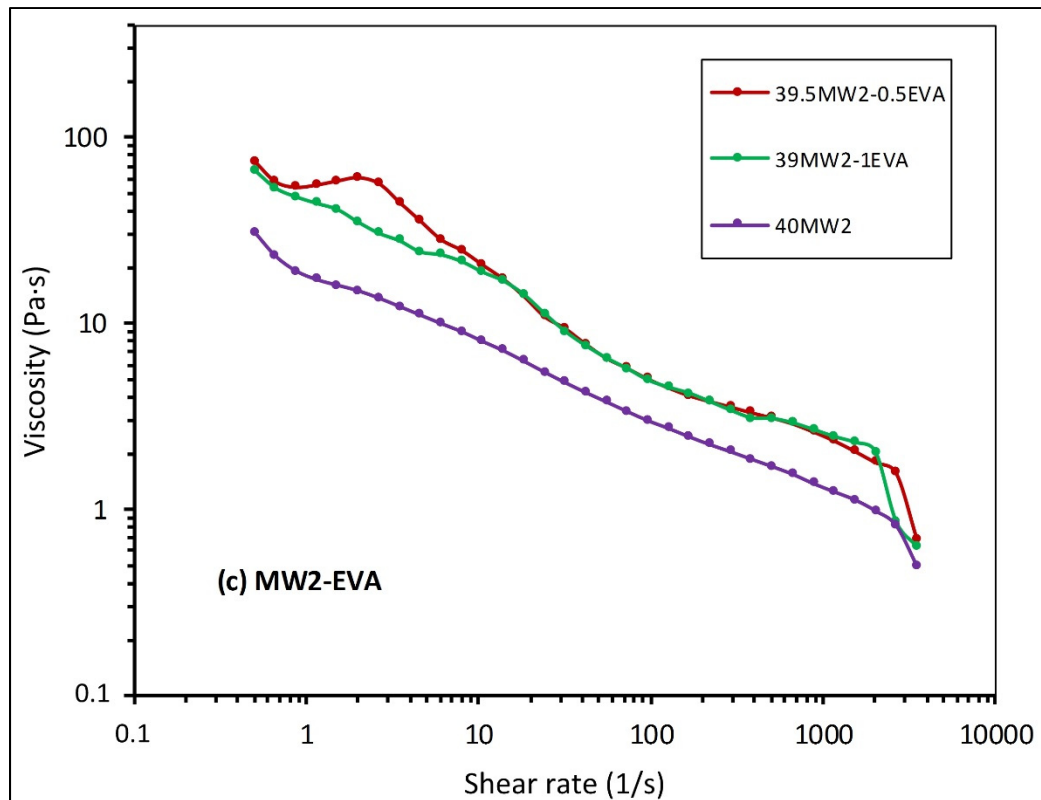


Figure 4.8 (Continued).

#### 4.6.2 Combination of stearic acid with ethylene vinyl acetate into single wax-based feedstocks

This section proposes to study the impact of combination of single wax-binder with surfactant agent and thickening agent on viscosity of wax-based feedstocks. Large amount of feedstocks was prepared using two categories of blend (0.5SA-EVA and 1SA-EVA) in order to confirm the threshold proportion of stearic acid determine above as well as to catch the possible chemical interactions occurring between SA and EVA.

##### 0.5 vol. % of SA-EVA Group

The purpose of this section is specifically to confirm the threshold proportion of stearic acid (SA) and ethylene–vinyl acetate (EVA) into waxes-based feedstocks. To reach this objective, a small quantity of SA (0.5 vol. %) was firstly combined with EVA into single waxes-based

feedstocks. This small value of SA was set based on the results obtained in section 4.4 where it was demonstrated that 0.2 vol. % of stearic acid was enough to produce a surfactant effect, and this value is the threshold of the surfactant agent. It is maybe a critical limit. For this reason, it is decided to increase the value of the surfactant agent to 0.5 vol. % in order to be sure that the effect of the surfactant is fully achieved. Therefore, the proportion of SA was fixed while the thickening agent and the single waxes were varied to balance a solid loading of 60 vol. % of powder to demonstrate the thickening effect as well as to propose a binder mapping that could be used in the future for the feedstocks tailoring. In this respect, EVA was combined with five waxes (i.e., separately to PW, BW, CW, MW1, and MW2) and with 0.5 vol.% of SA using a proportion of 0.5 to 5 vol.%. of EVA (excepted for PW-0.5SA-EVA feedstock where it was possible to blend up to 10 vol.% of EVA).

Viscosity profiles obtained with these five different wax-SA-EVA feedstocks are presented in Figure 4.9. The viscosity of all feedstocks decreases as the shear rate increases, which is the shear thinning behavior generally wanted for LPIM feedstocks. Expected trend was obtained for all viscosity profiles where an addition of EVA leads in an increase in viscosity.

In this respect, it was noted that an increase to 2 vol. % of EVA was required to visualize a significant thickening effect. In general, the viscosity profile of wax-SA-EVA feedstock indicates a pseudoplastic behavior followed by a near-Newtonian plateau for shear rates higher than  $100\text{ s}^{-1}$ . Some of feedstocks was also characterized by a near-Newtonian plateau at low shear which were partially (in PW-0.5SA-EVA and BW-0.5SA-EVA) or clearly (in MW1-0.5SA-EVA and MW2-0.5SA-EVA) visible. As explained above, this plateau-like behavior is generally explained by the lack of binder molecule chains alignment due to the too low shear deformation applied at low speed. For PW-0.5SA-EVA and BW-0.5SA-EVA, this plateau was observed only when small quantity of EVA was added into the waxes-based feedstock, while this plateau seems to disappear with more quantity of EVA was added to the mixture. This could be explained by the longer molecule chains of EVA compared to paraffin wax promoting the alignment (i.e., pseudoplastic effect could be more visible if there is something to align). Finally, it is interesting to note that the thickening effect seems to be more pronounced for certain binder families (PW, BW, and CW) compared to other (MW1 and MW2).

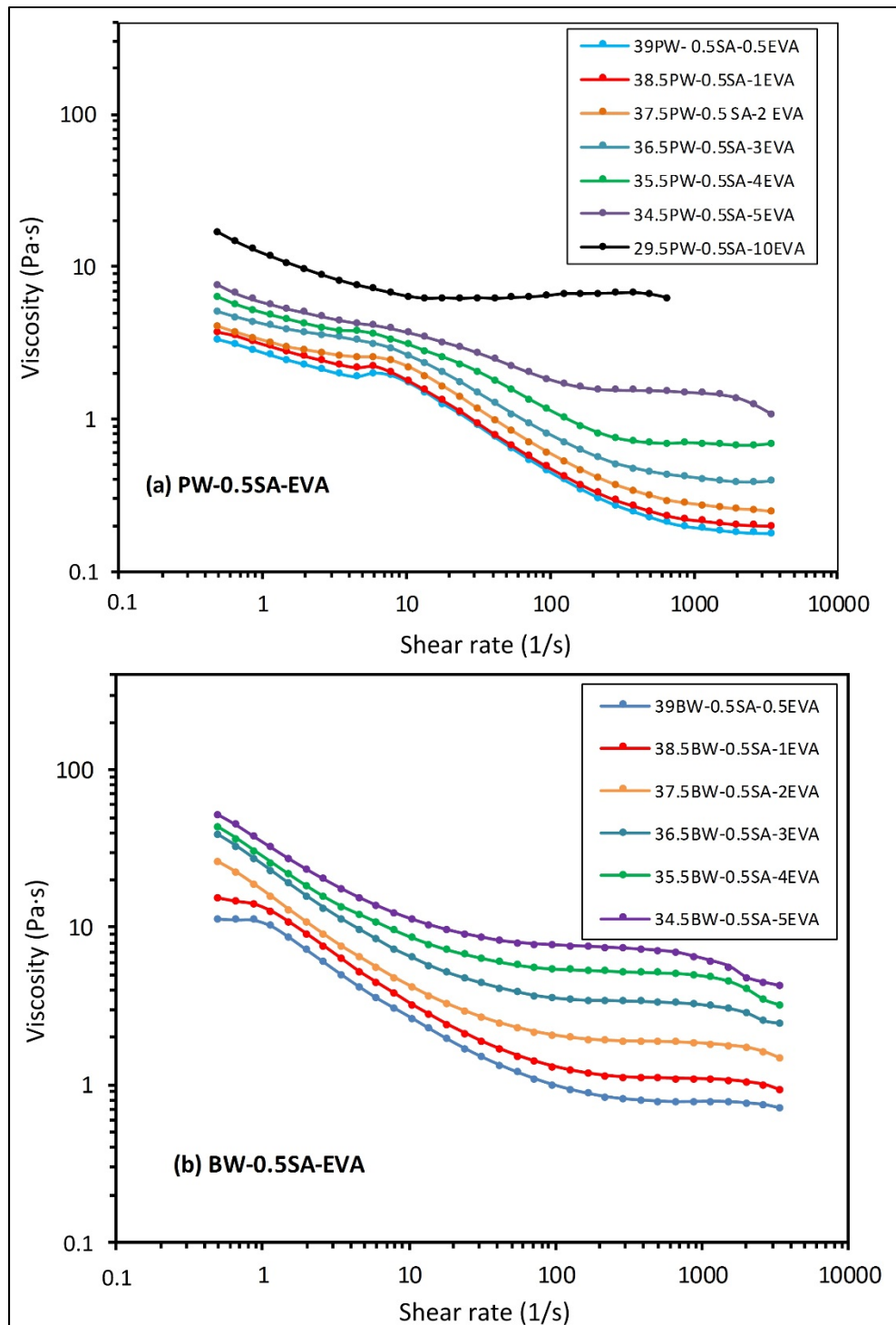


Figure 4.9 Viscosity profiles obtained with different wax-based feedstocks: a) PW+0.5SA+EVA, b) BW+0.5SA+EVA, c) CW+0.5SA+EVA, d) MW1+0.5SA+EVA, and e) MW2+0.5SA+EVA.

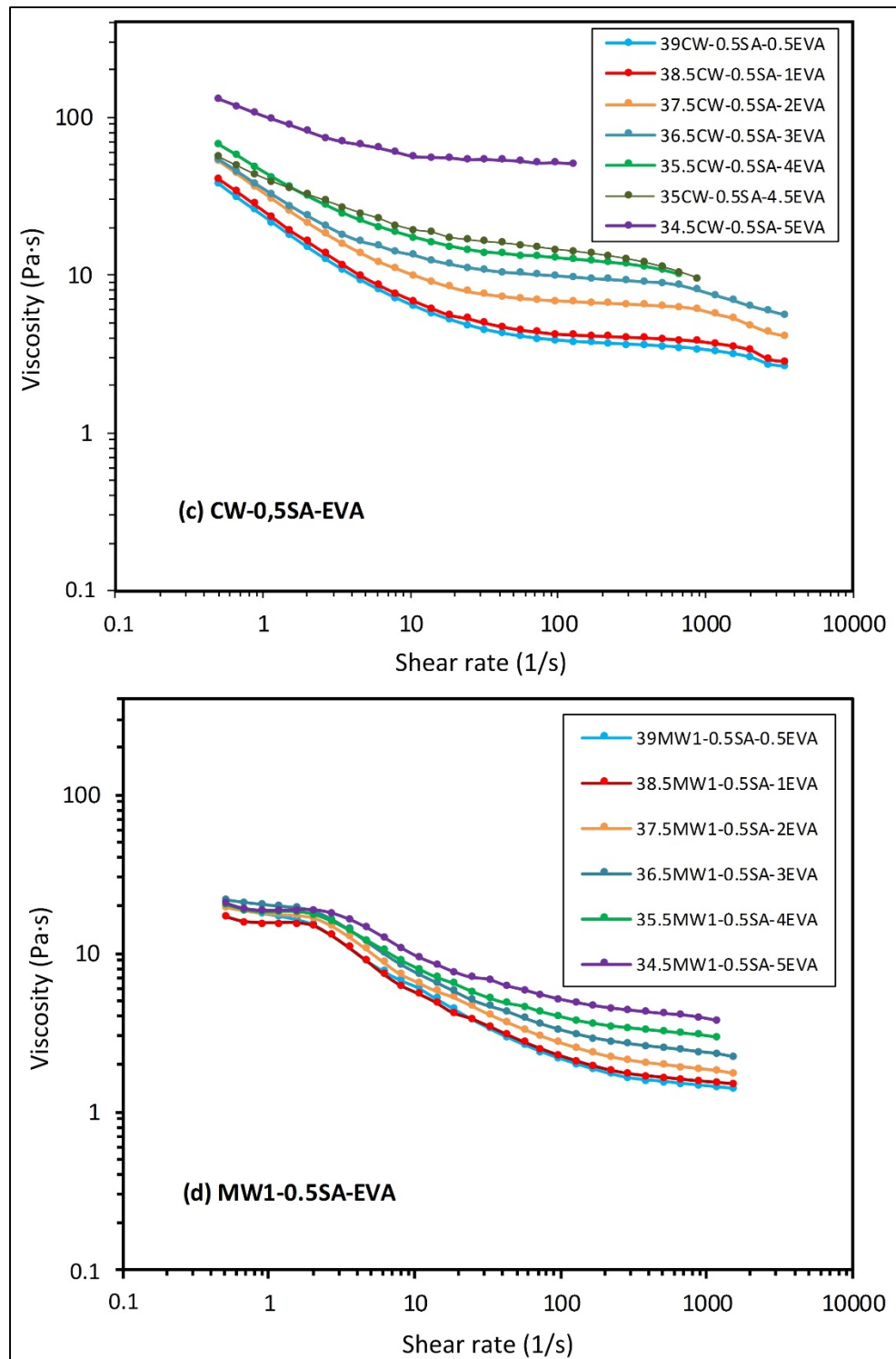


Figure 4.9 (Continued).

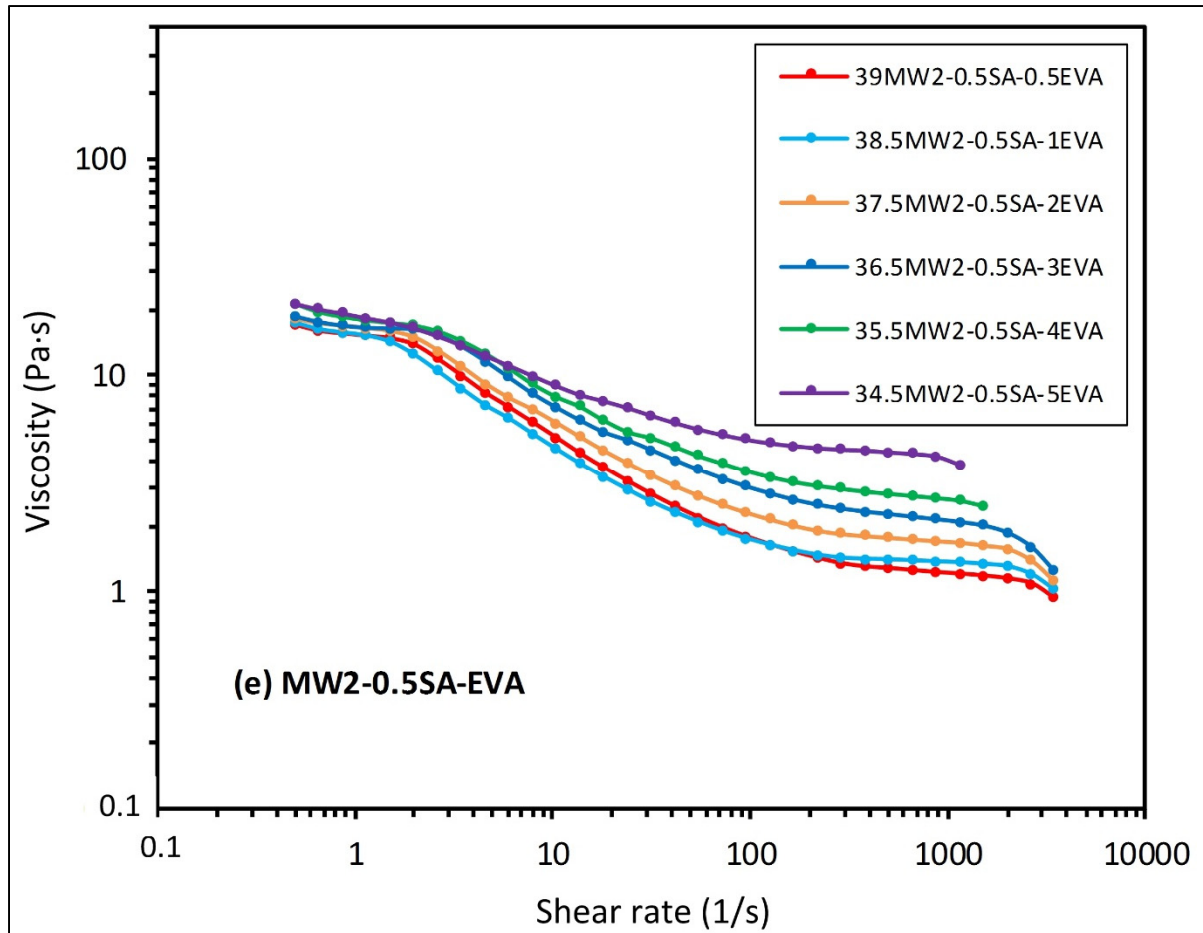


Figure 4.9 (Continued).

### 1 vol. % of SA-EVA Group

A test plan including a larger proportion of SA was proposed to confirm if the threshold proportion of 0.5 vol. % of SA could be maintained to produce the surfactant effect in the future (i.e., discard the possible chemical interaction between SA and EVA). Moreover, the proportion of SA was increased to use a similar quantity compared to many authors in literature (Demers, Turenne et al. 2015, Demers V. 2017). Therefore, it was planned to repeat the rheological tests for all waxes-SA-EVA with the 1 vol. % of stearic acid (SA).

The proportion of EVA varying from 0.5 to 3 vol. % was added into five different waxes (PW, BW, CW, MW1, and MW2) and with 1 vol. % of SA (excepted for PW-1SA-EVA feedstock where 4, 5 and 10 vol. % of EVA were added) to define the threshold proportion of EVA

promoting thickening effect and to better understand the impact of this ingredient on viscosity of feedstock. Figure 4.10 indicated that the viscosity of all feedstocks decreases as the shear rate increases (shear thinning behavior already studied above). Similar trend than the previous section was observed where the viscosity increases as the EVA proportion increases (i.e., similar trend from the bottom to top correspond to the proportion of EVA from low to higher quantity). It is interesting to note that there is no significant difference between 0.5SA-EVA and 1SA-EVA results (see Figure 4.9 and Figure 4.10). This confirms that 0.5 vol. % of SA is really sufficient to produce surfactant effect (i.e., no measurable chemical interaction between EVA and SA altering the conclusion drawn above) and demonstrating that EVA is a suitable constituent to tailor the viscosity of LPIM feedstocks.

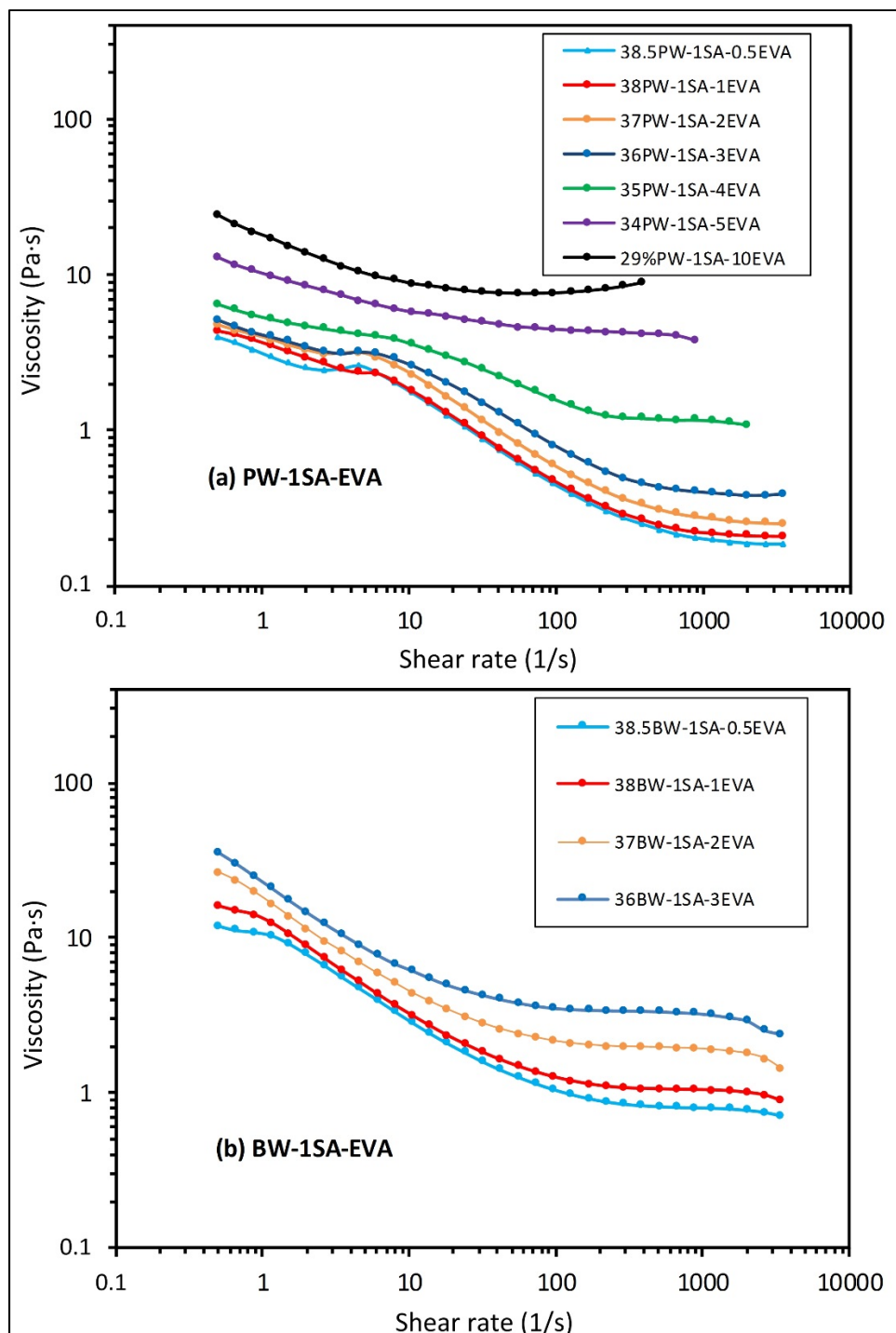


Figure 4.10 Viscosity profiles obtained with different wax-based feedstocks: a) PW+1SA+EVA, b) BW+1SA+EVA, c) CW+1SA+EVA, d) MW1+1SA+EVA, and e) MW2+1SA+EVA.

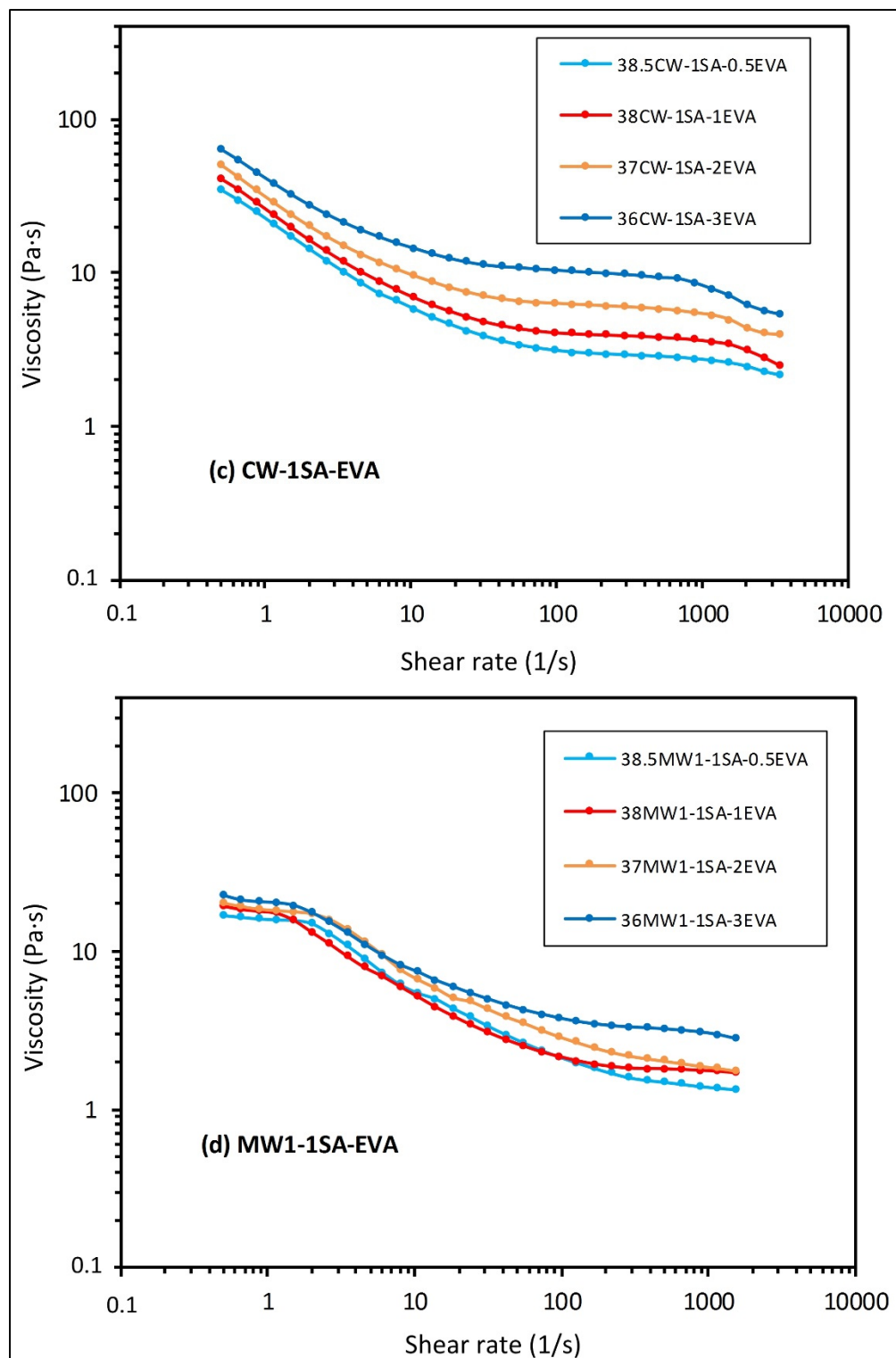


Figure 4.10 (Continued).

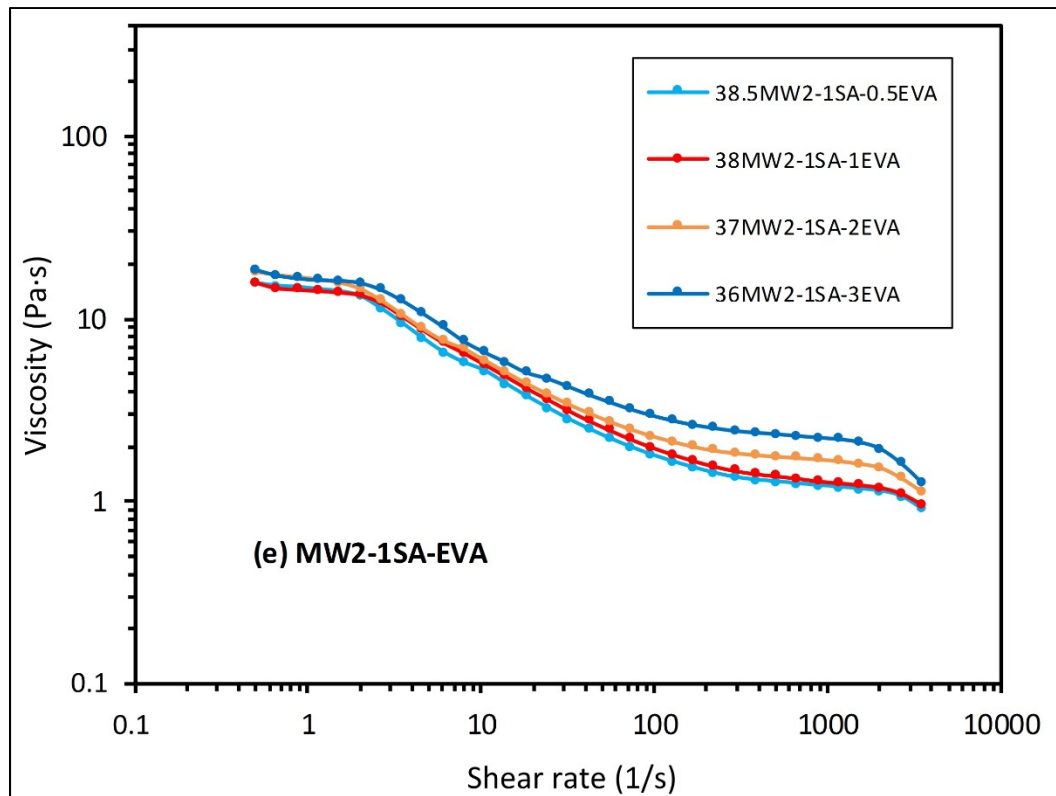


Figure 4.10 (Continued).

#### 4.6.3 Comparison between thickening agents

The role of thickening agents such as ethylene vinyl acetate (EVA) and low-density polyethylene (LDPE) is to tailor the viscosity properties of LPIM feedstock in order to propose the lower viscosity during injection and higher viscosity during dead time of the process to avoid segregation. This short test plan including a second thickening agent was conducted with paraffin wax-based feedstocks, which were combined with 0.5 % vol. of stearic acid and with different proportion of ethylene vinyl acetate (i.e., typical results presented above in Figure 4.9a and reported in Figure 4.11a), and different proportion of low-density polyethylene (LDPE) as it illustrated in Figure 4.11b. As expected, the viscosity profiles of feedstocks in both situations decreases with the increase of shear rate (shear thinning behavior). Moreover, it is clear that an addition of LDPE produces a higher impact on viscosity value. Indeed, this specific constituent is commonly used in the formulation of conventional high-pressure powder

injection molding feedstock (see section 1.1.1) where this latter often used in a proportion up to 15 vol. % producing a feedstock viscosity up to 1,000 to 10,000 Pa·s. Also, it can be concluded that an addition of a small quantities of thickening agents in paraffin wax-based feedstocks generate no significant differences in viscosity values in both case (i.e. EVA or LDPE) while an addition of 3 vol. % of each ingredient produce a significant increase in viscosity.

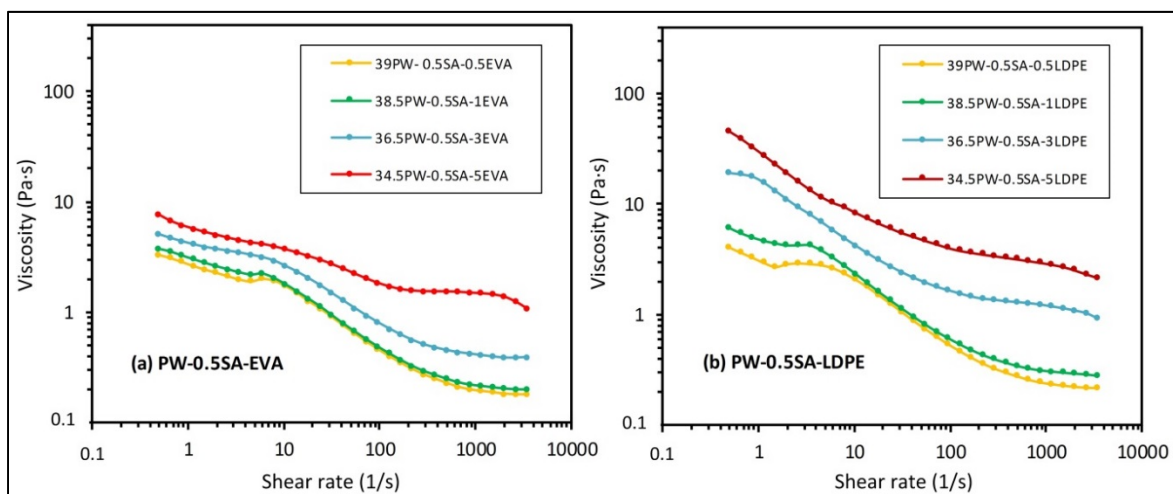


Figure 4.11 Viscosity profiles obtained with paraffin wax-based feedstocks: (a) paraffin wax+ stearic acid + Ethylene vinyl acetate (PW-SA-EVA) and (b) paraffin wax + stearic acid + low density polyethylene (PW-SA-LDPE).

#### 4.6.4 Combination of stearic acid with ethylene vinyl acetate into multiple waxes-based feedstocks

Figure 4.12 presents the viscosity profiles obtained with the feedstocks formulated from similar combination of stearic acid with ethylene vinyl acetate but using more complex combination of multiple waxes-based binders. The viscosity of all feedstocks decreases with shear rate (shear thinning behavior). The viscosity profile of the feedstock made entirely of BW (40BW), is characterized by a typical “S” curves where a near-Newtonian plateau is followed by a pseudoplastic behavior which is turned in a second near-Newtonian behavior at high shear rate (Figure 4.12b). Although that the shape of the curve is not changed, an addition of PW into BW (feedstock 20PW-20BW) produces a decrease in viscosity compared to the feedstock

40BW (Figure 4.12b). Likewise, an addition of surfactant agent and a thickening agent (SA-EVA) into this multiple binder-based (PW-BW) produces an increase in viscosity due to the presence of the EVA as shown in Figure 4.12b. On the other hand, an addition of PW into CW (feedstock 20PW-20CW) change the shape of the single CW binder viscosity profile and causes similar but more pronounced effect (i.e., decrease in viscosity) than a blend with BW (Figure 4.12c). Moreover, the combination of the (PW-CW) mixture with a surfactant agent and a thickening agent (SA-EVA) produces an increase in viscosity up to reach its initial viscosity profile (i.e., feedstock 40CW) in term of shape and magnitude (Figure 4.12c). The third combination proposed in this study consists in the interaction between two natural waxes (20BW-20CW) where the viscosity value seems to results proportionally from the viscosity values of their initial ingredient for entire shear rate (i.e., located between the curves obtained with the single-binder formulations 40CW and 40BW, Figure 4.12d). It is interesting to note that the combination of the BW-CW mixture with a surfactant agent and a thickening agent (SA-EVA) produces a higher increase in viscosity compared to the similar feedstock formulated with PW-CW (i.e., 19.5PW-18CW-0.5SA-2EVA vs 18BW-19.5CW-0.5SA-2EVA), where this latter feedstock could be suitable for increasing viscosity at low shear rate while producing an acceptable viscosity at high shear rate (Figure 4.12 c vs d). Finally, an addition of PW in the mixture of natural waxes (feedstock 14PW1-13BW-13CW) produces a decrease in viscosity compared to the feedstock 20BW-20CW (Figure 4.12 a). Besides, the combination of the PW-BW-CW mixture with a surfactant agent and a thickening agent (0.5AS-EVA) produces an increase in viscosity according to the proportion of the thickening agent but finally, produce similar behavior than the less complex feedstock 19.5PW-18CW-0.5SA-2EVA. In other words, it seems that there is no advantage to use the feedstock 11.5PW-13BW-13CW-0.5SA-2EVA instead of 19.5PW-18CW-0.5SA-2EVA in term of rheological properties.

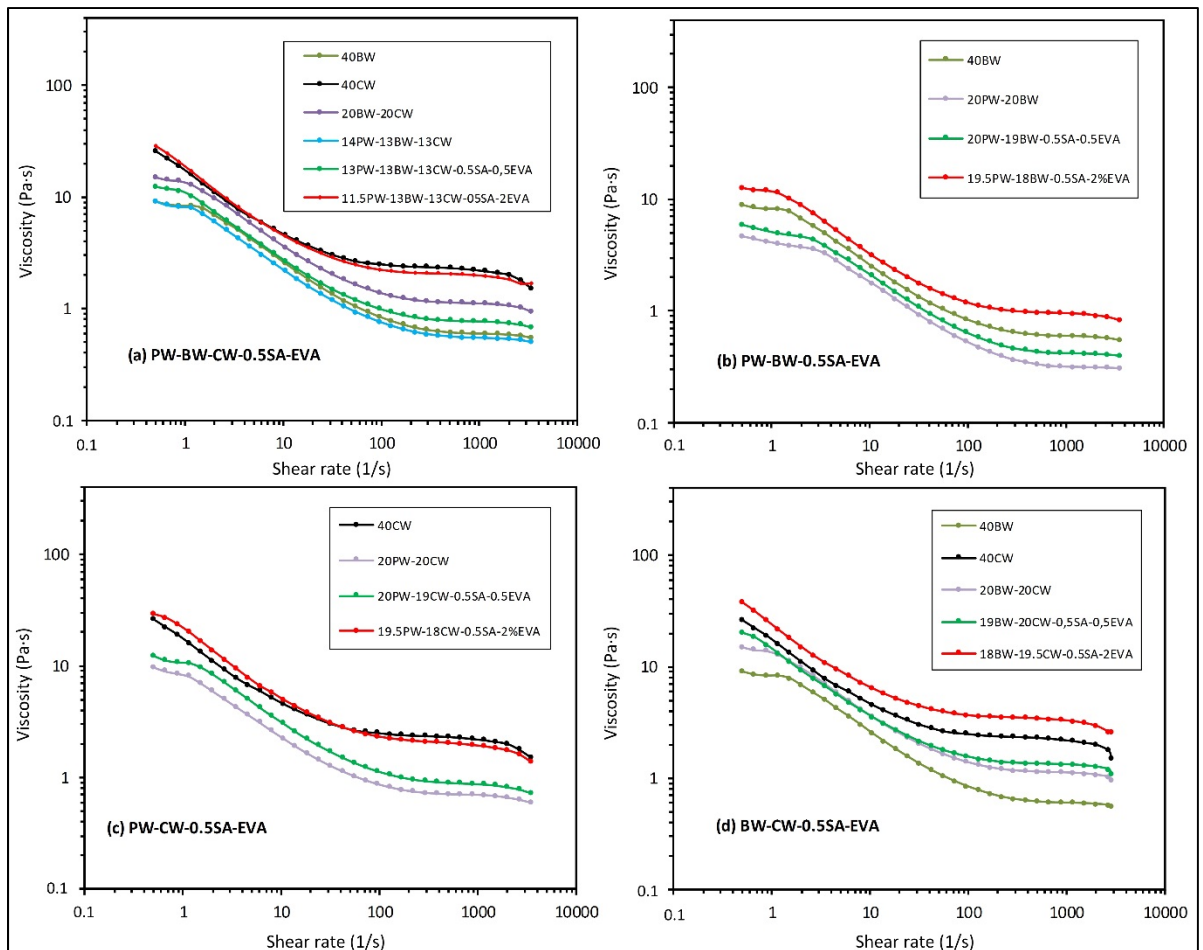


Figure 4.12 Viscosity profiles obtained with different multi waxes-based feedstocks:  
a) PW++BW+CW+0.5SA+EVA, b) BW+BW+0.5SA+EVA, c) PW+CW+0.5SA+EVA,  
d) BW+CW+0.5SA+EVA.

#### 4.6.5 Combination of stearic acid with, ethylene vinyl acetate and oleic acid into single wax-based feedstocks

The objective of this section is to study the combination of two surfactant agents (stearic acid and oleic acid) into a blend of ethylene–vinyl acetate (thickening agent) and single wax-based feedstocks. According to the conclusions obtained above (see section 4.6.2), it was proposed to set the proportion of stearic acid at 0.5 vol. % into five different waxes (PW, BW, CW, MW1, and MW2) and to change the proportion of EVA and OA using 0.5, 2 or 5 vol. % of each constituent as reported in Figure 4.13.

For all feedstocks family, two kind of rheological behaviors (depending on the proportions of EVA) were visible in Figure 4.13. The two groups of curves present the expected shear thinning effect. For low EVA contain (wax-0.5SA-0.5EVA-0.5OA and wax-0.5SA-0.5EVA-2OA), the viscosity values vary from 0.4 to 2.4 Pa·s at typical injection shear rate of 100 s<sup>-1</sup>. However, an increase in EVA proportion from 0.5 to 5 vol. % produces a significant increase in viscosity varying from 2.4 to 16.2 Pa·s at typical injection shear rate of 100 s<sup>-1</sup>. Finally, there is no effect on viscosity profile of mixture when two surfactant agents (stearic acid and oleic acid) and thickening agent (ethylene–vinyl acetate) are combined with single wax-based feedstocks. Meaning that the surfactant effect is not improved if different surfactant agents are used and the viscosity of feedstock can be controlled with thickening agent (EVA).

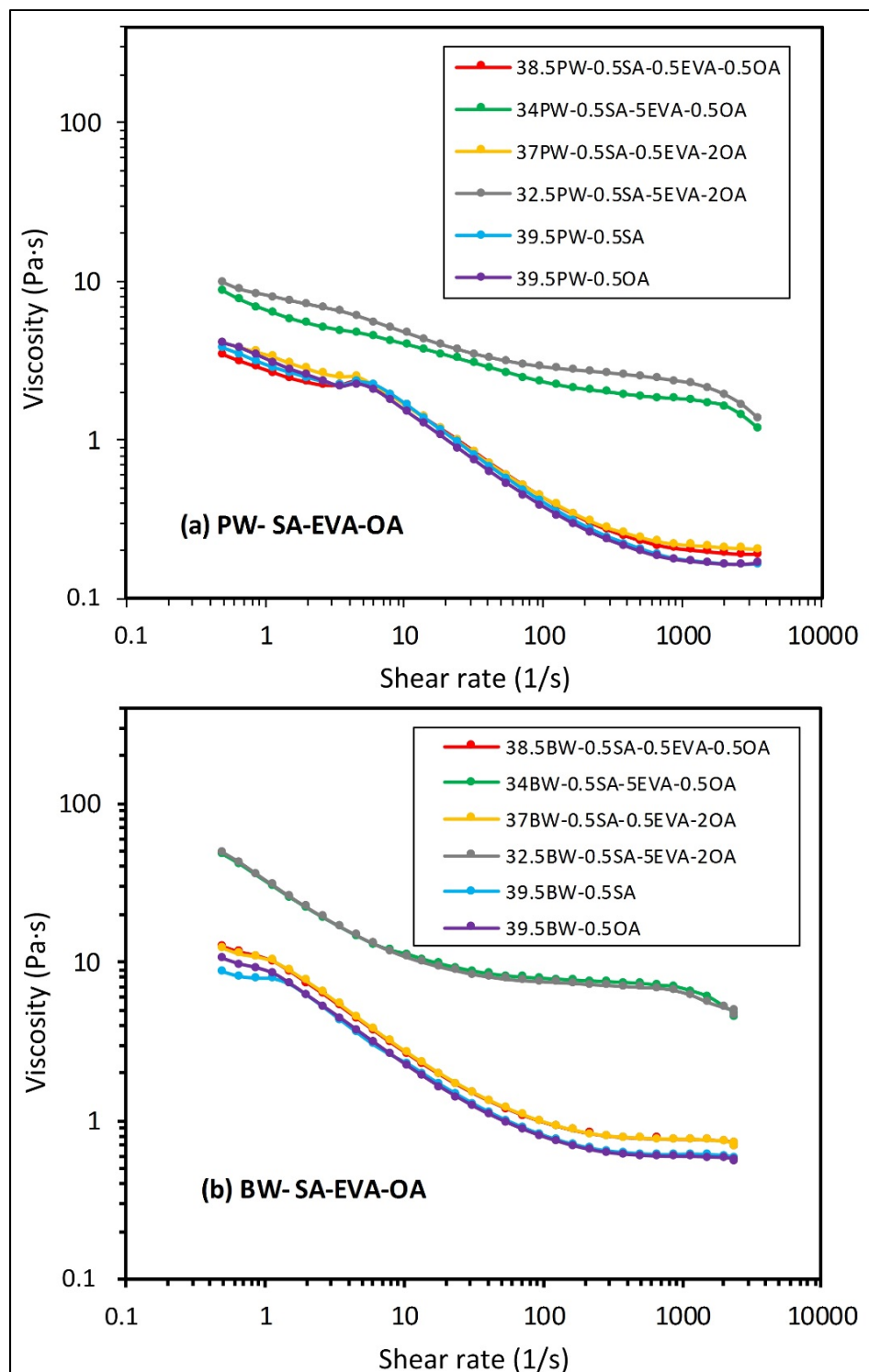


Figure 4.13 Viscosity profiles obtained with different wax-based feedstocks:  
a) PW+SA+EVA+OA, b) BW+SA+EVA+OA, c) CW+SA+EVA+OA, d)  
MW1+SA+EVA+OA, and e) MW2+SA+EVA+OA.

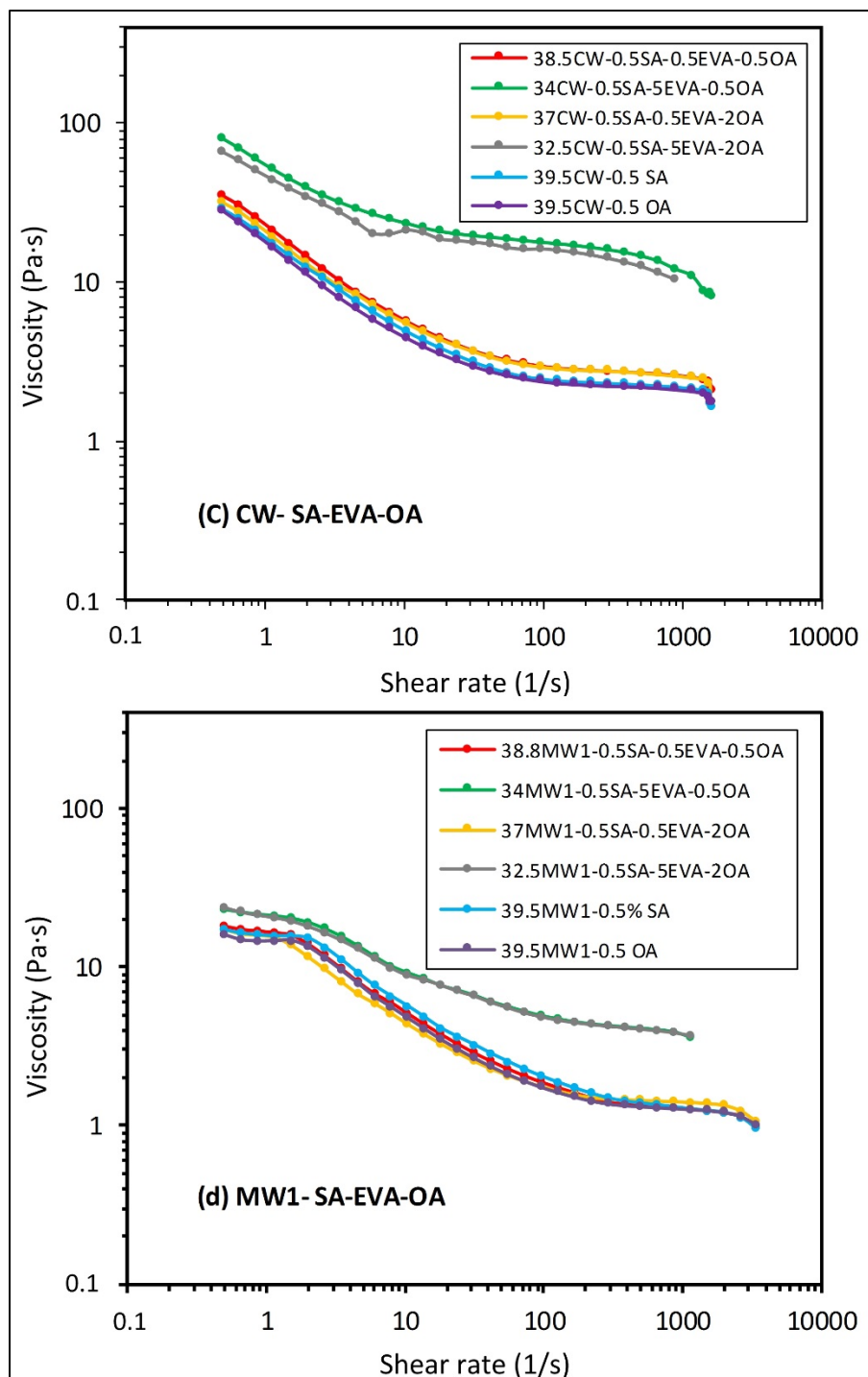


Figure 4.13 (Continued).

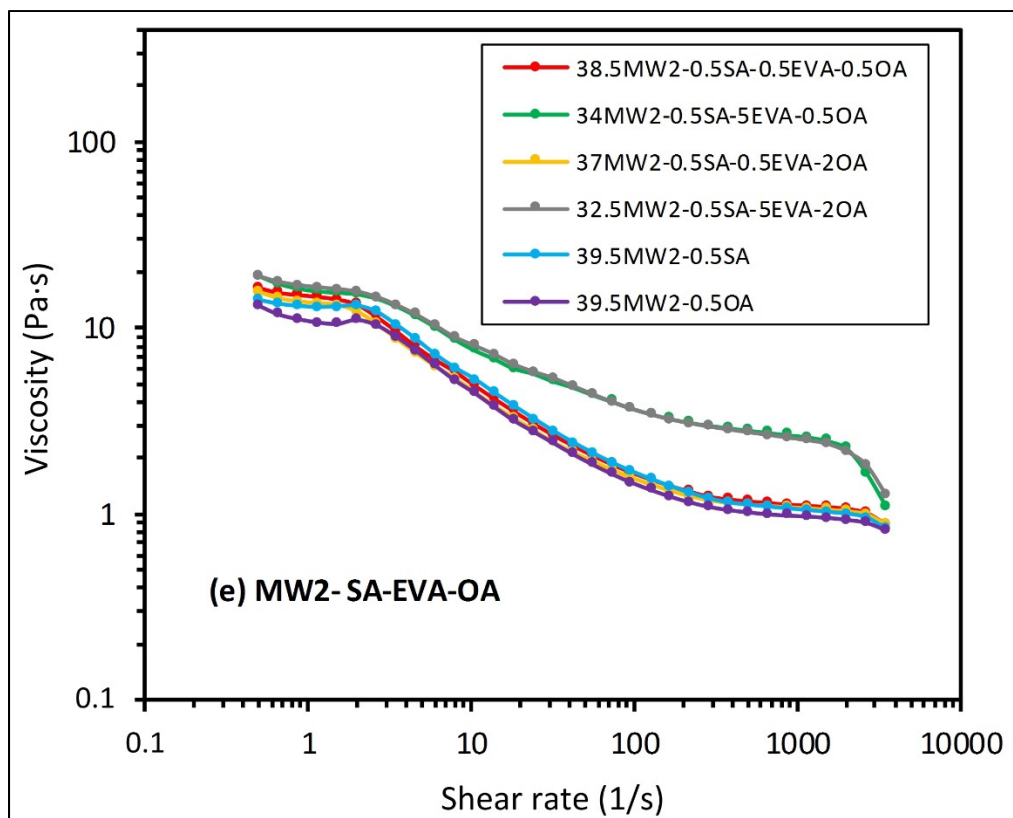


Figure 4.13 (Continued).

#### 4.6.6 Combination of stearic acid with, ethylene vinyl acetate and oleic acid into multiple waxes-based feedstocks

The rheological behaviors of mixtures made from the combination of two surfactant agents (stearic acid and oleic acid) into a blend of EVA and single wax-binder have shown that a use of two surfactant agents does not promote the surfactant effect. The purpose of this section is to confirm this conclusion with multiple waxes-binders. To minimize the time spent for this specific point, it was proposed to limit this demonstration to the mixture containing the three main wax constituents (i.e., PW, BW, and CW) used in LPIM. Figure 4.14 shows two kind of rheological behaviors (i.e., the dependence of EVA on viscosity) as previously seen in Figure 4.13 where an addition of two surfactant into a multiple waxes-binder has no significant effect on the viscosity profiles.

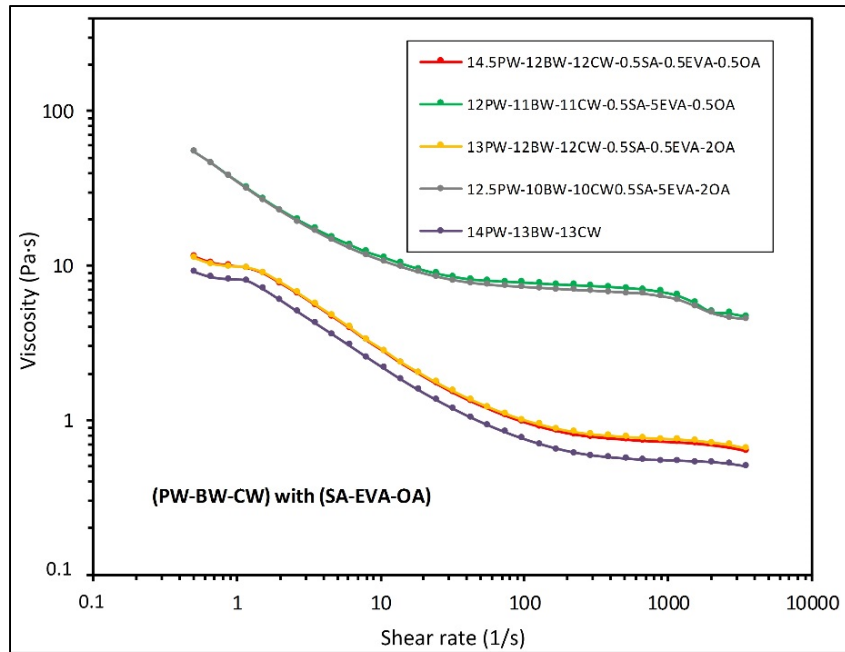


Figure 4.14 Influence of two surfactant agents on the viscosity Profiles of multiple waxes-based feedstocks.

#### 4.7 Influence of powder characteristics on viscosity of wax-based feedstocks

So far, the influence of binder on viscosity was demonstrated. This section presents the influence of powder characteristics such as powder size and powder shape on viscosity.

##### 4.7.1 Impact of powder size on viscosity

At constant solid loading, it is well known that smaller particle size produces higher feedstock viscosity. In order to validate but mostly quantify this fact for typical LPIM mixtures, four family of feedstocks were prepared using two different particle sizes (3 and 12  $\mu\text{m}$ ) and tested using the improved rheological testing protocol developed in the framework of this Master project (i.e., the protocol developed in section 4.2 above).

The influence of particle size on viscosity is presented in Figure 4.15. For all feedstock families, it can be clearly seen that the viscosity profiles obtained with small particle size are significantly higher than those obtained with a large particle size. It is interesting to note that the

shape of the viscosity profiles for all feedstocks seems to be driven only by the binder constituents used in formulations (i.e., no real impact of the particle size on the different stages of the viscosity profiles). In this respect, the viscosity values of all feedstock groups decreases with an increase of shear rate irrespectively to the particle size. However, an important conclusion is that the shear thinning behavior seems to be more pronounced for feedstocks formulated with small particle size. Moreover, it seems that a use of finer powder is suitable to increase the viscosity at low shear rate without producing a real detrimental effect on viscosity at moderate shear rate and especially at high shear rate. This could be seen as a potential advantage to use a finer powder (i.e., advantage for sintering stage of the process) without real impact on moldability properties of feedstocks. It is proposed to study this specific point in the future.

For the PW-SA feedstocks (Figure 4.15a), all viscosity profiles present a near-Newtonian plateau observed at low shear rate followed by a clear shear thinning behavior, where the viscosity decreases as the shear rate increases, and where a second near-Newtonian plateau is finally seen at high shear rate. However, the second near-Newtonian plateau is not clearly observed for the small particle size, which can be explained by the requirement of more energy (i.e., higher speed) to overcome the interparticular friction coming from finer particle size and the difficulty to form particles layers leading in flowing particles over each other and producing a decrease in viscosity.

For the PW-SA-EVA-OA feedstocks family, two kind of rheological behaviors (dependent on the proportions of EVA) are visible in Figure 4.15b, where an addition of two surfactant agents into a multiple waxes-binder has no significant effect on the viscosity profiles. The two groups of curves present the expected shear thinning effect, and the viscosity profiles obtained with small particle size are significantly higher than those obtained with a large particle size. However, the viscosity of the shear thinning behavior seems to be more visible for feedstocks formulated with the small particle size.

For the (0.5SA-EVA and 1SA-EVA) feedstocks, the viscosity of all feedstocks decreases as the shear rate increases. Expected trend was obtained for all viscosity profiles where an addition of EVA leads in an increase in viscosity. There is no significant difference between

0.5SA-EVA and 1SA-EVA results (see Figure 4.15c-d). However, the shape of the viscosity profiles obtained with large particle size feedstocks was characterized by a near-Newtonian plateau at low shear, and this plateau was observed only when small quantity of EVA was added to the waxes-based feedstock, while this plateau seems to disappear with more quantity of EVA added to the mixture. This plateau-like behavior is generally demonstrated by the lack of binder molecule chains alignment due to the too low shear deformation applied at low speed.

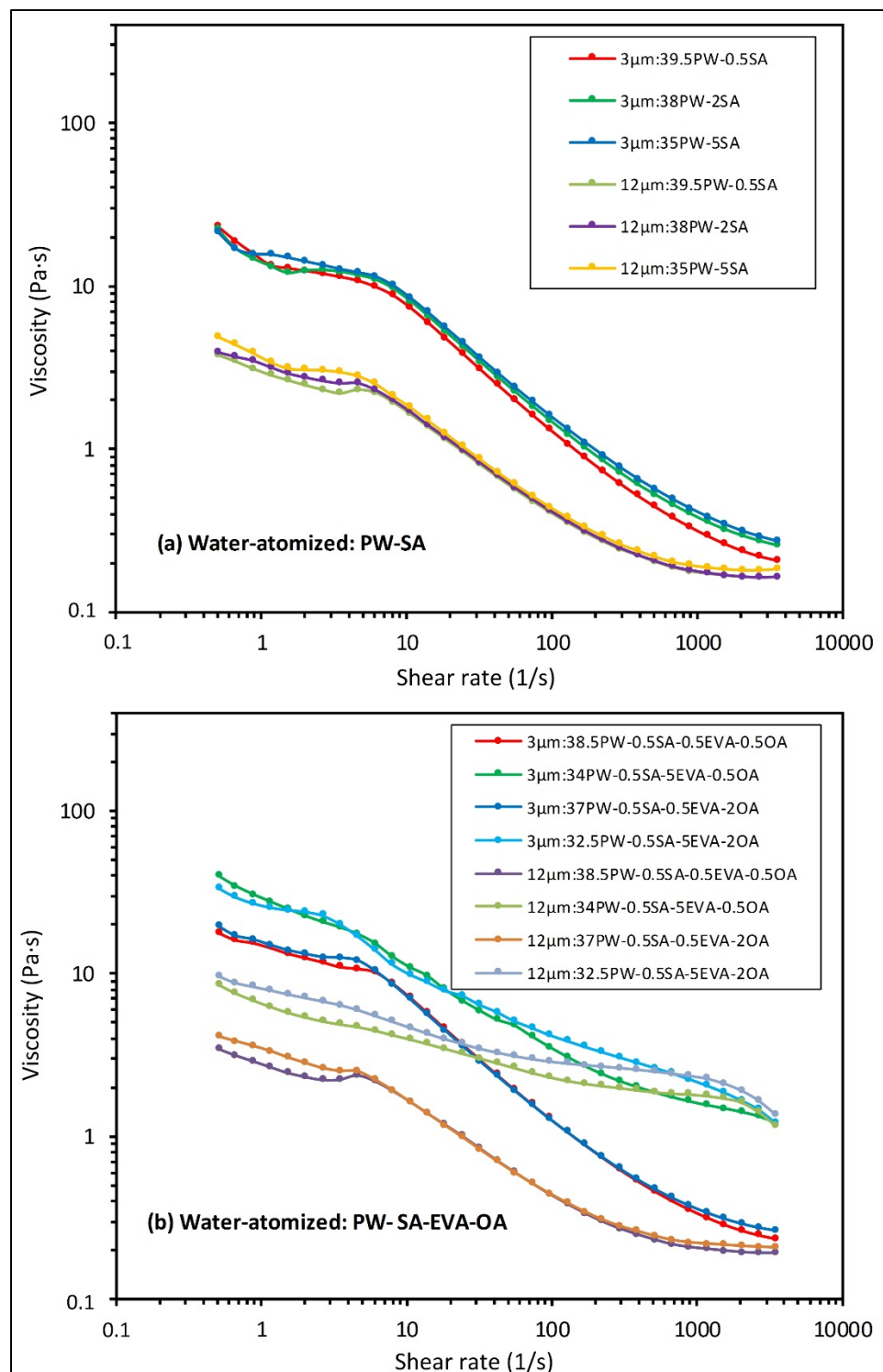


Figure 4.15 Viscosity profiles of water atomized feedstocks for powder sizes 3 and 12  $\mu\text{m}$ .

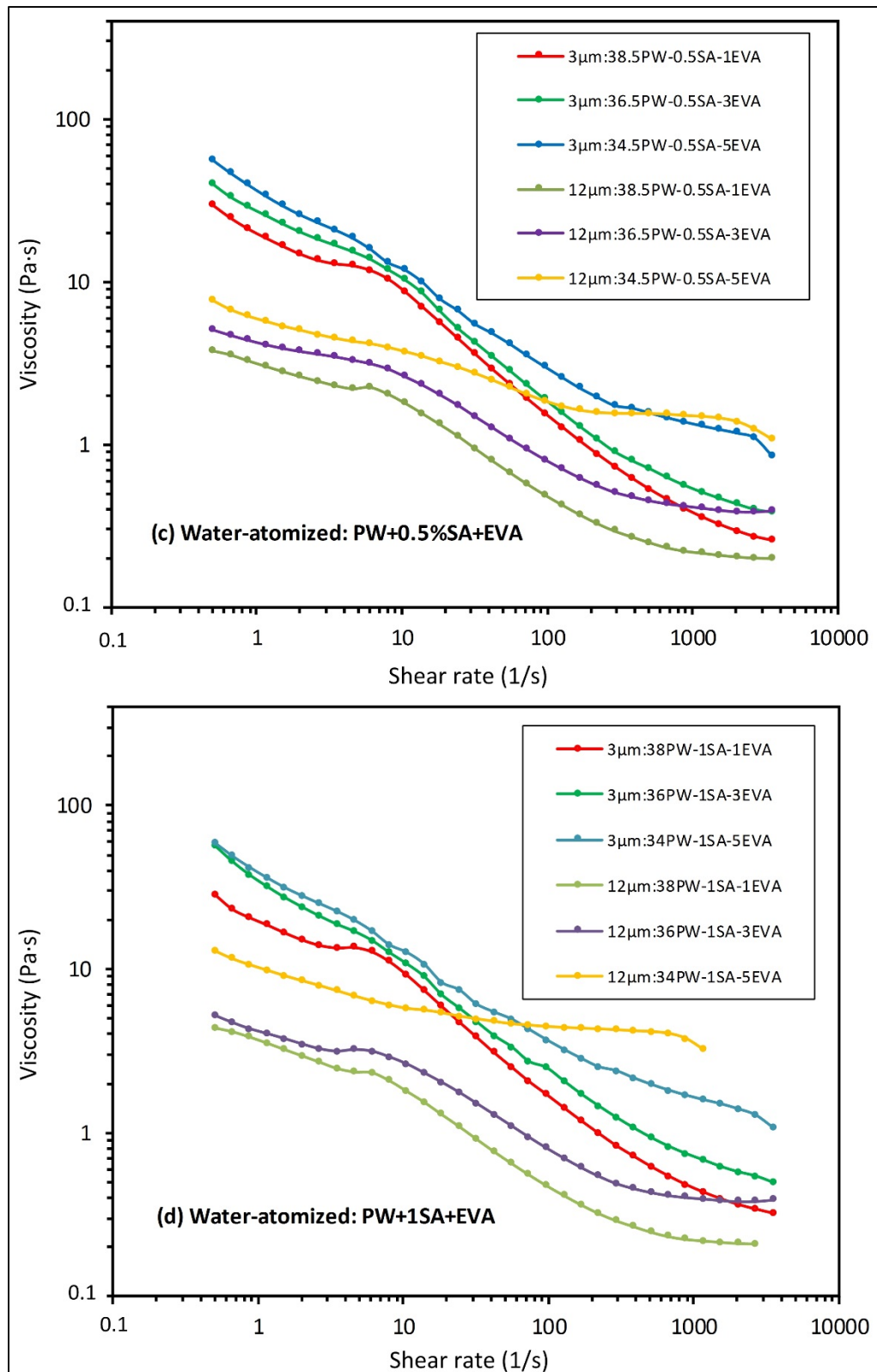


Figure 4.15 (Continued).

#### 4.7.2 Impact of powder shape on viscosity

Similarly, to powder size, the powder shape produces an impact on feedstock viscosity. At constant solid loading and similar surface texture, the feedstock viscosity decrease as the sphericity of powder increase where irregular shape produces higher feedstock viscosity compared to spherical shape. This is simply explained by the interparticle friction, which is more prominent for irregular shape powder leading in higher viscosity. As presented in the literature review section, the particle shape of powder is directly related to the fabrication method. For example, gas atomization produces spherical particles, while water atomization produces particles that are more irregular. In order to study the impact of particle shape on viscosity, four groups of feedstocks were prepared using two different particle shapes (near-spherical produced by water-atomization and spherical produced by gas-atomization) having similar particle size ( $12 \mu\text{m}$ ) and tested using the same rheological protocol.

Figure 4.16 presents the influence of particle shape on the feedstock viscosity. For all groups, the viscosity of feedstocks formulated using spherical powder was lower than that obtained with near-spherical powder, especially at typical shear rate representing the injection ( $\sim 100 \text{ s}^{-1}$ ) and at high shear rate. Similarly to the results obtained in the previous section, the viscosity values of all feedstock groups decreases with an increase of shear rate irrespectively to the particle shape. Note that this pseudoplastic effect is slightly more visible for the viscosity profiles obtained with spherical particle. For the PW-SA feedstocks (Figure 4.16a-b), all viscosity profiles present the same trend where a near-Newtonian plateau observed at low shear rate is followed by a clear shear thinning behavior, and a second near-Newtonian plateau finally seen at high shear rate. However, spherical powder seems to be less sensitive to the surfactant proportion at low shear rate and the hook in viscosity profile at very low share rate seems to be less pronounced compared to near-spherical powder. For the PW-SA-EVA-OA feedstocks, two kind of viscosity profiles (dependent on the proportions of EVA) are shown in Figure 4.16c-d. The two groups of curves present the expected shear thinning effect where the viscosity values of a spherical powder particle shape are lower than that obtained with an irregular powder particle shape especially at typical injection and high shear rate.

For the (0.5SA-EVA and 1SA-EVA) feedstocks, the viscosity of all feedstocks decreases as the shear rate increases (Figure 4.16e-f). Expected trend was obtained for all viscosity profiles where an addition of EVA leads in an increase in viscosity, and the shear thinning behavior is more pronounced in the viscosity profiles obtained with spherical shape. There is no significant difference between 0.5SA-EVA and 1SA-EVA results (see Figure 4.16e-f and Figure 4.16g-h). However, the shape of viscosity profile for near-spherical shape feedstocks was characterized by a near-Newtonian plateau at low shear, and this plateau was observed only when small quantity of EVA was added to the waxes-based feedstock, while this plateau seems to disappear with more quantity of EVA added to the mixture. This plateau-like behavior is generally demonstrated by the lack of binder molecule chains alignment due to the too low shear deformation applied at low speed.

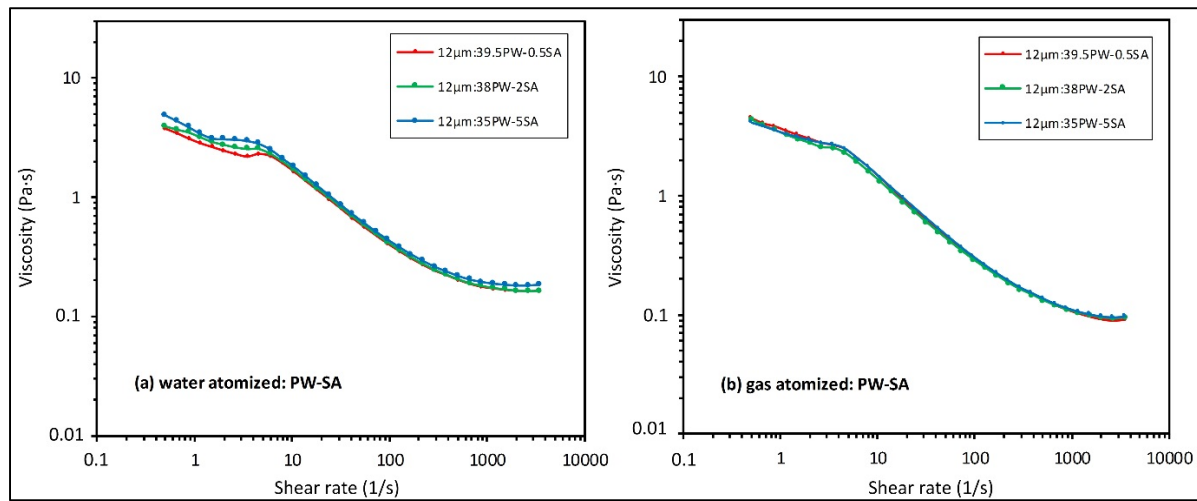


Figure 4.16 Viscosity profiles of representative water atomized and gas atomized powder feedstocks (for same powder size of 12  $\mu\text{m}$ ).

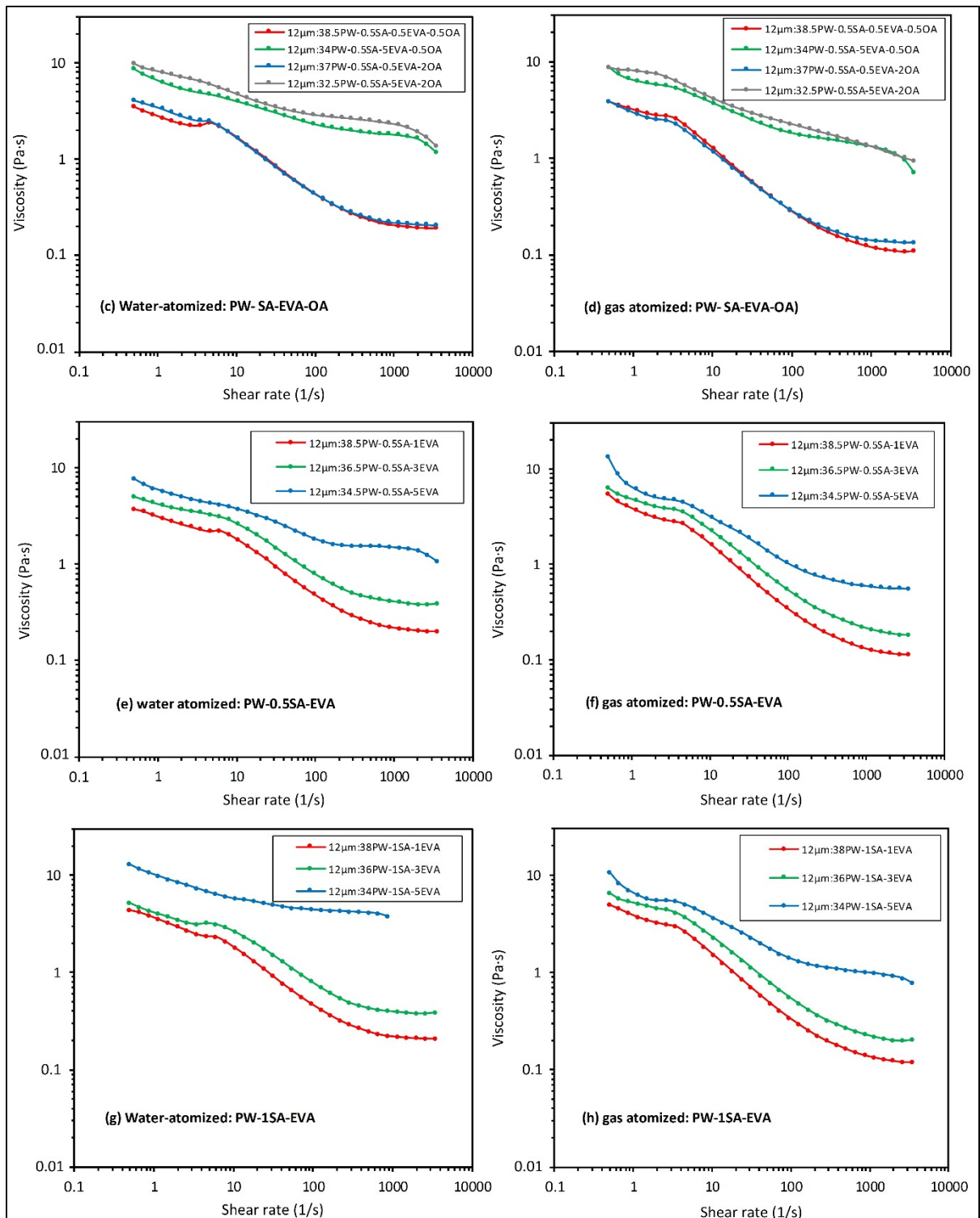


Figure 4.16 (Continued).

#### 4.8 Influence of binder on viscosity and slopes of the viscosity profiles

Based on previous sections, results have demonstrated that the rheological behavior is significantly affected by the binder formulation used for LPIM feedstocks. Therefore, 40 different feedstocks were selected from each feedstock families in order to study specifically the influence of binder constituents on shear sensitivity index and viscosity at low and high shear rate (see section 3.2.2 for details about the methodology).

Four rheological parameters were extracted from the viscosity profiles to study the behavior of feedstocks during different injection phases of the LPIM process. The minimum and the maximum viscosity values can be correlated with the behavior of feedstock during the injection ( $\eta_1$  obtained at  $\dot{\gamma} = 1 \text{ s}^{-1}$  in Figure 4.18) and mixing steps ( $\eta_2$  obtained at  $\dot{\gamma} = 100 \text{ s}^{-1}$  in Figure 4.18), respectively. In addition, flow behavior indexes between mixing and injection were extracted from the viscosity profile, which are reported in Figure 4.17. During injection (i.e., between  $100 \text{ s}^{-1}$  and  $3500 \text{ s}^{-1}$ ), the viscosity value should be as low as possible to permit the complete filling of the mold cavity without defects. During mixing stage (i.e., between  $1 \text{ s}^{-1}$  and  $100 \text{ s}^{-1}$ ) and after mold filling (i.e.,  $<1 \text{ s}^{-1}$ ) the viscosity value should be as high as possible to prevent a powder-binder separation and sustain the feedstock homogeneity. Note that the viscosity and flow behavior index values of each feedstock are summarized in Appendix I.

From Figure 4.17, it seems that the values of flow behavior index are almost the same for each feedstock. Although several research teams used this specific parameter to quantify rheological properties of feedstocks, it could be stated from this project that this value is not relevant to describe the influence of binder constituents. From Figure 4.18, it seems that viscosity values are more adapted to discretize the impact of binder constituents. All of the selected 40 feedstocks exhibited a viscosity values lower than  $20 \text{ Pa}\cdot\text{s}$ , which is commonly desired for LPIM feedstocks (excepted for CW-SA-EVA feedstocks that exhibit very high viscosity values at the mixing as well as at the injection stages, which is not suitable for LPIM feedstocks).

At the injection stage, the best feedstocks are PW-based feedstocks, but this feedstock family does not exhibits a perfect behavior at the mixing stage due to their relatively low viscosity values. However, MW1, MW2, and BW based feedstock are good candidates for LPIM molding, because these feedstocks generate high viscosity values at low shear rate (which is required to maintain the feedstocks homogeneity and avoiding segregation of the mixtures) combined with low viscosity values at the injection stage, which is suitable to promote the mold filling .

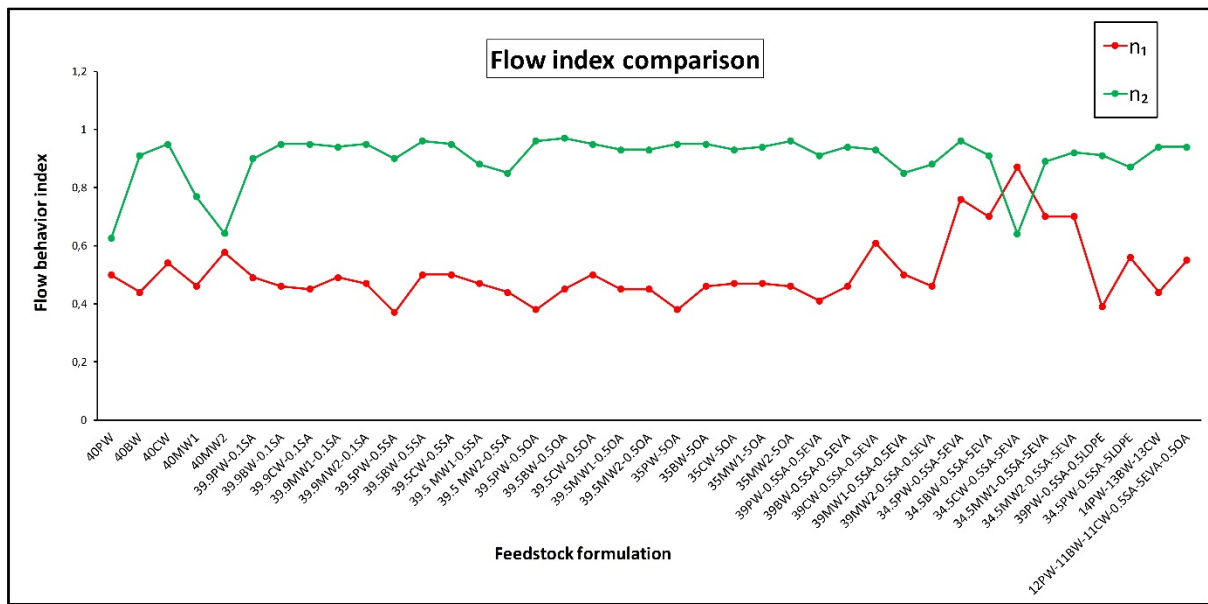


Figure 4.17 Flow behavior index according to feedstock formulations.

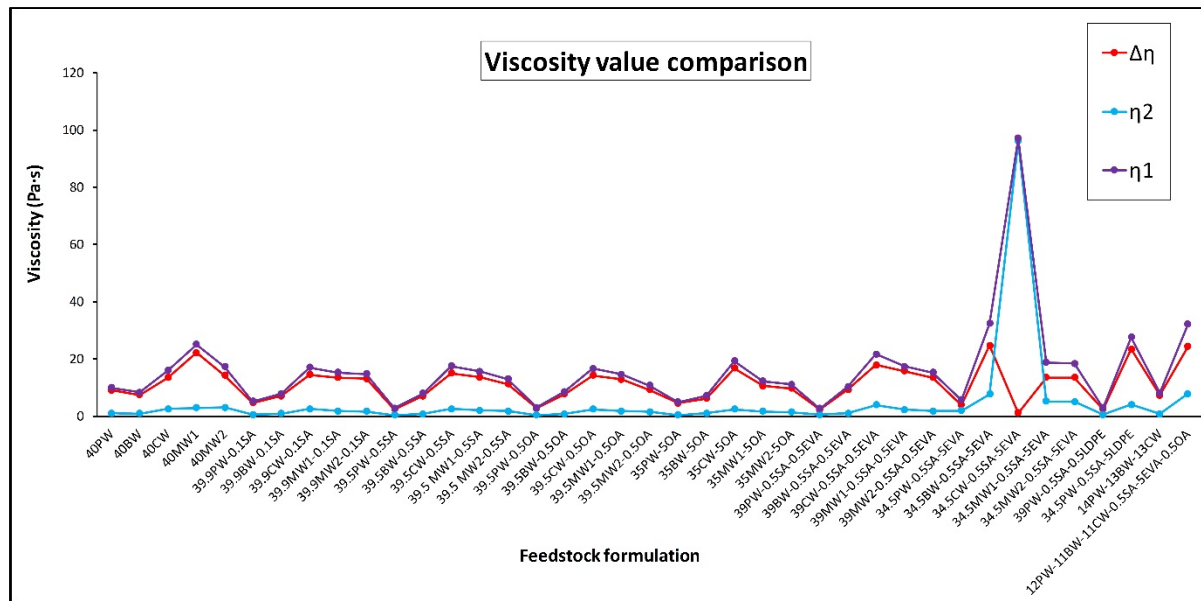


Figure 4.18 Evolution of the viscosity according feedstock formulations.

## CONCLUSION

The viscosity of feedstock is one of the most important rheological parameters influencing the success of the molding stage during low-pressure powder injection molding process. Although trends qualifying the influence of binder and powder characteristics are well known, it is clear that data available in literature are not sufficient to assess the moldability properties of feedstock and to optimize feedstock formulations as well as final properties of the manufactured components. So far, the efforts to optimize the mechanical properties of LPIM metallic materials typically involve debinding and sintering using feedstocks whose optimal moldability has not yet been demonstrated. Therefore, assessing the full potential of the LPIM technique is still limited by a poor understanding of the fundamental mechanisms underlying the moldability of LPIM feedstocks linked with the rheological behavior of feedstock specifically on a poor understanding of the impact of binder constituents on rheological behavior. Therefore, this work was focused on the extensive study of the impact of low-viscosity binder systems on rheological properties of feedstocks. Rotational rheometer was used to evaluate the viscosity profile of different 17-4PH stainless steel based feedstocks, while differential scanning calorimetry was used to set the common testing temperature for this systematic rheological test campaign. The results obtained in this study are summarized below:

- 1) Initial test protocol developed one year ago in our research group was improved by introducing a thermal equilibrium stage consisting in two minutes of blending before to record the viscosity profile.
- 2) The viscosity of all feedstocks decreases as the shear rate increases, which is the shear thinning behavior generally required for LPIM feedstocks.
- 3) The addition of PW in the mixture of single natural wax or multi natural waxes produces a decrease in viscosity.
- 4) Stearic acid and oleic acid are two equivalent surfactant agents that can be used for enhancing the powder-binder interaction, promoting the homogeneity of the feedstock, and decreasing the viscosity of the feedstocks. These two surfactants proposed different advantages and limitations. When small quantity must be used, it is suggested to use

the stearic acid as a surfactant agent instead of using oleic acid because it is difficult to use very small amount of oleic acid. However, oleic acid seems to present a certain advantage in increasing viscosity at low shear rate (e.g., during the blending phase of the process) without producing any change in low viscosity visible at high shear rate (i.e., during the injection phase). In this respect, results confirm that a quantity as small as 0.2 vol. % of stearic acid is enough to produce the surfactant effect.

- 5) Ethylene–vinyl acetate (EVA) is a good constituent to increase the viscosity and possibly decrease the segregation compared with other conventional thickening agent (low-density polyethylene (LDPE)) that detrimentally increases the feedstock viscosity. Also, an addition of a small quantities of thickening agents in paraffin wax-based feedstocks generate no significant differences in viscosity values in both case (i.e. EVA or LDPE) while an addition of 3 vol. % of each ingredient produce a significant increase in viscosity.
- 6) The viscosity values resulting from a combination of main binder, surfactant agent, and thickening agent depends essentially on the proportion of thickening agent (EVA) into feedstock while the latter can be used to tailor a proper feedstock viscosity avoiding segregation.
- 7) The use of two surfactant agents induces no effect on rheological behavior compared to feedstocks using only one surfactant agent.
- 8) The viscosity profiles obtained with small powder size as well as spherical shape are significantly higher than those obtained with a large particle size and near-spherical powder. No real impact of the powder size and powder shape on the different stages have been seen in the viscosity profiles. However, the shear thinning behavior seems to be more pronounced for feedstocks formulated with small particle size and spherical particle.

With all these important results, this project finally proposed the first complete database describing the influence of each binder constituents that was still missing today to develop optimal feedstock for LPIM process.

## RECOMMENDATIONS

Following the conclusions drawn above, there is some recommendation that could be taken into account for futures works in the LPIM research group at ÉTS:

- Regarding the new test protocol developed during this work, it is recommended to use this new testing approach for all projects where rheological profiles must be recorded from low-viscosity feedstocks.
- The advantage of oleic acid is to produce an increase in viscosity at low shear rate (e.g., during the blending phase of the process) without producing any change in low viscosity visible at high shear rate (i.e., during the injection phase) could be studied in a future work involving real scale injection to confirm this beneficial influence of oleic acid on moldability of feedstocks.
- It could be also interesting to study the effect of the volume fraction of the metal powder on viscosity of feedstock and its interaction with threshold proportion of surfactant agent and thickening agent.
- Finally, it could be relevant to obtain the viscosity profile of feedstock under different temperature in order to calculate the moldability index using Weir's model for typical LPIM feedstock.



## APPENDIX I

Note, the green color indicates the feedstock tests that have done while the red one refers to the unattainable feedstock tests.

**First,** water-atomized stainless steel 17-4PH (average size 12µm) with different binders of different feedstock families:

Test	Temperaure (°C)	powder	Binder							comment
			Atmix PF	PW	BW	CW	MW#1	MW#2	SA	
1	90	60	39.5						0.5	
2	90	60	39						1	
3	90	60	38						2	
4	90	60	35						5	
5	90	60				39.5			0.5	
6	90	60			39				1	
7	90	60			38				2	
8	90	60			35				5	
9	90	60					39.5		0.5	
10	90	60					39		1	
11	90	60					38		2	
12	90	60					35		5	

**Impact of EVA on viscosity and confirm the threshold proportion of EVA (if exist)**

Test	Temperaure (°C)	powder Atmix PF	Binder							comment
			PW	BW	CW	MW#1	MW#2	SA	EVA	
13	90	60	39.9					0.1		
14	90	60	39.75					0.25		
15	90	60	39.5					0.5		
16	90	60	39					1		
17	90	60	38					2		
18	90	60	35					5		
19	90	60		39.9				0.1		
20	90	60		39.75				0.25		
21	90	60		39.5				0.5		
22	90	60		39				1		
23	90	60		38				2		
24	90	60		35				5		
25	90	60			39.9			0.1		
26	90	60			39.75			0.25		
27	90	60			39.5			0.5		
28	90	60			39			1		
29	90	60			38			2		
30	90	60			35			5		
31	90	60				39.9		0.1		
32	90	60				39.75		0.25		
33	90	60				39.5		0.5		
34	90	60				39		1		
35	90	60				38		2		
36	90	60				35		5		
37	90	60					39.9	0.1		
38	90	60					39.75	0.25		
39	90	60					39.5	0.5		
40	90	60					39	1		
41	90	60					38	2		
42	90	60					35	5		

Impact of SA on viscosity and  
confirm the threshold  
proportion of SA (if exist)

Test	Temperaure (°C)	powder Atmix PF	Binder							comment
			PW	BW	CW	MW#1	MW#2	SA	EVA	
43	90	60	39.9							0.1
44	90	60	39.75							0.25
45	90	60	39.5							0.5
46	90	60	39							1
47	90	60	38							2
48	90	60	35							5
49	90	60		39.5						0.5
50	90	60		39						1
51	90	60		38						2
52	90	60		35						5
53	90	60			39.5					0.5
54	90	60			39					1
55	90	60			38					2
56	90	60			35					5
57	90	60				39.5				0.5
58	90	60				39				1
59	90	60				38				2
60	90	60				35				5
61	90	60					39.5			0.5
62	90	60					39			1
63	90	60					38			2
64	90	60					35			5

Impact of OA on viscosity and  
confirm the threshold  
proportion of OA (if exist)

Test	Temperaure (°C)	powder Atmix PF	Binder							comment
			PW	BW	CW	MW#1	MW#2	SA	EVA	
65	90	60	39					0.5	0.5	
66	90	60	38.5					0.5	1	
67	90	60	37.5					0.5	2	
68	90	60	36.5					0.5	3	
69	90	60	35.5					0.5	4	
70	90	60	34.5					0.5	5	
71	90	60	29.5					0.5	10	
72	90	60	24.5					0.5	15	
73	90	60		39				0.5	0.5	
74	90	60		38.5				0.5	1	
75	90	60		37.5				0.5	2	
76	90	60		36.5				0.5	3	
77	90	60		35.5				0.5	4	
78	90	60		34.5				0.5	5	
79	90	60			39			0.5	0.5	
80	90	60			38.5			0.5	1	
81	90	60			37.5			0.5	2	
82	90	60			36.5			0.5	3	
83	90	60			35.5			0.5	4	
84	90	60			35			0.5	4.4	
85	90	60			34.5			0.5	5	
86	90	60				39		0.5	0.5	
87	90	60				38.5		0.5	1	
88	90	60				37.5		0.5	2	
89	90	60				36.5		0.5	3	
90	90	60				35.5		0.5	4	
91	90	60				34.5		0.5	5	
92	90	60					39	0.5	0.5	
93	90	60					38.5	0.5	1	
94	90	60					37.5	0.5	2	
95	90	60					36.5	0.5	3	
96	90	60					35.5	0.5	4	
97	90	60					34.5	0.5	5	

**Impact of combination of  
0.5SA+EVA**

Test	Temperaure (°C)	powder	Binder							comment	
			Atmix PF	PW	BW	CW	MW#1	MW#2	SA	EVA	
98	90	60	38,5						1	0.5	
99	90	60	38						1	1	
100	90	60	37						1	2	
101	90	60	36						1	3	
102	90	60	35						1	4	
103	90	60	34						1	5	
104	90	60	29						1	10	
105	90	60	24						1	15	
106	90	60		38.5					1	0.5	
107	90	60		38					1	1	
108	90	60		37					1	2	
109	90	60		36					1	3	
110	90	60		38.5					1	0.5	
111	90	60		38					1	1	
112	90	60		37					1	2	
113	90	60		36					1	3	
114	90	60			38.5				1	0.5	
115	90	60			38				1	1	
116	90	60			37				1	2	
117	90	60			36				1	3	
118	90	60				38.5		1	0.5		
119	90	60				38		1	1		
120	90	60				37		1	2		
121	90	60				36		1	3		

Impact of combination of  
1%SA+EVA

Test	Temperaure (°C)	powder	Binder							comment	
			Atmix PF	PW	BW	CW	MW#1	MW#2	SA	EVA	
122	90	60	37	1	1				0.5	0.5	
123	90	60	29	5	5				0.5	0.5	
124	90	60	19	10	10				0.5	0.5	
125	90	60	13	13	13				0.5	0.5	
126	90	60	11.5	13	13				0.5	2	
127	90	60		19	20				0.5	0.5	
128	90	60		18	19.5				0.5	2	
129	90	60	20	19					0.5	0.5	
130	90	60	20		19				0.5	0.5	
131	90	60	19.5	18					0.5	2	
132	90	60	19.5		18				0.5	2	

Addition of PW into  
BW+CW+0.5SA+EVA

Test	Temperaure (°C)	powder	Binder							comment	
			Atmix PF	PW	BW	CW	MW#1	MW#2	SA	EVA	
133	90	60	40								
134	90	60		40							
135	90	60			40						
136	90	60				40					
137	90	60					40				
138	90	60		20	20						
139	90	60	14	13	13						
140	90	60	20	20							
141	90	60	20		20						

Impact of natural waxes,  
PW,MW#1, MW#2

Test	Temperaure (°C)	powder	Binder							comment	
			Atmix PF	PW	BW	CW	MW#1	MW#2	SA	EVA	
142	90	60	38.5						0.5	0.5	0.5
143	90	60	34						0.5	5	0.5
144	90	60	37						0.5	0.5	2
145	90	60	32.5						0.5	5	2
146	90	60		38.5					0.5	0.5	0.5
147	90	60		34					0.5	5	0.5
148	90	60		37					0.5	0.5	2
149	90	60		32.5					0.5	5	2
150	90	60			38.5				0.5	0.5	0.5
151	90	60			34				0.5	5	0.5
152	90	60			37				0.5	0.5	2
153	90	60			32.5				0.5	5	2
154	90	60				38.5			0.5	0.5	0.5
155	90	60				34			0.5	5	0.5
156	90	60				37			0.5	0.5	2
157	90	60				32.5			0.5	5	2
158	90	60					38.5		0.5	0.5	0.5
159	90	60					34		0.5	5	0.5
160	90	60					37		0.5	0.5	2
161	90	60					32.5		0.5	5	2
162	90	60	14.5	12	12				0.5	0.5	0.5
163	90	60	12	11	11				0.5	5	0.5
164	90	60	13	12	12				0.5	0.5	2
165	90	60	12.5	10	10				0.5	5	2

Impact of combination of (OA-SA+EVA)

**Second**, impact of powder size on viscosity (water-atomized stainless steel 17-4PH (average size 3µm) with different different feedstock families):

Test	Temperaure(°C)	powder	Binder							comment	
			Atmix PF	PW	BW	CW	MW#1	MW#2	SA	EVA	
166	90	60	38.5						0.5	1	
167	90	60	36.5						0.5	3	
168	90	60	34.5						0.5	5	
	90										
169	90	60	38						1	1	
170	90	60	36						1	3	
171	90	60	34						1	5	

impact of SA+EVA

Test	Temperaure(°C)	powder	Binder							comment	
			Atmix PF	PW	BW	CW	MW#1	MW#2	SA	EVA	
172	90	60	38.5						0.5	0.5	0.5
173	90	60	34						0.5	5	0.5
174	90	60	37						0.5	0.5	2
175	90	60	32.5						0.5	5	2

Impact of (SA+EVA+OA)

Test	Temperaure(°C)	powder	Binder							comment	
			Atmix PF	PW	BW	CW	MW#1	MW#2	SA	EVA	
176	90	60	39.5						0.5		
177	90	60	38						2		
178	90	60	35						5		

Impact of SA

**Third**, impact of powder shape on viscosity (gas-atomized stainless steel 17-4PH (average size 12µm) with different feedstock families):

Test	Tempera ure(°C)	powder	Binder								comment	
			Atmix PF	PW	BW	CW	MW#1	MW#2	SA	EVA	Oleic acid	
179	90	60	38.5						0.5	1		
180	90	60	36.5						0.5	3		
181	90	60	34.5						0.5	5		
	90											
182	90	60	38						1	1		
183	90	60	36						1	3		
184	90	60	34						1	5		

impact of SA+EVA

Test	Tempera ure(°C)	powder	Binder								comment	
			Atmix PF	PW	BW	CW	MW#1	MW#2	SA	EVA	Oleic acid	
185	90	60	38.5						0.5	0,5	0.5	
186	90	60	34						0.5	5	0.5	
187	90	60	37						0.5	0.5	2	
188	90	60	32.5						0.5	5	2	

Impact of (SA+EVA+OA)

Test	Tempera ure(°C)	powder	Binder								comment	
			Atmix PF	PW	BW	CW	MW#1	MW#2	SA	EVA	Oleic acid	
189	90	60	39.5						0.5			
190	90	60	38						2			
191	90	60	35						5			

Impact of SA

**Fourth**, comparison between thickening agents:

Test	Temperaure(°C)	powder	Binder								comment	
			Atmix PF	PW	BW	CW	MW#1	MW#2	SA	LDPE	Oleic acid	
192	90	60	39						0.5	0.5		
193	90	60	38.5						0.5	1		
194	90	60	36.5						0.5	3		
195	90	60	34.5						0.5	5		

impact of SA+LDPE

## APPENDIX II

### Rheological parameters of feedstocks

Viscosity and flow behavior index values of each feedstock.

Feedstock group	Feedstock identification	$\eta_1$ (Pa·s)	$\eta_2$	$\Delta\eta$	$(n_1)$	$(n_2)$
waxes based	40PW					
	40BW	8.3	0.85	7.4	0.44	0.91
	40CW	16	2.5	13.4	0.54	0.95
	40MW1					
	40MW2					
waxes based-SA	39.9PW-0.1SA	5.1	0.47	4.6	0.49	0.9
	39.9BW-0.1SA	7.84	0.84	7	0.46	0.95
	39.9CW-0.1SA	17	2.47	14.5	0.45	0.95
	39.9MW1-0.1SA	15.2	1.8	13.4	0.49	0.94
	39.9MW2-0.1SA	14.7	1.6	13.1	0.47	0.95
	39.5PW-0.5SA	2.8	0.4	2.4	0.37	0.90
	39.5BW-0.5SA	7.9	0.8	7	0.5	0.96
	39.5CW-0.5SA	17.5	2.5	15	0.5	0.95
	39.5 MW1-0.5SA	15.6	2	13.6	0.47	0.88
	39.5 MW2-0.5SA	12.9	1.7	11.2	0.44	0.85
waxes based-OA	39.5PW-0.5OA	3	0.4	2.7	0.38	0.96
	39.5BW-0.5OA	8.5	0.8	7.7	0.45	0.97
	39.5CW-0.5OA	16.6	2.4	14.2	0.5	0.95
	39.5MW1-0.5OA	14.6	1.8	12.8	0.45	0.93
	39.5MW2-0.5OA	10.7	1.5	9.2	0.45	0.93
	35PW-5OA	4.9	0.42	4.5	0.38	0.95

	35BW-5OA	7.2	0.93	6.2	0.46	0.95
	35CW-5OA	19.2	2.4	16.7	0.47	0.93
	35MW1-5OA	12.2	1.6	10.6	0.47	0.94
	35MW2-5OA	11	1.4	9.7	0.46	0.96
0.5SA-EVA	39PW-0.5SA-0.5EVA	2.6	0.47	2.2	0.41	0.91
	39BW-0.5SA-0.5EVA	10.3	1	9.3	0.46	0.94
	39CW-0.5SA-0.5EVA	21.7	3.9	17.8	0.61	0.93
	39MW1-0.5SA-0.5EVA	17.3	2.2	15.7	0.5	0.85
	39MW2-0.5SA-0.5EVA	15.2	1.8	13.4	0.46	0.88
	34.5PW-0.5SA-5EVA	5.7	1.9	3.9	0.76	0.96
	34.5BW-0.5SA-5EVA	32.3	7.7	24.6	0.7	0.91
	34.5CW-0.5SA-5EVA	97.1	96	1.1	0.87	0.64
	34.5MW1-0.5SA-5EVA	18.7	5.2	13.5	0.7	0.89
	34.5MW2-0.5SA-5EVA	18.4	5	13.4	0.7	0.92
0.5SA-LDPE	39PW-0.5SA-0.5LDPE	2.94	0.54	2.4	0.39	0.91
	34.5PW-0.5SA-5LDPE	27.5	4	23.4	0.56	0.87
Multi waxes	14PW-13BW-13CW	8.1	0.76	7.3	0.44	0.94
	12PW-11BW-11CW-0.5SA-5EVA-0.5OA	32.1	7.8	24.3	0.55	0.94

## REFERENCES

- . "[www.tainstruments.com/wp-content/uploads/CA-2016-Rheology.pdf](http://www.tainstruments.com/wp-content/uploads/CA-2016-Rheology.pdf)."
- Abdoos, H., H. Khorsand and A. Yousefi (2014). "Torque rheometry and rheological analysis of powder–polymer mixture for aluminum powder injection molding." *Iranian Polymer Journal* **23**(10): 745-755.
- Abdoos, H., H. Khorsand and A. Yousefi (2014). "Torque rheometry and rheological analysis of powder–polymer mixture for aluminum powder injection molding." *Iranian Polymer Journal* **10**(23): 745-755.
- Adames, J. M. (2007). *Characterization of polymeric binders for metal injection molding (MIM) process*, University of Akron.
- Amin, M., N. Muhamad, K. R. Jamaludin, S. Abdullah and M. N. A. Rahman (2012). "Rheological investigation of MIM feedstocks prepared with different particle sizes."
- Amin, S. Y. M., N. Muhamad, K. R. Jamaludin, A. Fayyaz and H. S. Yunn (2014). "Characterization of the feedstock properties of metal injection-molded WC-Co with palm stearin binder system." *Sains Malaysiana* **43**(1): 123-128.
- AN, R. (2012). "Metal powder injection molding (MIM): key trends and markets." *Handbook of metal injection molding*: 1.
- Aslam, M., F. Ahmad, P. S. M. B. M. Yusoff, K. Altaf, M. A. Omar, H. Abdul Khalil and M. R. Raza (2016). "Investigation of rheological behavior of low pressure injection molded stainless steel feedstocks." *Advances in Materials Science and Engineering* **2016**.
- Binet, C., D. Heaney, R. Spina and L. Tricarico (2005). "Experimental and numerical analysis of metal injection molded products." *Journal of Materials Processing Technology* **164**: 1160-1166.
- Cheng, L., K. Hwang and Y. Fan (2009). "Molding properties and causes of deterioration of recycled powder injection molding feedstock." *Metallurgical and Materials Transactions A* **40**(13): 3210-3216.
- Choi, J.-P., H.-G. Lyu, W.-S. Lee and J.-S. Lee (2014). "Investigation of the rheological behavior of 316L stainless steel micro-nano powder feedstock for micro powder injection molding." *Powder Technology* **261**: 201-209.
- Demers, V., F. Fareh, S. Turenne, N. Demarquette and O. Scalzo (2018). "Experimental study on moldability and segregation of Inconel 718 feedstocks used in low-pressure powder injection molding." *Advanced Powder Technology* **29**(1): 180-190.

- Demers, V., S. Turenne and O. Scalzo (2015). "Impact of binders on viscosity of low-pressure powder injection molded Inconel 718 superalloy." *Journal of Materials Science* **50**(7): 2893-2902.
- Demers V., E. M. M., Bocher P. (2017). " Moldability of low-pressure powder injection molding feedstocks." *Proceedings of the 2017 International Conference on Powder Metallurgy & Particulate Materials, Las Vegas, USA, June 2017, pp. 401-414.*
- Dihoru, L., L. Smith and R. German (2000). "Experimental analysis and neural network modelling of the rheological behaviour of powder injection moulding feedstocks formed with bimodal powder mixtures." *Powder metallurgy* **43**(1): 31-36.
- Fareh, F. (2016). *Caractérisation des mélanges développés pour le moulage basse pression des poudres métalliques (LPIM)*, École de technologie supérieure.
- Fareh, F. and V. Demers (2016). "Rheological behavior of Inconel 718 feedstocks used in low-pressure powder injection molding."
- Fareh, F., V. Demers, N. Demarquette, S. Turenne and O. Scalzo (2017). "Influence of segregation on rheological properties of wax-based feedstocks." *Powder Technology* **320**: 273-284.
- Fareh, F., V. Demers, N. R. Demarquette, S. Turenne and O. Scalzo (2016). "Molding properties of inconel 718 feedstocks used in low-pressure powder injection molding." *Advances in Materials Science and Engineering* **2016**.
- Fareh, F., V. Demers, S. Turenne and O. Scalzo (2016). *Segregation measurement of inconel 718 feedstocks used in low-pressure metal injection molding*. Materials Science Forum, Trans Tech Publ.
- G Lamarre, S. (2016). *Conception, fabrication et validation d'une presse à injection basse pression pour le procédé des poudres métalliques*, École de technologie supérieure.
- German, R. and A. Bose (1997). "Powder Injection Molding of Metal and Ceramics: Metal Powder Industries Federation." *Princeton, NJ*.
- German, R. M. (1990). "powder injection molding, metals powder industries federation."
- German, R. M. (1996). *Sintering theory and practice: A Wiley-Interscience Publication*.
- German, R. M. (1997). *Injection Molding of Metals and Ceramics*, Met. Powder Ind, Federation.
- German, R. M., K. F. Hens and S.-T. P. Lin (1991). "Key issues in powder injection molding." *American Ceramic Society Bulletin* **70**(8): 1294-1302.

- Ghanbari, A., M. Alizadeh, E. Ghasemi, R. Y. Rad and S. Ghaffari (2015). "Preparation of optimal feedstock for low-pressure injection molding of Al/SiC nanocomposite." *Science and Engineering of Composite Materials* **22**(5): 549-554.
- Gonçalves, A. C. (2001). "Metallic powder injection molding using low pressure." *Journal of materials processing technology* **118**(1): 193-198.
- González-Gutiérrez, J., G. B. Stringari and I. Emri (2012). Powder injection molding of metal and ceramic parts. *Some Critical Issues for Injection Molding*, InTech.
- Hausnerová, B. (2010). "Rheological characterization of powder injection molding compounds." *Polimery* **55**(1).
- Hausnerová, B., V. Kasparkova and E. Hnátková (2016). *Rheological and thermal performance of newly developed binder systems for ceramic injection molding*. AIP Conference Proceedings, AIP Publishing.
- Hausnerová, B., L. Marcaníková, P. Filip and P. Sáha (2011). "Optimization of powder injection molding of feedstock based on aluminum oxide and multicomponent water-soluble polymer binder." *Polymer Engineering & Science* **51**(7): 1376-1382.
- Hausnerova, B., B. N. Mukund and D. Sanetrnik (2017). "Rheological properties of gas and water atomized 17-4PH stainless steel MIM feedstocks: Effect of powder shape and size." *Powder Technology* **312**: 152-158.
- Hens, K. and R. German (1993). "Advanced processing of advanced materials via powder injection molding." *Advances in Powder Metallurgy & Particulate Materials--1993*. **5**: 153-164.
- Hidalgo, J., C. Abajo, A. Jiménez-Morales and J. Torralba (2013). "Effect of a binder system on the low-pressure powder injection moulding of water-soluble zircon feedstocks." *Journal of the European Ceramic Society* **33**(15-16): 3185-3194.
- Hidalgo, J., A. Jiménez-Morales and J. M. Torralba (2012). "Torque rheology of zircon feedstocks for powder injection moulding." *Journal of the European Ceramic Society* **32**(16): 4063-4072.
- Honek, T., B. Hausnerová and P. Sáha (2005). "Relative viscosity models and their application to capillary flow data of highly filled hard-metal carbide powder compounds." *Polymer Composites* **26**(1): 29-36.
- Huang, B., S. Liang and X. Qu (2003). "The rheology of metal injection molding." *Journal of Materials Processing Technology* **137**(1-3): 132-137.
- Huang, B., S. Liang and X. Qu (2003). "The rheology of metal injection molding." *Journal of Materials Processing Technology* **137**(1): 132-137.

- Karataş, Ç., A. Sözen, E. Arcaklıoglu and S. Erguney (2008). "Investigation of mouldability for feedstocks used powder injection moulding." *Materials & Design* **29**(9): 1713-1724.
- Khakbiz, M., A. Simchi and R. Bagheri (2005). "Analysis of the rheological behavior and stability of 316L stainless steel-TiC powder injection molding feedstock." *Materials Science and Engineering: A* **407**(1-2): 105-113.
- Kowalski, S. (2005). *Rheology based investigation of a polymer-mineral powder mix for low pressure injection moulding*, Université Jean Monnet, Saint Etienne.
- Kukla, C., I. Duretek, J. Gonzalez-Gutierrez and C. Holzer (2016). "Rheology of PIM feedstocks." *Metal Powder Report*.
- Lamarre, S., V. Demers and J. Chatelain (2016). "Experimental study of the rheological properties and moldability of wax-based feedstocks used in low-pressure powder injection molding."
- Lamarre, S. G., V. Demers and J.-F. Chatelain (2017). "Low-pressure powder injection molding using an innovative injection press concept." *The International Journal of Advanced Manufacturing Technology* **91**(5-8): 2595-2605.
- Li, Y.-m., X.-Q. Liu, F.-h. Luo and J.-L. Yue (2007). "Effects of surfactant on properties of MIM feedstock." *Transactions of Nonferrous Metals Society of China* **17**(1): 1-8.
- Li, Y., L. Li and K. Khalil (2007). "Effect of powder loading on metal injection molding stainless steels." *Journal of Materials Processing Technology* **183**(2-3): 432-439.
- Liang, S. T., Y.; Huang, B. and Li, S., (2004). "Trans. Nonferrous Met.".
- Liu, Z., N. Loh, S. Tor and K. Khor (2002). "Characterization of powder injection molding feedstock." *Materials characterization* **49**(4): 313-320.
- Loebbecke, B., R. Knitter and J. Haußelt (2009). "Rheological properties of alumina feedstocks for the low-pressure injection moulding process." *Journal of the European Ceramic Society* **29**(9): 1595-1602.
- Machaka, R., P. Ndlangamandla and M. Seerane (2018). "Capillary rheological studies of 17-4 PH MIM feedstocks prepared using a custom CSIR binder system." *Powder Technology* **326**: 37-43.
- Mangels, J. A. (1994). "Low-pressure injection molding." *American Ceramic Society Bulletin;(United States)* **73**(5).
- Mangels, J. A. and R. M. Williams (1983). "Injection molding ceramics to high green densities."

- Medvedovski, E. and M. Peletsman (2012). "Low pressure injection moulding mass production technology of complex shape advanced ceramic components." *Advances in Applied Ceramics* **111**(5-6): 333-344.
- Moballegh, L., J. Morshedian and M. Esfandeh (2005). "Copper injection molding using a thermoplastic binder based on paraffin wax." *Materials Letters* **59**(22): 2832-2837.
- Mohamad Nor, N., M. H. Ismail, N. Abu Kasim, N. Muhamad and M. Taib (2014). *Characterization and rheological studies on ready-made feedstock of stainless steel 316L in metal injection molding (MIM) process*. Applied Mechanics and Materials, Trans Tech Publ.
- Mohd Amin, A., M. H. I. Ibrahim and R. Asmawi (2014). "Mixing homogeneity and rheological characterization for optimal binder formulation for metal injection moulding." *Applied Mechanics and Materials* **607**: 181-184.
- Nishimura, K. and K. Yoshino (1995). Binder system for use in the injection molding of sinterable powders and molding compound containing the binder system, Google Patents.
- Park, S.-J., Y. Wu, D. F. Heaney, X. Zou, G. Gai and R. M. German (2009). "Rheological and thermal debinding behaviors in titanium powder injection molding." *Metallurgical and Materials Transactions A* **40**(1): 215-222.
- Qu, X., J. Gao, M. Qin and C. Lei (2004). "Rheologic behavior and PIM processing of WC-TiC-Co powder feedstock." *Journal of University of Science and Technology Beijing(English Edition)* **11**(4): 334-337.
- Quevedo Nogueira, R. E. F., A. C. Bezerra, F. C. dos Santos, M. R. d. Sousa and W. Acchar (2001). *Low-Pressure Injection Molding of Alumina Ceramics Using a Carnauba Wax Binder: Preliminary Results*. Key Engineering Materials, Trans Tech Publ.
- R.M. German (1995). "Powder Injection Molding."
- Rei, M., E. Milke, R. Gomes, L. Schaeffer and J. Souza (2002). "Low-pressure injection molding processing of a 316-L stainless steel feedstock." *Materials Letters* **52**(4): 360-365.
- Rei, M., E. Milke, R. Gomes, L. Schaeffer and J. Souza (2002). "Low-pressure injection molding processing of a 316-L stainless steel feedstock." *Materials Letters* **52**(4-5): 360-365.
- Schlechtriemen, N., R. Knitter, J. Haußelt and J. R. Binder (2013). "Impact of powder morphology on quality of low-pressure injection moulded reaction-bonded net shape oxide ceramics." *Journal of the European Ceramic Society* **33**(4): 709-715.

- Sotomayor, M., B. Levenfeld and A. Várez (2011). "Powder injection moulding of premixed ferritic and austenitic stainless steel powders." *Materials Science and Engineering: A* **528**(9): 3480-3488.
- Sotomayor, M., A. Várez and B. Levenfeld (2010). "Influence of powder particle size distribution on rheological properties of 316 L powder injection moulding feedstocks." *Powder Technology* **200**(1-2): 30-36.
- Sotomayor, M., A. Várez and B. Levenfeld (2010). "Influence of powder particle size distribution on rheological properties of 316L powder injection moulding feedstocks." *Powder Technology* **200**(1): 30-36.
- Sri Yulis, M. A., J. Khairur Rijal and M. Norhamidi (2009). "Rheological properties of SS316L MIM feedstock prepared with different particle sizes and powder loadings."
- Suri, P., S. V. Atre, R. M. German and J. P. de Souza (2003). "Effect of mixing on the rheology and particle characteristics of tungsten-based powder injection molding feedstock." *Materials Science and Engineering: A* **356**(1-2): 337-344.
- Tatt, T. K., N. Muhamad, A. Muchtar, A. B. Sulong and H. S. Yunn (2012). "Rheological behaviour of novel feedstock for manufacturing porous stainless steel via (MIM)-PSH." *Jurnal Teknologi (Sciences and Engineering)* **59**(SUPPL. 2): 187-191.
- Torralba, J., J. Ruiz-Román, L. Cambronero, J. Ruiz-Prieto and M. Gutierrez-Stampa (1997). "P/M high speed steels obtained by metal injection moulding." *Journal of materials processing technology* **64**(1): 387-395.
- Vervoort, P., R. Vetter and J. Duszczyk (1996). "Overview of powder injection molding." *Advanced Performance Materials* **3**(2): 121-151.
- Weir, F., M. Doyle and D. Norton (1963). "Moldability of plastics based on melt rheology. Part II—practical applications." *Polymer Engineering & Science* **3**(1): 37-41.
- Zlatkov, B., E. Griesmayer, H. Loibl, O. Aleksić, H. Danninger, C. Gierl and L. Lukić (2008). "Recent advances in PIM technology I." *Science of Sintering* **40**(1): 79-88.
- Zorzi, J. E., C. A. Perottoni and J. A. H. d. Jornada (2003). "Wax-based binder for low-pressure injection molding and the robust production of ceramic parts."